national accelerator laboratory TM-547
1501

SUMMARY REPORT ON PHASE I OF THE POPAE DESIGN STUDY (Part 1)

T.L. Collins, D.A. Edwards, J. Ingebretsen, D.E. Johnson,
S. Ohnuma, A.G. Ruggiero, L.C. Teng

February 1975

The initial phase of the POPAE Design Study consists of an investigation of the lattice and layout of the storage rings, and an examination of site factors. Part 1 of the summary report - this Technical Memorandum - contains introductory comments and material relating to the proton storage rings. The electron ring and site discussion will be issued as Part 2.

PREFACE

The potential role of storage rings in the high energy physics program at the Fermi National Accelerator Laboratory was recognized early in the project. In the summer of 1968, following the design development of the present Fermilab accelerator, a study was made of a system of 100 GeV proton storage rings; however, with the construction of the Laboratory underway, a continuation of that design effort was not then feasible.

Four years later, as the accelerator came into operation and the experimental program was initiated, it became timely to examine the question of what major additional facilities would be appropriate to further exploit the potential of the Laboratory. Of course, storage rings were not the only possibility - new experimental areas, a large multiparticle spectrometer, and a bubble chamber as successor to the 15 foot chamber then under construction had been suggested. In order to advise the Laboratory as to which course to pursue, the Director asked a representative group of physicists to serve as a Long Range Advisory Committee. Following a Summer Study at Aspen, Colorado in 1973, attended by some 80 physicists from throughout the United States and abroad, the Long Range Advisory Committee recommended, in December of that year, that the primary goal for new construction at the Fermilab be a storage ring system on a scale suitable to permit the collision of 1000 GeV protons with 1000 GeV protons and with 20 GeV electrons. The Committee, observing that in their specific choice of proton energies they had been influenced by the possibility of an Energy Doubler, qualified their recommendation with the statement that the largest step in energy and luminosity consistent with technical and economic reality be undertaken.

Following the concurrence of the Trustees of the Universities Research Association with the Committee findings, in the Spring of 1974, the Director initiated a design effort on the recommended facility and assigned to it the acronym POPAE (Protons on Protons and Electrons). This report summarizes the first phase of that activity.

Our study has been based on the plans outlined at the Aspen Summer Study. In addition, we have been guided by discussions at two "workshops" conducted in recent months. The first of these was organized by L. C. Teng of Fermilab and the emphasis was on machine problems - beam dynamics of storage rings, superconducting magnets, and so on. The second was arranged by M. L. Goldberger of Princeton University and was concerned with the high energy physics aspects, both theoretical and experimental, of POPAE. It is our hope that the design will continue to evolve with the aid of meetings of this sort in order that the plan reflect the interests of the prospective users.

In assembling and editing this report, I have attempted to make the text an accurate synthesis of the views and contributions of the various authors. Should the reader find obscure passages or errors of interpretation, the responsibility is mine.

D.A. Edwards

CONTENTS

(Part 1)

Contents (cont'd)

I. INTRODUCTION

A. Design Goals and Constraints

POPAE as conceived at the 1973 Aspen Summer Study and recommended for design development by the Long Range Advisory Committee is a storage ring facility on a scale suitable to permit the collision of 1000 GeV protons with 1000 GeV protons and with 20 GeV electrons. The luminosities were specified at $10^{34}cm^{-2}sec^{-1}$ for proton-proton and $10^{32}cm^{-2}sec^{-1}$ for the electron-proton intersections. The general location of the facility as sketched at Aspen was to be to the east of the present main accelerator, encircling the Fermilab Village.

This phase of our study as described in this report has been carried out with adherence as closely as possible to the above outline. There are many ways that storage rings of various dimensions can be placed on the Fermilab site - here, we have been concerned only with the elaboration of the specific case suggested at Aspen.

We have found some modifications to be useful for the purposes of our study. The major change has been in the shape of the layout. At Aspen, a 240 meter length for each of the eight symmetrically disposed long straight sections was estimated to be sufficient to accommodate both the experiments and the machine components to attain beam optics necessary for the interaction region. Further study indicated that 240 meters was insufficient, and in order to retain the 1000 GeV scale and general locations of the rings, we have considered a racetrack form for POPAE, with approximately the same total straight section length as the Aspen version.

Another less significant change has been a slight repositioning of POPAE in order to avoid the region of most probable expansion of fixed target experimental areas at the Fermilab. Thus, the layout appearing in this report does not make use of the present external beam lines for proton injection to one of the storage rings.

In common with the 1973 Summer Study plan, we have not yet taken into account any potential geometrical interference with a site-filling fixed target accelerator; however, it is a requirement that a fully developed design not foreclose that option.

B. The Design Procedure

In order to proceed with the evolution of a design, it is necessary to impose some constraints in addition to those in the preceding section. For this study, we will assume that we are designing proton storage rings to receive their injected beam from the present Fermilab synchrotron up to the energy at which it has demonstrated successful operation, namely, 400 GeV, and that the magnetic field of the bending magnets in the storage rings will be 18 kilogauss.

These presumptions remove from present consideration a number of unanswerable questions which can be debated endlessly and, most likely, profitlessly. Foremost among these are, first, the probability of existence of the Energy Doubler and the intangibles concerning its suitability as an injector for a storage ring, and, second, the magnetic field levels that can be achieved by high quality, economical, and reliable superconducting magnets.

The physical scale of POPAE is unchanged by this approach, for the Aspen group had based their layout on 1000 GeV protons steered by 45 kilogauss magnets. But our more limited focus provides a mechanism for proceeding through the design process without wrestling with a host of unknowns. Of immediate and great benefit is the unambiguous definition of the proton injector performance, for the injector characteristics are of paramount importance in the design of storage rings for protons.

We will not deliberate upon the manner in which 1000 GeV proton energies in the storage rings are to be eventually achieved; 400 GeV proton storage rings are interesting in themselves and could represent an intermediate step to the 1000 GeV region. Though this report assumes that the protons are to be injected at the energy of storage (aside from the modest energy changes involved in stacking the beam), we do not exclude the eventual examination of acceleration of the high current beam in the storage rings to above 400 GeV in the event that an appropriate injector is not provided.

We have no illusions about the prospect that a facility conforming to our design procedure would actually be constructed. One need only observe that the present Fermilab synchrotron was initially conceived and funded as a 200 GeV machine, yet now offers the promise of operation at energies in the neighborhood of 500 GeV. The same evolution would doubtless occur in this context, in a way that we cannot visualize at this writing. However, the procedure that we have adopted creates a relatively definite perimeter within which to conduct our study for the near term, and it is likely that such a study will form a basis for subsequent excursion beyond these boundaries.

A word about magnets is appropriate at this stage - even though we speak of 18 kilogauss dipole magnets, it is presumed that whatever dipole magnets are used in the proton storage rings that they will of necessity be constructed of low or vanishing resistivity conductors in view of the present climate of opinion regarding energy utilization.

We select 18 kilogauss as a figure consistent both with the design constraints imposed on us and with a field level that is surely attainable with high quality in magnets having iron yokes and superconducting coils.

Thus, throughout this report, unless otherwise specified, we take the proton energy to be 400 GeV and all dipole magnets, whether in injection lines or in the rings, are at or below the 18 kilogauss level. In the same spirit, quadrupole gradients are limited to 9 kilogauss per inch.

C. Summary and Status

The layout of the present version of POPAE on the Fermilab site is sketched in Figure 1. The proton storage rings have two long straight sections, one of length 928 m to the west and the other of length 1159 m to the east. That the straight section lengths are unequal is a consequence of the east-west asymmetry of the system as regards injection. On the western side of POPAE, a number of short straight sections have been introduced into the "semi-circles" at either end to accommodate injection equipment; these short straight sections are not necessary on the eastern side and the corresponding space can be filled with bending magnets thereby increasing the east long straight section length.

The two long straight sections are parallel to each other and parallel to the eastern boundary of the site. The racetrack shape permits rings of a scale consistent with the design procedure to fit in this general location on the site without crowding the power transmission line to the east or the main accelerator to the west.

Insofar as the machine optics are concerned, several interaction regions are possible in each long straight. Nevertheless, the layout under current consideration contains but two experimental regions on each side. There are several reasons for this. Foremost among these is the feeling that a facility of this magnitude should not from the outset be tailored to today's preconceptions of its use but should rather be planned with the potential for future development. In the abstract, one can scarcely take exception to this sentiment. For a fixed target accelerator, it is relatively easy to allow for future expansion of experimental areas with a minimum of repercussions for the design and placement of accelerator enclosures and systems. In a storage ring, however, the experimental areas lie between pieces of machine, which play the role of beam transport systems repetitively delivering beam to those areas. If at a later stage, an expansion of experimental facilities is found desirable, one will be confronted with an existing complex of machine enclosures, components, injection transports, and so on, reconstruction of which would be unrealistic to contemplate. Rather, the ultimate extent of the experimental facilities for a storage ring system must be judged from the beginning. Of course, this argument must ultimately be tempered by the realities of costs.

A second reason for not immediately fitting the long straight sections to the mix of interaction regions that have been recommended to be suitable arises from the suspicion that as time goes on and potential users think about other varieties of experiments that may be conducted at a facility such as this, additional insertion requirements will arise. It is obviously, we hope, preferable that the design exercise not be reset to the beginning with each new added feature.

Finally, we offer two other reasons for leaving space in the long straight sections. One is experimental: what degree of decoupling or shielding is needed between detection apparatus at neighboring interaction regions in one straight section? The other has to do with beam dynamics. Any modern storage ring design, regardless of its apparent symmetry, will be nevertheless a periodic focusing system of one-fold rotational symmetry when operated for the diverse interaction region requirements for which it has been constructed, and, at least during the initial phases of its running, will need an allocation of adequate space for beam optics systems which are necessary for the compensation of the consequences of low periodicity.

In Figure 1, we have indicated that there are two high luminosity regions for proton-proton collisions in the west straight section. At the south end of the east straight section, there is a multi-purpose interaction region for the study of processes, such as elastic proton-proton scattering, which can sacrifice peak luminosity in preference to improved access to particles emitted at small angles from the interaction point.

The other experimental area on the east side is for electron-proton interactions. We have, relatively briefly, examined two versions of the electron ring selection between which will depend on response to this report and on cost estimates that have not yet been made. The small dotted oval in Figure 1 represents a 10 GeV electron storage ring in an enclosure of its own. The second option is a 20 GeV electron storage ring following the same tunnel as the proton storage rings.

This report represents a first pass through the conceptual design of a storage ring system consistent with the goals, constraints and biases stated above, and may be used as a basis for a new phase. The next two chapters treat the proton and electron storage rings, primarily from the machine builders point of view. Site factors are discussed in Chapter IV, using topographic and subsurface data developed prior to and during the construction of the Laboratory.

II. THE PROTON STORAGE RINGS

A. Introduction

Generally speaking, the luminosity at a beam crossing point is proportional to the current in each beam and the length through which the beams overlap and inversely proportional to an effective cross sectional area of the beams. In pressing toward high luminosity, primarily one seeks to increase the currents and reduce their areas. The length of the overlap region is less useful as a variable, for experiments are apt to prefer that the "target" size remain within bounds appropriate to the detection apparatus.

High luminosity is of no value if it is accompanied by intolerable backgrounds. The minimization of beam loss deserves as great an emphasis in storage ring design as the improvement of luminosity; unfortunately, it is a more difficult subject to quantify and the ingenuity displayed by particles in straying from their assigned course is considerable. Certain of the loss mechanisms - particularly some of the more catastrophic ones - are reasonably well understood as a result of experience on accelerators and storage rings, and accommodation can be made in the design from the outset. Beyond those predictable processes, prudence dictates that space allowances be made in the lattice and in the aperture so that a degree of freedom will be available for necessary modifications and additions during operation.

There are three principal means or steps in achieving small beam size. Of these, the most fundamental has little to do with the storage rings themselves; rather it is built into the injector. Perhaps the most important single input parameter to the design of a proton storage ring, not only for luminosity but for losses as well, is the transverse emittance of the proton source. For this reason, the next section is devoted to the beam properties of the Fermilab proton synchrotron. Secondly, the optics in the storage ring can be arranged to reduce the beam area at the intersection point, and this is the role of the "insertions" discussed in Section D below. Thirdly, scraping or trimming of the beam can be used to enhance the current density and to assist in localizing the intersection region.

High current is obtained by filling the storage rings with a suitably large number of protons from pulse after pulse of the injector. Employing stacking in momentum space, the ISR has achieved beam currents of 30 amperes in each ring. In achieving long term stability of a single high current beam, a number of phenomena must be taken into account, such as

- beam induced pressure instability
- transverse and longitudinal wall impedance instabilities
- incoherent single beam tune shift
- nonlinear resonances and access to them by intra-beam diffusion
- effects of trapped electrons or ions

The extent to which these processes represent limitations tends to be reflected in the choice of aperture, some discussion of which will be found in Section E below and will doubtless appear as a continuing topic in subsequent phases of this study.

A single-beam characteristic whose roles as a potential performance limitation is difficult to assess is the kinetic energy stored in the beam. A 10 ampere beam containing 2×10^{15} 400 GeV protons represents an energy of 128 MJ. Though a large number, there is no <u>a priori</u> reason to consider it to be outside the bounds of possibility. We comment on the problems associated with disposal of such a beam in Section H.

Given two beams of suitable intensity and cross sectional area, when they are brought into collision, each beam acts with an extremely nonlinear force on the other. It has become conventional to characterize this inter-beam effect by a single parameter - the so-called linear tune shift. What the limiting value of this parameter may be is not known experimentally. In the absence of a limit derived from experience, the value of .005 for proton-proton collisions is often used as a reference figure. Beam-beam tune shifts below .005 are felt to be safe, while tune shifts above .005 are pushing toward some potential limit. In this report, we do not regard any particular value of the tune shift as a hard and fast limit; we have, however, sought to insure that interesting luminosities would be achieved in POPAE without large values of the linear tune shift.

B. The Injector

The Fermilab accelerator and its operation for the fixed target experimental program has been described extensively elsewhere;[1] here we will only discuss its characteristics as an injector for the proton storage rings.

The accelerator consists of three major subsystems - the linac, booster and main ring. The linac accelerates protons to a kinetic energy slightly over 200 MeV. At a current of 100 mA, the emittance containing 90% of the beam is typically 10π mm mrad and some 20% less under optimum conditions. The linac pulse length is such that the linac beam may be injected into the booster for several turns; the ultimate performance figures for the accelerator system insofar as intensity is concerned were based on four turn injection to the booster.

Today, a multi-turn mode of injection into the booster is normally employed. Thereby, the transverse phase space area in the horizontal plane of the booster beam is increased by more than a factor of two at injection. Horizontal-vertical coupling may then increase the vertical phase space area as well. For storage ring use, in order to capitalize on the small linac emittance, it is desirable that the single turn mode of injection into the booster be used, provided that the filling time for the storage rings is reasonable and that the momentum width of the stacked beam is not excessive.

The main ring has a circumference 13¼ times that of the booster, and is filled by a sequence of 13 pulses from the rapid cycling 15 Hz booster.

To date, single turn injection into the booster has yielded main ring proton beams of up to ~ 10^{13} protons per main ring cycle. We feel that the gradual increase of booster performance over the years, particularly as the debuncher between the linac and booster is exploited and as additional radiofrequency cavities are installed in the booster to improve acceleration efficiency, insures that 10^{13} protons per main ring cycle will be a conservative estimate of booster performance for single turn injection.

A circulating beam in the main ring of 10^{13} protons represents a current of 76 mA. The storage rings are 35% larger in circumference and 10A is the sort of current that one would like to store in each. Thus, to fill one ring, some 2×10^{15} protons would be required, or 200 main ring cycles for each storage ring.

At 5 seconds per accelerator cycle, 17 minutes would be required to deliver 2×10^{15} particles to one of the storage rings. Allowing for filling efficiencies of the order of 50%, one requires only one hour of accelerator time to fill both storage rings to 10A. Recognizing that the one hour filling time is apt to be comparable to the time required to set up the accelerator for the filling operation and to convert back to the fixed target experimental program, we conclude that the low-emittance single turn into the booster mode is both reasonable in filling time and desirable for luminosity, and we will base our performance estimates upon this presumption.

The emittance of the main ring beam at 300 GeV was studied by two techniques in the spring and summer of 1973 and the results were reported in the proceedings of the 1973 Aspen Summer Study.[2] With single turn injection into the booster, the main ring intensity at that time was about 4 x 10^{12} protons per cycle. The beam profile could be well represented by a gaussian out to 3 standard deviations, and the measurements yielded

$$\sigma = 2/3 \text{ mm at } \beta = 79 \text{ m}$$
$$3/4 \text{ mm at } \beta = 98 \text{ m}$$

in the horizontal plane and very slightly smaller results in the vertical. If we define the emittance, ε, as the phase space area in one transverse dimension containing 95% of the particles, then for a Gaussian beam

$$\varepsilon = \frac{6\pi\sigma^2}{\beta}$$

and from the average of the two measurements we have

$$\varepsilon = \frac{1}{30}\pi \text{ mm mrad at 300 GeV}$$

A scaling of the linac emittance with momentum would predict an emittance of ~0.029π mm mrad.

Since mid-1973, though the main ring intensity obtained from single turn injection into the booster has increased, there has been no apparent increase in the emittance. Pending a remeasurement, we will use the figure above for both the horizontal and vertical emittances at 300 GeV and scale inversely with momentum to obtain the emittance at other energies.

The longitudinal emittance has been obtained from observation of debunching at high energy after the rf system is turned off and from the phase length of the bunches. In canonical coordinates, $\Delta E/\omega_{rf}$ and $\Delta\phi_{rf}$, the bunch area is 0.1 eV·sec.

Above we mentioned a 5 second cycle for acceleration to 400 GeV. This short a cycle cannot be performed at present, but a limited number of accelerator systems modifications, some of which are already underway, will permit this cycle time to be achieved. Additional accelerating stations are being installed in the main accelerator to increase the ramp rate to 150 GeV/sec. At this ramp rate, a main ring cycle might consist of a 1 second injection dwell time (as at present), 2.67 second acceleration time, 0.33 second flat top and 1 second recovery time to the injection level. The average main ring power for this mode is 45 MW, which is acceptable. The rms power is 80 MW, which exceeds the present 60 MW rms power limitation of the feeder between the master substation and the main ring. However, it is presently planned to upgrade this feeder to 80 MW, though on an unspecified time scale. An increase of the duty factor of the main ring radiofrequency system to that considered here would probably require an additional anode power supply.

C. Description of the Lattice

The proton storage ring lattice has been developed on the basis of the following considerations[3], in addition to those defined by the design procedure in Chapter 1:

1. We assume the two proton storage rings to be located one on top of the other. The two oppositely circulating beams are brought together in the vertical plane to collide with each other.
2. The most economical normal cell is the FODO cell, and the most advantageous phase advance per cell for the placement of beam manipulating elements is 90°. We take the normal cell length to be 60 m, essentially the same as that in the main ring. Four bending magnets, each about 6 m in length, are placed between successive quadrupoles.
3. To facilitate the design of matched insertions in the straight sections, all pairs of corresponding quadrupoles in the two rings are assumed to have opposite focusing actions on the two beams, hence the same gradient polarity.
4. The lattice modifications to accommodate injection to the clockwise and counterclockwise rings will be identical in both rings and the injection points will be symmetrically to the north and south of the midpoint of the west long straight section.
5. The bending elements in the north and south arcs will be distributed so as to bring the momentum dispersion function to zero or nearly so throughout the long straight sections.

For injection, we follow the method outlined in the 1968 Fermilab storage ring report[4], which utilizes full aperture kickers to produce a transient localized orbit distortion positioning the injected beam orbit on the "other" side of a septum. It is also desirable to modify the momentum dispersion function in the injection area so that this function will be large at the septum position. An arrangement which provides space for the injection elements and accomplishes the modification of the momentum dispersion function is sketched below.

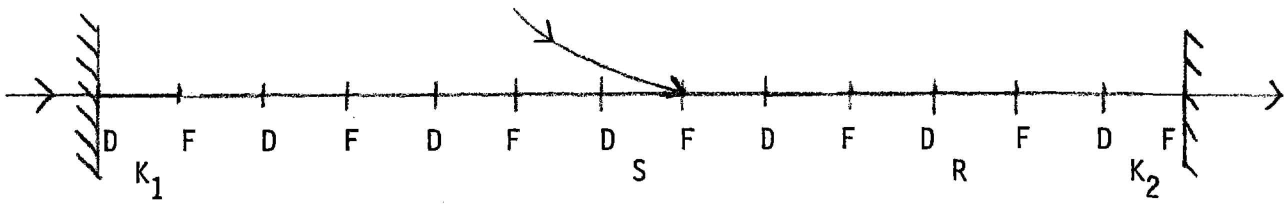

All of the half-cells have their normal complement of four bending magnets except those labeled K_1, K_2, S and R. The bending magnets are left out of the half-cell at S to provide space for the injection septum. The absence of these magnets will create a distortion in the dispersion function in addition to the one we want; to localize it to the vicinity of S, we also leave four bending magnets out at R, 180^{o} in betatron phase away. Four bending magnets are also left out at both K_1 and K_2, the kicker locations. The kickers should be an odd number of quarter wavelengths upstream and downstream of the septum. We can also enhance the dispersion function at S by taking this odd number to be 3 (or 7, 11, etc.), so that between K_1 and K_2 we have a perturbation in the dispersion function of the form:

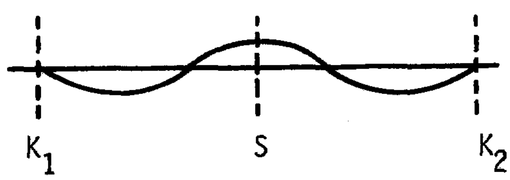

The injection portion of the lattice then consists of a set of four half-cells without dipoles distributed among normal cells as sketched above which can be moved through the north and south arcs in half-cell increments to yield a variety of injection points.

Dispersion reduction for the long straight sections can also be effected by omission of dipoles from the normal lattice.

Consider two series of cells I and II with bending magnets in alternate half-cells, as sketched below. For clarity the diagram is

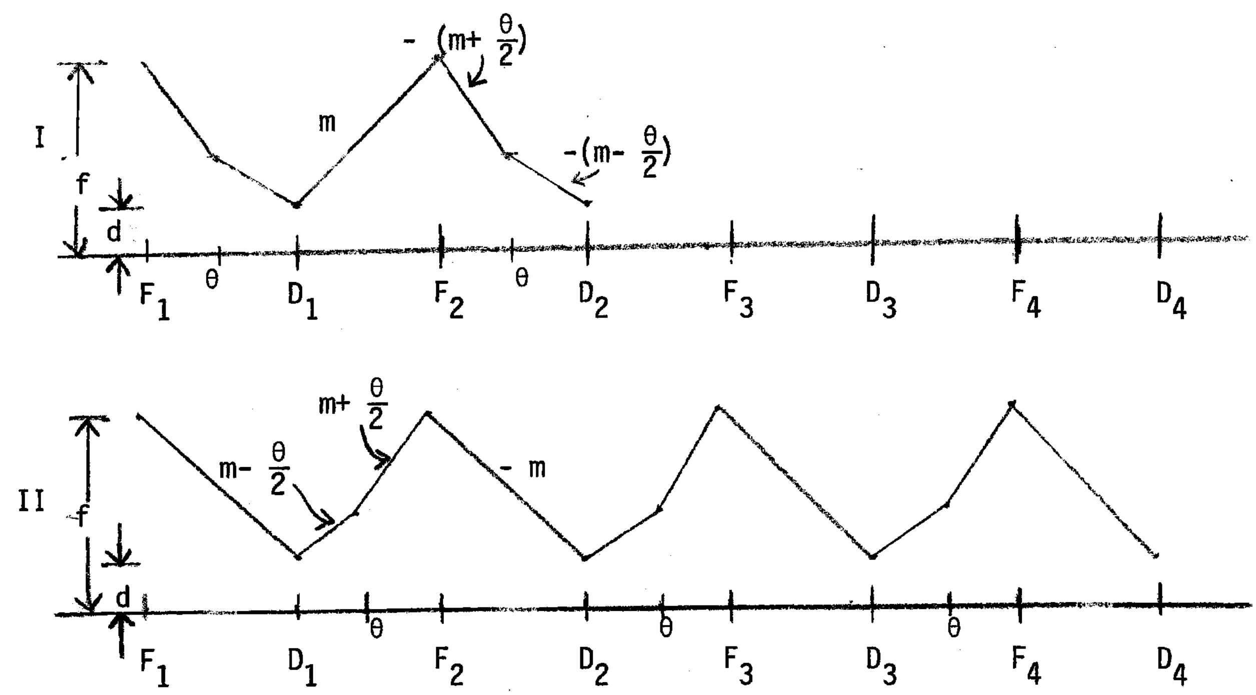

drawn in thin element approximation although the argument is quite independent of this approximation. The sum of these dispersion functions gives that of the normal cells. Since series II is simply series I traced backward, the designations of the values and slopes of the dispersion functions given in the figure are self-evident. If now one terminates series I at D_2 after a phase advance of 180^0, the dispersion and slope at D_4 will be the negatives of those at D_2. Adding the truncated series I to series II, the dispersion and slope at D_4 are then d - d = 0 and $-m + (m- \frac{\theta}{2}) = - \frac{\theta}{2}$ respectively. A $\frac{\theta}{2}$ bend (2 cell dipoles) at D_4 will make dispersion zero to the right of D_4 which is then the beginning of the straight section. Similarly if series II is terminated at F_2 and added to the un-terminated series I, the dispersion and slope at F_4 will be f - f = 0 and $m - (m+ \frac{\theta}{2}) = - \frac{\theta}{2}$ respectively which is also made zero to the right by the $\frac{\theta}{2}$ bend. This dispersion transition section then looks like

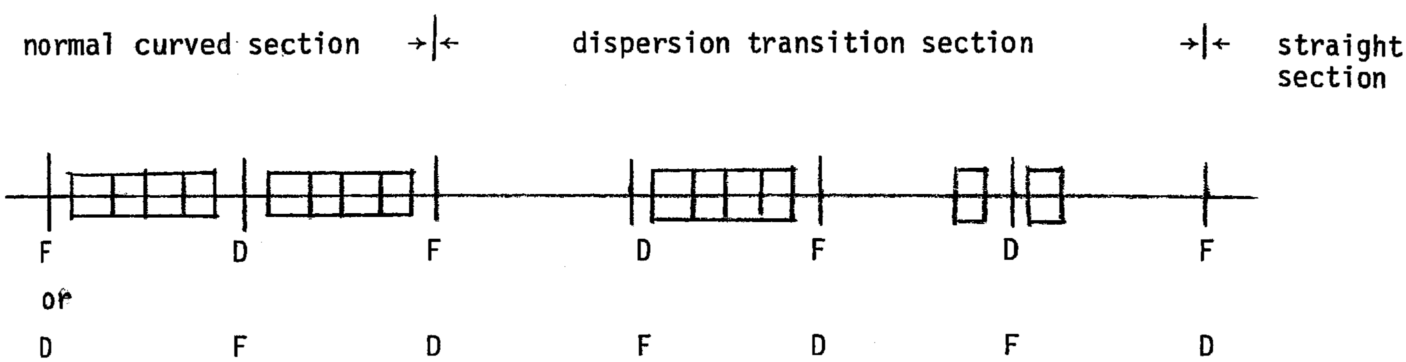

the geometry being identical for both rings.

The normal cell as discussed in greater detail in Section E below does not have its bending magnets disposed symmetrically about the middle of the half-cell. Nor can the equivalent of two bending magnets be superimposed upon a quadrupole. So slight modification of the above idealized arrangement - in particular in the positions and strengths of the final bending magnets - would be necessary to zero the dispersion in a long straight section, and so the degree to which it is set precisely to zero is a matter of convenience. We have assumed that minor dispersion adjustments would most appropriately be performed in the neighborhood of the interaction regions and have been satisfied with the removal of the bulk of the dispersion at the ends of the straight sections by the arrangement described above.

After an examination of a large number of specific cases, we have chosen the injection point so that the downstream end of the injection septum will be located at an angle of 15.6122^{0} with respect to the direction of the west long straight section. This choice yields a west long straight section length of about 930 m and reasonable clearance of POPAE from the site boundary and the main accelerator.

Each semi-circular arc, proceeding from west to east consists of the dispersion transition section, then the injection sequence, then 41½ normal cells, and finally another dispersion transition section.

The straight section lengths have been adjusted so that the path length of the injection orbit corresponds to a harmonic number h = 1507 at the frequency of the main accelerator rf system. The west straight section is then 928 m long and the east straight section 1159 meters.

The resulting lattice is summarized schematically in Figure 2; the contents of the long straight sections will be described in the next section.

D. The Insertions

Each long straight section consists of a sequence of several matched insertions. A modular design approach[5] has been used, in the sense that a standard set of matching conditions has been assumed at either end of each insertion. Namely, the momentum dispersion function, η, and its derivative with respect to position along the orbit, η', have been taken to be zero, while the amplitude functions join properly onto those in a normal cell.

Thus far, there are four insertion types, exclusive of that for the e-p crossing discussed in the next chapter. These are (1) a high luminosity crossing insertion for experiments on rare events, two of which are in the west straight section, (2) a high angular resolution crossing insertion for experiments on small angle events in the east straight section, (3) a phase adjusting non-crossing insertion, one of which appears in the lattice of each beam between experimental crossings, and (4) a non-colliding crossing for the west straight section. The design of these insertions has been carried out using the computer program MAGIC[6] to obtain the desired behavior of the amplitude function, and TRANSPORT[7] to adjust the dispersion function and the geometry of the crossings. The locations of the various insertions in the straight sections are shown in Figure 3.

1. Symmetry Considerations

In principle, as long as the desired beam geometry, optics, and dispersion characteristics are obtained in an insertion, there need not be any requirement of symmetry either in the focusing sequence or between the two rings. However, since there exists an excessive degree of flexibility in the design of insertions, imposing some symmetry conditions will simplify the design and make the operation of the rings easier.

First, we assume all crossings of the two beams to be in the vertical plane and all optics matching quadrupoles in the two beams are paired with one directly above the other and having equal strength. There are, then, two alternative arrangements: each pair of quadrupoles could have either the same focusing actions on the two beams, hence opposite gradient polarities (denoted by F/F) or the opposite focusing actions, hence identical gradient polarities (denoted by F/D). In the focusing sequence in each beam, we consider also two alternative symmetry arrangements: the quadrupole focusing actions can have either reflection symmetry about the midpoint (symmetric) or reflection symmetry with change of sign (antisymmetric). In an antisymmetric insertion, the beam optics in the horizontal and the vertical planes are midpoint-reflections of each other, hence the phase advances of betatron oscillations in the two planes are identical. For this reason, we consider antisymmetric insertions generally more desirable although the different optics in the two planes obtainable in a symmetric insertion can be advantageous in some special cases.

The vertical geometry of the beams is determined by the requirements: (1) the beam at either end of the insertion must be horizontal and at prescribed elevations, (2) the crossing angle must have the desired value, (3) the vertical dispersion must be matched from zero to zero across the insertion, and (4) the vertical dispersion must satisfy prescribed conditions at the crossing point and, in some cases, at other locations in addition. The F/F arrangement applied to an antisymmetric insertion yields a geometry for the two beams which does not possess reflection symmetry about the midpoint. This makes the design of such a crossing insertion more complicated. For the present design, we have adopted the

F/D arrangement for the insertions as being simpler and more symmetric. In addition to simplifying the design for antisymmetric insertions, the F/D arrangement also permits the use of quadrupoles common to both beams. To further exploit the simplicity thus acquired, we extended this arrangement to the entire rings as stated in Section C above.

2. High Luminosity Insertion

The basic requirements for this insertion are that (a) the beams be focused to the smallest width reasonably possible at the (vertical) crossing in order to achieve high luminosity, (b) space adequate for experimental equipment be allowed between the beam transport elements on either side of the crossing point, (c) the length of the luminous region be reasonably short and well defined, and that (d) space be available next to the outgoing beams for detecting forward secondaries. In addition, it is desirable that the beam width and crossing angle be variable so that a variety of experimental conditions can be produced with given beam currents in the machine.

The dependence of the luminosity and the length of the luminous region on the various parameters can be inferred from the simplest of models. The general expression for the luminosity per unit volume in the collision between two particles species having volume densities n_1 and n_2 traveling with velocities $\vec{v}_1$ and $\vec{v}_2$ is

$$\frac{d\mathcal{L}}{dV} = n_1 n_2 |\vec{v}_1 - \vec{v}_2| \tag{1}$$

For highly relativistic particles and small crossing angle α, $|\vec{v}_1-\vec{v}_2| \simeq 2c \cos\frac{\alpha}{2} \simeq 2c$. If each beam had a sharply defined rectangular cross-section of width w (perpendicular to crossing plane) and height h within which the particle density is uniform, then for equal currents $I_1=I_2=I$

$$n = \frac{I}{ec\ wh} \tag{2}$$

and

$$\mathcal{L} = 2c \left(\frac{I}{ec}\right)^2 \frac{1}{wh} \frac{h}{\alpha} \tag{3}$$

with a distribution of luminosity along the interaction region of the form

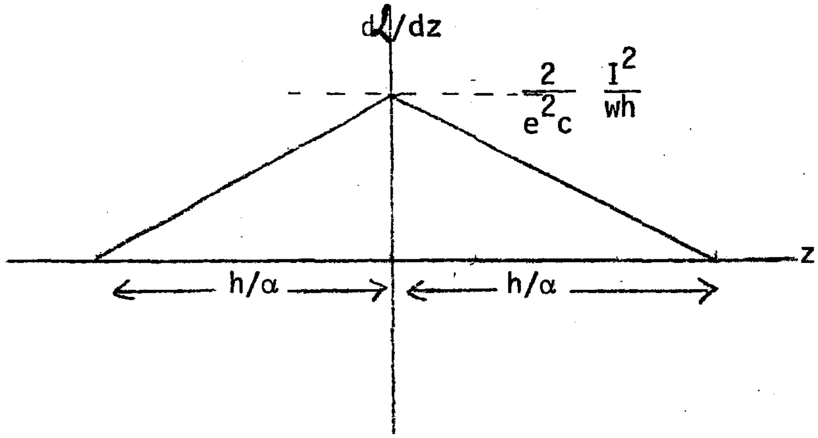

where the longitudinal coordinate z bisects the angle α included between the two beams. The total luminosity, $\mathcal{L}$, is then independent of beam height, and is inversely proportional to the beam width and crossing angle. For a fixed crossing angle, the length of the luminous region varies directly as the beam height.

The two quantities influencing the beam width are the horizontal momentum dispersion function η_H and the horizontal amplitude function, β_H. The former is made zero in the design. Then $w \propto \sqrt{\beta_H}$, and condition (a) above is equivalent to a desire for small β_H.

Condition (c) implies that h/α should be small. But luminosity is inversely proportional to α, so we want the beam height, h, to be small. Again, there are two contributions to the beam height. Because the two beams are initially parallel with one above the other, vertical bends must be introduced to effect the crossing. The vertical bends are so designed as to produce zero vertical momentum dispersion function at the center of the crossing region. Its derivative, on the other hand, need not vanish; however, η_V' should be sufficiently small so that the resulting dispersion function throughout the luminous region be negligible. The beam height then varies as $\sqrt{\beta_V}$, so we require that β_V be small.

The desire for small β_V and β_H runs counter to condition (b). The smaller the value of β at the crossing point, the larger its value elsewhere in the insertion. High β value at a quadrupole accentuates the effects of chromatic aberration and as the free region about the interaction point gets longer, this situation becomes aggravated. We have assumed that the total free drift space on either side of the crossing point should not be less than 20 m. The maximum tolerable value of β in the insertion is not easily determined. We have chosen not to allow β to exceed by more than an order of magnitude its maximum value in the normal cell. Then, with a maximum value of β in the insertion of ~1000 m and a 21 m free length, we have found that the lower limit for both β_H and β_V at the crossing is about 1 meter.

In both planes, β is a minimum at the center of the crossing region. Denoting the minimum value by β^*, at a distance z from the crossing point in the field-free drift space, the amplitude function is given by

$$\beta(z) = \beta^* + \frac{z^2}{\beta^*} \quad (4)$$

We have assumed that the luminous region should not exceed 1 m in length; at $z = \pm 0.5$ m and for $\beta^* = 1$ m, β is only 25% larger than it is at $z = 0$. This variation in β can for all practical purposes be ignored in luminosity estimates, as shown below.

Let us refer to the luminosity per unit length, $d\mathcal{L}/dz$, as the "brightness," b(z). For Gaussian beams having the same emittance ε (as defined in Section B) in both planes, we have

$$b(z) \equiv \frac{d\mathcal{L}}{dz} = c \left(\frac{I}{ec}\right)^2 \frac{3}{\varepsilon} \frac{1}{\left[\beta_H(z)\beta_V(z)\right]^{\frac{1}{2}}} \exp\left\{-\frac{3\pi\alpha^2}{2\varepsilon} \frac{z^2}{\beta_V(z)}\right\} \quad (5)$$

If we require that

$$\frac{b(z = \pm 0.5 \text{ m})}{b(z = 0)} = 10^{-4} \quad (6)$$

as a typical condition for localization of the luminous region, then (5) indicates that as a function of β_V^*, α reaches a minimum of ~0.76 mrad at $\beta_V^* \cong 0.5$ m as shown in Figure 4. For the design value of $\beta_V^* = 1$ m, the condition (6) yields $\alpha = 0.87$ mrad. At $z = 0.5$ m with this crossing angle, the beams are separated by 0.44 mm which corresponds to 6 standard deviations and represents the limit of our knowledge concerning the beam profiles.

The discussion of the preceding paragraph suggests that a nominal crossing angle of 1 mrad is reasonable. The brightness versus longitudinal position given by equation (5) is shown in Figure 5 for $\beta_H^* = \beta_V^* = 1$ m and $\alpha = 1$ mrad. The brightness curve is indistinguishable on the scale of the figure from the pure Gaussian beam shape associated with constant amplitude functions. Numerical integration of equation (5) yields a luminosity of $1.14 \times 10^{34} \text{cm}^{-2}\text{sec}^{-1}$. For constant β, (5) may be integrated directly to give

$$\mathcal{L} = \int_{-\infty}^{\infty} b(z)dz = 2c\left(\frac{I}{ec}\right)^2 \frac{1}{2\sqrt{\pi}\sigma^*\alpha} \qquad (7)$$

and comparison with equation (3) yields the conventional identification[8] of the beam width, w, with $2\sqrt{\pi}\,\sigma$. Use of (7) then leads to the same luminosity: $1.14 \times 10^{34} \text{cm}^{-2}\text{sec}^{-1}$. For comparison, the triangular brightness distribution for rectangular beams of uniform density is also shown in Figure 5.

The beam-beam tune shift under these conditions exceeds the canonical figure of .005. Since we are dealing with Gaussian beams with $\beta_H^* = \beta_V^*$ at the crossing point, we may use the results of Keil, Pellegrini, and Sessler,[9] viz:

$$\delta\nu_H = \delta\nu_0 \left[1 + \frac{1}{(2\pi)^{1/2}} \frac{\sigma^* L}{\beta^{*2}\alpha}\right] \qquad (8)$$

where

$$\delta\nu_0 = \left(\frac{2}{\pi}\right)^{1/2} \left(\frac{I}{ec}\right) \frac{r_p\beta^*}{\gamma\alpha\sigma^*} \qquad (9)$$

is the "short range" tune shift, r_p is the classical radius of the proton, and the factor in brackets represents the enhancement due to the variations in β within the free length L between beam transfer magnets. For the crossing conditions above, $\delta\nu_0 = 0.010$; taking L = 21 m gives

$$\delta\nu = 0.010 \left[1 + 0.54\right] \qquad (10)$$

which is larger than the traditional limit of 0.005. However, on the one hand, this limit is pessimistic and uncertain; on the other, the luminosity calculated above is rather high. The present design provides entirely adequate luminosities at a tune shift of 0.005 and allows improvements should the true limit prove to be higher.

Because of the rather small crossing angle, to keep the "long range" tune shift from becoming excessively large, the beams must be separated at both ends of the crossing region drift space by strong, large aperture common dipoles. For the F/D arrangement, these dipoles can be located immediately next to the focusing quadrupole pairs either on the inboard side or on the outboard side. To investigate the forward secondaries as stated in condition (d), one must detect particles which pass through the apertures of both the dipole and the quadrupole pair. If the dipoles are on the inboard side, they will sweep the charged secondaries onto the yokes of the quadrupoles. On the other hand, if the dipoles are on the outboard side, most of the charged particles can pass through the apertures of the quadrupoles and be swept out of the beam by the following large aperture dipoles into the detectors. Of course, the quadrupole pairs must then be used commonly by both beams. We have adopted this design. Furthermore, in the beam branches going away from the crossing point, the common dipole is followed by a 25 meter free drift length to facilitate placement of detectors.

The high luminosity insertion conforming to the specifications developed above is represented in Figure 6. A tabulation of the insertion elements is to be found in Appendix I, Table 1.

3. High Angular Resolution Insertion

The primary role of this insertion is to permit the study of scattering and production processes at rather small angles. For certain of these processes, the demand on luminosity is rather minimal. The insertion described here has had its parameters selected to make feasible measurements on elastic proton-proton interactions in the angular region where nuclear and coulomb amplitudes are comparable - that is, in the region where $\sqrt{|t|} \approx .045$ GeV/c. At 400 GeV, this corresponds to a scattering angle of 0.1 mrad. We must insure that the angular width of the beam at the crossing point be substantially less than this figure. At the high luminosity intersection described above, $\beta^* = 1$ m and the full angular width of the beam arising from betatron oscillations is 0.32 mrad. Thus, β^* must be raised by at least two orders of magnitude to reduce the angular width of the beam. As in the preceding case, however, we impose the constraint that β should not exceed 1000 m or so at any point in the insertion. We have chosen $\beta^* = 500$ m, yielding $\delta\theta = 0.014$ mrad, and presumed that should further reduction in $\delta\theta$ be necessary, additional improvement can be obtained by reducing the beam emittance ε through scraping.

Because of the momentum spread in the beam, a non-vanishing slope of the vertical dispersion function at the crossing would also contribute to the angular width. For a beam stack with the design momentum width of

$\delta p/p$ = 0.3%, an η' of 0.1 would already result in a contribution to $\delta\theta$ of 0.3 mrad. We have therefore required that η' vanish throughout the region of overlap of the beams. In order to not constrain too severely the design of the insertion, we have not required that η itself vanish. A non-zero dispersion function will contribute to the beam height, hence to the length of the luminous region. This is dealt with in the design feature considered below.

The particle detectors will be located downstream in the outgoing branches and right next to the beams. The small-angle scattered particles will go through all the beam transport elements following the beam optics and be detected within the beam pipe. For a long luminous region, we require that all particles scattered at the same angle over the entire length of the luminous region be focused at the detector; that is to say, we want a parallel-to-point optics from the crossing point to the detector. For β' = 0 at the interaction point, this implies a 90^{o} phase advance for betatron oscillations between these locations. The amplitude function at the detector point should be large enough so as not to put excessive demand on the spatial resolution of the detector. With β^* = 500 m, and a 90^{o} phase advance, corresponding to an angular definition of 0.014 mrad at the crossing point, a β value at the detector of 20 m gives a spatial definition of 1.4 mm at the detector. Several types of detectors exist which can give spatial resolutions far below this value. In addition, the vertical dispersion function at the detector should be made zero so that the spatial definition there would not be degraded by momentum spread.

The crossing angle is chosen to be 10 mrad; this value reflects a compromise between the growth of the beam-beam tune shift with decreasing crossing angle on the one hand, and the lower luminosity and larger total vertical bending required with bigger crossing angles on the other. The beam crossing is taken to be in the downward direction; we assume that for the relatively large crossing angle, this orientation will facilitate the installation of long spectrometers which detect forward going particles. The distribution of vertical bending magnets is adjusted to improve access to the neighborhood of the outgoing branches of the beams.

Since changes in β along the luminous region are clearly unimportant in this case, the luminosity may be calculated from equation (3). For $\beta^* = 500$ m, $\sigma^* = 1.44$ mm at 400 GeV; the luminosity is then $5 \times 10^{31} cm^{-2} sec^{-1}$ with 10 amperes in each beam. This is a very high luminosity for certain of the processes of interest. At $\sqrt{|t|} = 0.045$ GeV, the elastic scattering cross section, $d\sigma/dt$, is about 100 mb/GeV^2. In a $\Delta|t|$ interval of 10^{-4}, the counting rate at $= 5 \times 10^{31} cm^{-2} sec^{-1}$ would be 500/sec - a luminosity of $10^{28} cm^{-2} sec^{-1}$ would surely be adequate. On the other hand, at $\sqrt{|t|} \sim 1$ GeV, higher luminosity is needed. For example, if the cross section at the dip near $\sqrt{|t|} = 1$ GeV remains near 0.03 μb/GeV^2, then in a $\Delta|t|$ interval of 0.05 GeV^2, the peak luminosity would yield ~4 counts per minute. Clearly, somewhere in the region $|t| \sim 5$ GeV^2 counting rates will become unreasonably low.

The linear beam-beam tune shift is 0.022 and is intended to be comparable with that in the high-luminosity insertion; the remarks pertaining to the beam-beam interaction in the discussion of that insertion are applicable here as well.

A high angular resolution insertion meeting the requirements developed above is shown in Figure 7. The parameters of the elements are shown in Table 2 of Appendix I.

4. Phase Adjusting Insertion

The phase adjusting insertion is a sequence of eight quadrupoles occupying 90 m of straight section in each storage ring - in effect, replacing four quadrupoles of the normal lattice. These eight magnets are powered separately from the normal lattice quadrupoles, and as the name of the insertion implies, by varying their excitation, the phase advance of betatron oscillations through the insertion may be adjusted over a range of 100^{o} - from 105^{o} to 205^{o}. The phase advance is the same in both planes of motion. The disposition of elements is shown in Figure 8 and their parameters tabulated in Tables 3 and 4 of Appendix I.

In our provisional lattice, three phase adjusting insertions are included in each of the proton storage rings, so that one is interposed between each pair of proton-proton interaction regions. They play a number of roles in our design procedure. First, they provide a mechanism for tune adjustment, permitting us to retain a 90^{o} phase advance in the normal cells and also enabling us to allow the phase advance through the intersecting insertions to be a free parameter. Second, they allow us to explore the variation of the beam parameters as the intersecting insertions are retuned to operating conditions other than those for which their design was optimized. Third, by manipulating the individual phase adjusting insertions, the effects of chromatic aberration on the luminosity may be decoupled from one intersection to another. We will discuss this latter role in Section F below.

The introduction of phase adjusting insertions is a natural consequence of our modular design procedure, and in these storage rings where straight section space has been reserved for future developments, they are reasonable items to include at this stage. At a more advanced point in our work, it may prove feasible to eliminate one or more of this type of insertion; however, for the present, the phase adjusting insertion introduces an essential element of flexibility into the lattice design.

5. The Non-Colliding Crossing Insertion

With three intersection points where the proton beams collide, there must be at least one more place at which the beams interchange their relative position in the vertical plane without colliding. The two alternatives are an odd or an even number of crossings in each long straight section; we have elected the former. As a consequence, the beam that is at the higher elevation in the north arc is at the lower elevation in the south arc. The injection geometry is then the same for both proton storage rings, and the additional crossing in the west straight section may be of use in reducing backgrounds arising at one high luminosity region due to interactions at the other.

In any event, no matter where located, there is a need for a lattice segment which interchanges the relative up-down position of the two beams.

The non-colliding crossing is shown in Figure 9. Note that this insertion is of the symmetric type, in contrast to the others. Arranging the crossing point to occur at the mid-point of a quadrupole in the normal sequence maximizes the drift on either side so that the beams are more readily separated before encountering the nearest lattice elements.

E. The Normal Cell

1. Layout

The normal cell resembles that of the main accelerator - a straightforward FODO cell with a length of 60 m. The provisional disposition of quadrupole and dipole magnets is shown in Figure 10, and listed in Table 6 of Appendix I. As noted in Section C, the phase advance of betatron oscillations through the normal cell is nominally 90°.

The straight section of length 3 m in each half cell is intended to accommodate vacuum equipment, correction and compensating elements, and beam monitoring devices. At this early stage in the design procedure, we do not feel that a 3 m allowance for these items is excessive; the rapidity with which components populated the 2 m normal cell straight sections of the main accelerator as it was brought into operation suggests that a somewhat greater space will be needed in the storage rings, where the demands on the corresponding systems are greater than in the conventional synchrotron. Our current prejudice is that such functions as chromaticity compensation, nonlinear resonance correction, and beam steering be accomplished by elements located in these straight sections rather than by separately excited windings of the main dipoles and quadrupoles of the cell. Not only is the design and fabrication of the main magnets thereby simplified, but overall reliability will likely be improved. The other intermagnet gaps are quite small - 0.4 m between the magnetic ends. We assume that this is an adequate space for the physical magnet ends and interconnections between magnets, and that a cold-bore vacuum system will not require a pumping station between each pair of magnets. Clearing electrodes may also be found in these gaps, though it is possible that they may be incorporated in the magnet vacuum chamber.

In both the north and south arcs of the storage rings, the 3 m straight sections are to the west of the dipole magnets of each half cell. This arrangement enables the injection elements to be identically situated for both rings.

2. Comments on Magnets and Vacuum System

Though the design of magnets is not included in this phase of the study, a few remarks are in order here to indicate the sort of magnets that we have in mind while selecting dimensions and intermagnet spacings for the calculations of this report.

We visualize the 18 kG dipoles of the normal cell as superconducting "window-frame" magnets having an aperture which is approximately square. They may be characterized as a low field version of the magnets developed by Danby and collaborators at BNL.[10] Even with a gap as large as 10 cm, the outline of the steel yoke need be no larger than an ordinary 8½" x 11" sheet of writing paper. The superconducting coil fits as closely as possible to the cold steel frame to minimize the field inhomogeneities arising from wire placement errors. Corresponding magnets of the two proton storage rings are in a common cryostat. We have taken the vertical separation between proton beams to be 30 cm. By extension of the roughly square steel geometry, the quadrupoles are envisioned to be of the Panofsky-Hand configuration.

As implied in the layout of the normal cell, we have assumed that a cold bore vacuum system will prove to be feasible, with a cryopumping beam tube replacing most of the vacuum stations of the conventional room temperature vacuum system. Recent studies of the cold bore approach have been encouraging;[11,12] of course, there is as yet no experience with such systems in particle accelerators.

Whatever the type of vacuum system, there is no reason to believe that the pressure requirements will be any less stringent than those in the ISR. Thus, at liquid helium temperatures, the pressure should not exceed some 5×10^{-13} Torr (at room temperature, the same particle density would be associated with a pressure of 3×10^{-11} Torr). And despite the pumping speed offered by the cold surfaces, the high desorption coefficients of helium and hydrogen adsorbed in sufficient quantity indicate that surface cleanliness will remain a consideration. Surface coverages are limited to about 10^{-3} of a monolayer for He and 0.3 of a monolayer for H_2.[12]

3. Aperture

The beam pipe is taken to be circular in cross section with an inner diameter of 7.6 cm (3 inches), primarily for reasons of vacuum stability. Benvenuti[12] has concluded that, based on current knowledge of surface coverages and desorption coefficients, a vacuum chamber of this size would be adequate for the maintenance of vacuum stability in the presence of a 10 ampere circulating current.

The injection and stacking procedure outlined in Section G below implies the need for a good field region some 5 cm in horizontal extent, at least in the injection region where the momentum dispersion function is a maximum. If the steel and coils forming the inner boundaries of the magnet aperture describe a square 10 cm on a side, a somewhat larger region of good field quality can likely be achieved to make allowance for orbit distortions, beam manipulation, and less rapid degradation of luminosity at lower energies.

The use of a circular beam pipe - particularly if it is made of a material such as aluminum which has a high conductivity at low temperature - has the consequence of removing certain of the high current phenomena from contention as aperture determining factors.

As an example, consider the single beam incoherent tune shift. Strictly speaking, in treating the image currents in the square steel boundary, one should sum the appropriate series for that geometry. In order to estimate the tune shift in a straight-forward way, let us treat the magnet boundary as also circular, with the same radius as the beam tube. Though approximate, this procedure insures that the leading terms in the series expansion of the magnetic image fields be of the proper order. The procedure is correct for magnets having circular steel boundaries, as in the ISABELLE design,[13] with of course the replacement of the beam pipe radius by the steel radius in the magnetic sum. Then, for a particle describing betatron oscillations about an orbit a mean distance x in the horizontal plane from the center of the beam pipe, in the presence of a ribbon-like stacked beam located in the median plane, the image contribution to the tune shift is

$$\delta\nu_y = -\delta\nu_x = \frac{r_p N R}{\gamma \pi \nu} \left(1 + \frac{\rho}{R}\right) F$$

where r_p is the classical radius of the proton, N is the total number of protons in the beam and F is given by

$$F = \frac{b^2}{4a} \sum_{n=3}^{\infty} \frac{1}{n} x^{n-3} \left\{ \left(\frac{x_s+a}{b^2}\right)^n - \left(\frac{x_s-a}{b^2}\right)^n \right\}$$

b = radius of beam pipe

a = half width of stacked beam

x_s = distance of center of stack from center of the beam pipe

Each term in the sum contains $2a/b^2$ as a factor, so F actually contains neither negative powers of a nor positive powers of b. The leading term varies as the inverse fourth power of b, rather than the $1/b^2$ dependence of the plane-parallel configuration. As a result, the tune shifts tend to be small. With a centered 10 ampere stack, the tune shift due to images at the center of the chamber is 6×10^{-4}, and the difference in tune between the injected beam and a particle at the middle of the stack is $\sim10^{-5}$. Even with the stack off-center, the tune shifts remain relatively small. For instance, if during the injection process, a 5 ampere stacked beam is located with one edge at the center of the beam pipe, the tune shift at that edge would be 3×10^{-4} and the injected beam would differ in tune by only 7×10^{-5} from the most distant particles in the stack.

As a second example, let us use the formula stated by Keil[14] to estimate the degree to which resistive wall effects are of concern. In the case of the transverse resistive wall instability, the tune spread required to provide Landau damping is

$$\delta\nu = \frac{2}{\pi\nu}\left(\frac{Z_0}{\sigma}\right)^{1/2}\left(\frac{Ie}{\gamma m_p c^2}\right)\frac{R^{5/2}}{b^3(n-\nu)^{1/2}}$$

With $\nu \approx 35\frac{1}{4}$, $n-\nu \approx 0.75$ for the lowest unstable mode. If we take for the conductivity, σ, that of aluminum at 4.5^0K, $\delta\nu \simeq 2 \times 10^{-5}$. The momentum spread necessary for longitudinal stability can be estimated from

$$\left(\frac{\delta p}{p}\right)^2 > \left(\frac{Z_0 R}{\sigma}\right)^{1/2} \frac{e}{\gamma m_p c^2} \frac{I\nu^2}{b} \quad .$$

This condition is most restrictive in the initial stages of formation of the beam stack when $(\delta p/p)/I^{1/2}$ is smallest. For a single injected pulse, the current is 0.07A; then the criterion above gives $(\delta p/p) > 8 \times 10^{-6}$ whereas the fully-debunched momentum spread of a single pulse would be 1.3×10^{-5}.

The discussion of the preceding two paragraphs is not meant to imply that we expect intensity dependent electromagnetic effects to be of little concern. Rather, the point is that by a suitable choice of wall geometry and material in the normal cells, this large portion of the storage rings will be relatively innocuous as a contributor to these phenomena.

F. Consequences of Low Periodicity

Traditionally, accelerator designers have favored lattices consisting of a reasonably large number of identical periods in order to reduce the density of resonances arising from systematic errors in magnet construction and from other sources associated with the periodicity of the magnet ring. Thus, for example, there are six superperiods in the Fermilab main accelerator and twelve in the Brookhaven AGS. Single period designs, such as the Cornell 12 GeV electron synchrotron, have been the exception rather than the rule.

Present storage ring designs tend to have lower rotational symmetry than the synchrotrons due to the introduction of the various experimental insertions. At the same time, these rings contain features, such as beams containing a relatively broad momentum spread and regions where the amplitude functions become very large, which can make periodicity-associated effects of more concern than in the synchrotrons. However, in contrast to the accelerators, a high periodicity conflicts directly with the intended use of the storage rings and so the consequences of a low symmetry structure must be examined.

In a ring containing N superperiods, one-dimensional structure resonances may appear at intervals in tune of N/k, where k = 1,2,3, ... etc. is the order of the resonance. Including both transverse degree of freedom, the same is true for the spacing of sum resonances ($i\nu_H + j\nu_V = k$) along the main diagonal of the tune diagram where $\nu_H = \nu_V$; off of the main diagonal, the spacing diminishes due to the fanning out of resonance lines of given order from their common intersection point on the diagonal. For our lattice, N = 1; therefore potential structure resonance lines coincide with imperfection resonance lines.

There are a number of measures that may be taken to reduce the effects of systematic errors. Considering that there are 784 bending magnets in the ring, these dipoles constitute the most likely source of odd-order resonance driving terms. During the development of magnets, as an appreciation is gained of the systematic higher order multipoles in their fields, some redistribution of dipoles in the rings can be made to reduce the strength of certain resonances in the working region of the tune diagram. Though admittedly of limited value, this may still be a useful exercise. A potentially more effective step is to limit the range of tunes explored by the beam through the reduction of chromaticity. This implies a reliance on feedback systems to provide the primary stabilization against coherent instabilities rather than the Landau damping consequent to non-zero chromaticity. Finally, we note the substantial space allowance in the lattice for correction and compensation magnets. A major motivation for the reservation of a 3 m drift space in the normal cell has been to permit the addition of a suitably diverse set of multipole elements.

A quantitative examination of many of the low periodicity effects must be deferred until a later phase of the study. One of these effects, however, is of such magnitude and so immediately predictable that it requires attention in this first pass through the design; we refer to the half-integral stop bands arising from chromatic aberration in the quadrupoles.

The standard matching procedure for a ring with a complex lattice having a variety of insertions leads to a system free of stopband influences for one given momentum. In a conventional synchrotron, the off-momentum mismatch is relatively unimportant; in a storage ring, with its greater demands on momentum aperture and more exotic insertions, chromatic aberration in the quadrupoles becomes much more of a "first order" problem.[15]

In addition the chromaticity of the lattice, having the same origin, must be controlled to adjust properly the working line in the tune diagram. For both functions, sextupole fields must (in effect) be added to quadrupoles to modify their chromatic aberration by virtue of the momentum dispersion of the orbit. Clearly, the sextupoles should be arranged in such a way that third integral resonances are not excited.

An obvious way of accomplishing this is to compensate the chromatic aberration of each quadrupole by adding to it a sextupole field given by

$$B'' = B'/\eta .$$

However, a major source of the aberration effects is in the insertions where it is desirable to have $\eta = 0$, thereby precluding this scheme of direct compensation.

That the insertions, and particularly the high luminosity insertions will contribute significantly in this regard may be inferred as follows. The increment to the chromaticity ξ linear in $\delta p/p$ from an insertion may be written

$$\Delta\xi \equiv \delta\nu/(\delta p/p) = -\frac{1}{4\pi}\int \beta(z)K(z)dz \quad ; \quad K = \frac{B'}{B\rho}$$

$$= -\frac{1}{4\pi}\int (\alpha' + \gamma)dz$$

where α, β, and γ are the usual Courant-Snyder parameters. Since α is required to be the same at the ends of the insertion, the first term in the integral vanishes and

$$\Delta\xi = -\frac{1}{4\pi}\int \gamma dz$$

So, the high luminosity insertions wherein γ becomes large have disproportionate leverage on the chromaticity, and by extension, on other chromatic aberration effects, compared to the fraction of the periphery of the ring occupied by these insertions, yet it is precisely here that it is most inconvenient to accommodate compensating sextupoles.

On the other hand, the normal cells of the semi-circular arcs present an attractive location for sextupoles, where the dispersion function is inherently non-zero. The $\pi/2$ phase advance per normal cell provides a natural means for chromatic aberration compensation without introduction of third-integral resonance driving terms. For, note that a group of four sextupoles of the same strength located at corresponding positions in successive cells contributes to the chromaticity without affecting the off-momentum stopbands or exciting third-integral resonances. A number of such groups, located near both the F and D quadrupoles, can adjust the chromaticity in both planes of motion. Similarly, groups of four sextupoles alternating in sign will influence the off-momentum stopbands without affecting the chromaticity or yielding third-integral driving terms.

We have applied the above prescription to our lattice. In Figure 11, we show the tunes in the horizontal and vertical planes without the introduction of sextupoles. As anticipated, substantial stopbands appear at the neighboring half-integral tune values, and the tune spread across the 0.3% in momentum width stack is slightly in excess of 0.2. If we place 80 sextupoles at the horizontally focusing quadrupoles with $B''\ell$ = 645 kG/m, and 80 sextupoles at vertically focusing quadrupoles with $B''\ell$ = 1290 kG/m in the normal cells of the north and south arcs, we obtain the tune versus momentum plots shown in Figure 12, wherein the tune spread has been reduced by somewhat more than a factor of 100. The graphs suggest that the chromaticity can be controlled adequately by this means.

The (by now) remote half integral stopbands demonstrate their presence by a momentum dependent "beat factor" in the amplitude function, which can lead to a reduction in luminosity in one or more of the crossing regions in comparison to that expected from the perfectly matched insertions. Actually, all that need be achieved is that the phase of the beat factor need be such that the values of the amplitude function at the crossing points not be significantly increased. Elsewhere, the amplitude functions must only remain within reason. We have found that the global compensation associated with sextupoles alternating in sign mentioned above may not be necessary; rather, the phase adjusting insertions can be set to compensate adequately for the beat factor. That this is so is in part a characteristic of our particular lattice. Since the high luminosity insertions are the major contributors to the effect and they are located close to each other, a suitable tune of the phase adjusting insertion between these can significantly reduce the amplitude of the wave in $\delta\beta/\beta$ throughout most of the ring. Figure 13 illustrates two settings of the phase adjusting insertions, one of which yields a reasonably insensitive dependence of the amplitude function on momentum at the intersection points. Only one of the high luminosity regions is represented in the Figure; the behavior of the amplitude function at the other is similar.

Our conclusion from the discussion of this section is that the chromatic aberration effects of the one-fold periodicity lattice can certainly be accommodated. With reasonable space allowed for correction magnets, other consequences of the low rotational symmetry are not likely to become performance limitations. We cannot emphasize the point of the preceding sentence too strongly. A versatile and easily manipulated set of correction magnets is an essential system in the storage rings that we outline here. Further study will aid in defining the scope of this system. However, we doubt that the correction requirements can be fully analyzed without operating experience, and we feel that an early reduction in the space allocated for this purpose would prove to be a very poor economy indeed.

G. Injection and Stacking

1. Geometry of Injection Beam Transport Lines*

Fast single-turn extraction from the main ring will be accomplished at straight sections B and C in a fashion identical to that now used at straight section A. As at straight section A, the extracted beam at B and C will be directed at an initial angle of 1.26° with respect to the orbit in the straight sections. From B0 and C0 station marks, we project each beam line 300 feet to allow space for focusing and matching elements and then bend at a 2700 foot radius away from the main ring through an angle of 5.22°. At the end of the 300 foot straight portion, the separation between the extracted beam and the main ring is about 12 feet so a separate tunnel can be started. The succeeding bend is to minimize the portion of the main ring tunnel that must be uncovered for the new construction. The bend radius of 2700 feet corresponds to a 90% packing of dipoles and so implies a quadrupole spacing about a factor of two greater than that in the normal cell of the main accelerator. The choice of 5.22° bend angle is arbitrary but reasonable and convenient in that it brings the beam from B0 to a direction perpendicular to the east site boundary, and the beam from C0 to an angle of -60° with respect to that boundary. We refer to the points we arrived at by this geometrical construction as the "extracted beam points"; they define the starting positions and directions of the injection transports to the storage rings.

* English units are used in this subsection to facilitate reference to existing site maps and drawings.

As described in Section C, the injection point in the storage ring is at the downstream end of a half cell containing no bending magnets. The injection aim point is taken to be 197 feet (one normal cell) in the upstream direction on a line tangent to the orbit at the injection point. The basis for this selection of the aim point is that the injection will be through a series of Lambertson septum magnets which deflect the beam downward into the ring. These septum magnets require a space of about one-half normal cell and another half-cell is needed for optics matching elements.

The extracted beam points and injection aim points must be connected by beam transport lines, made up of straight sections and curved portions whose radius of curvature should not be smaller than 2700 feet in accordance with our design procedure. For the particular locations of the injection aim points that we have selected, the connecting beam transport lines are as follows: for the transport line to Ring I (clockwise) a straight section of length 220 feet connects the extracted beam point at B to a 74.4° bend to the north injection aim point, and for Ring II (counterclockwise) a straight section of length 477 feet connects the extracted beam point at C to a 14.4° bend to the south injection point. This transport system would be composed of conventional magnets since they need be powered only during storage ring filling operations.

2. Injection and Stacking in the Storage Rings

Momentum stacking has proved to be very successful at the ISR, and we follow the same procedure for POPAE.

Prior to the arrival of each beam burst from the main accelerator, the two pulsed kicker dipoles mentioned in Section C perturb the injection orbit outward to the outside of the injection septum, so that the beam arriving from the main ring finds itself on the (perturbed) closed orbit appropriate to its momentum. The duration of the beam burst is 21 μsec; the kickers then have 7 μsec in which to turn off before the next passage of the injected beam which will be along the unperturbed closed orbit on the inside of the injection septum. After the injected beam is decelerated to the stack, the kickers are again turned on and the injection orbit moved to the outside of the septum awaiting the arrival of the next beam burst from the main ring. The turn-on of the kickers could be relatively slow.

Both the turn-on and the turn-off of the two kickers must be identical but with the downstream kicker delayed by the beam transit time of 1.2 μsec between the two kickers. Inequality of the two kickers or error in the delay times tends to leave a residual betatron oscillation in the stacked beam, thereby diluting its betatron phase space density. However, the required precision is not difficult to attain. The injection scheme proposed here employs full-aperture kickers but avoids the need for the rather complicated moving kicker-shield used for the ISR.

A 10 ampere beam in one of the proton storage rings corresponds to 1.8×10^{15} protons which requires 180 pulses from the injector each containing 10^{13} protons, if there is no loss during transfer. Assuming that during stacking the momentum phase-space density is diluted to 75%, the momentum width of the stack would be 180/0.75 = 240 times the debunched momentum width of a single pulse. A longitudinal emittance per rf bunch of ε_s = 0.1 eV·sec translates into a fractional momentum spread at 400 GeV of

$$\frac{\delta p}{p} = \frac{hc}{2\pi RE}\,\varepsilon_s = 1.3 \times 10^{-5} \qquad \begin{array}{l} h = \text{harmonic number} \\ 2\pi R = \text{ring circumference} \end{array}$$

when debunched. The momentum width of the stack would then be 0.3%.

At the injection septum, the momentum dispersion function is ~4.5 m leading to a contribution to the physical width of the stack from momentum of 14 mm. The horizontal amplitude function at the position is ~100 m, so for our emittance of $\pi/40$ mm-mrad at 400 GeV, the beam width from betatron oscillations is 3 mm. The physical width of the full stack is then about 17 mm.

We take the distance between the "edges" of the injected and stacked beams to be 10 mm. The distance from the center of the injected beam to the center of the nearest pulse in the stack is then 13 mm, or 0.3% in momentum. The initial pulse will be decelerated by 0.6% x 400 or 2.4 GeV to begin formation of the stack. Subsequent pulses will be decelerated through the same interval to stack on the "top." "Top" and "bottom" here refer respectively to momentum edges of the stack farthest and nearest to the injection momentum.

To estimate the stacking efficiency, defined as the ratio of the phase-space density of the stacked beam to that of the injected beam, we may use the phenomenological formula[16]

$$\text{efficiency} = \left[1 + \frac{2 \sin \phi_s}{3\alpha(\phi_s)\sqrt{n}}\right]^{-1}$$

where ϕ_s is the synchronous phase of deceleration through the stack, n is the total number of pulses stacked, and $\alpha(\phi_s)$ is the ratio of the moving bucket area at ϕ_s to the stationary bucket area for the same voltage. The smaller ϕ_s, the higher the efficiency. On the other hand, smaller ϕ_s leads to lower rf voltage and longer deceleration time, once one adds the requirement that the bucket be fit tightly around the beam bunch. ¯ addition to stacking efficiency the longitudinal beam stability condition requires low shunt impedance of the rf cavity, hence also favors low ϕ_s.

Therefore, a compromise must be made between the desires of shorter deceleration time on the one hand and higher stacking efficiency and lower cavity voltage on the other. For this design, we have selected $\phi_s = 50^o$ as a reasonable value. Then for the bucket area of 0.1 eV·sec, the deceleration rate is 0.24 GeV/sec, the cavity voltage, V, is 8.9 kV, and the stacking efficiency is 75% as assumed earlier. The time required for stacking each injected pulse will be 10 seconds.

Prior to extraction from the main accelerator, the bunches should be tailored to the appropriate size and shape for the storage ring. The same ϕ_s in the main ring will insure that the bucket shape will be identical in the two rings provided we match the bucket areas. This requires that $\frac{V}{h}\left(\frac{1}{\gamma_t^{\,2}} - \frac{1}{\gamma^2}\right)^{-1}$ (γ_t = transition energy in the units of mc^2) be the same for both rings. This condition gives a main ring cavity voltage of 14 kV and, together with $\phi_s = 50^o$, a deceleration rate of 0.54 GeV/sec.

We could consider tailoring the beam bunches to the appropriate size and shape in the storage ring after transfer and concurrent with deceleration but before arrival at the "bottom" of the stack. But it is inevitable that some beam will be lost during the size-and-shape tailoring. In the main ring when the tailoring is done on the controlled "flat-top" and not "on-the-fly" the beam loss may well be less. In any case beam loss is less harmful in the main ring than in the storage rings where experiments are performed internally in the rings, hence demand a high degree of radiation cleanliness. It is also possible to stack on the "bottom." In this manner, one may be able to reduce slightly the stacking time of 10 seconds, but with additional demands on the programming of the frequency and voltage of the storage ring rf. In the scheme described, the cavity voltage is fixed at 8.9 kV during stacking, and the frequency modulation is identical for every pulse from 53,104,924 Hz at injection to 53,105,329 Hz at stacking, with a required precision of ± 3 Hz.

Although the frequencies of the accelerating systems of the main ring and the storage ring can be locked before transfer, it is difficult to insure proper phasing of the beam bunches after injection because of the large distance between the two rings. The injected beam itself, however, can be used to establish the phasing on each pulse. During the first passage of the injected beam at the rf station, the cavity voltage is off, and by sensing the bunch timing, the cavity voltage is turned on at the proper phase in the 7 μsec time interval between the end of the injected pulse and the beginning of the second passage of beam through the rf cavity. Since the rf system must already be able to suppress empty buckets in order to avoid unnecessary dilution of the stack, this added bit of gymnastics introduces no additional demand.

H. Beam Extraction

There are three circumstances under which the beam will leave one of the storage rings, which can be characterized as (1) uncontrolled and unplanned, (2) controlled and unplanned, and (3) controlled and planned. By the first we mean the disaster in which the beam somehow encounters the wall - with over 100 MJ of stored energy in a 400 GeV 10 ampere beam, protective devices must be installed with sufficient redundancy to insure that this is a very rare event indeed. In the first section of this chapter, we remarked that the kinetic energy of the beam may conceivably represent a potential limit to the performance of the storage rings. It is to the degree that one is unable to prevent unintentional and uncontrolled beam extraction that the beam energy is such a limiting factor.

In the second category, we include those circumstances in which a sudden malfunction of a system or a growing disturbance of the beam is detected and the protective devices are activated to extract the protons into a beam transport culminating in a dump. In this case, extraction will need to be fast and comparable with the period of a single turn, though we assume that a period of time corresponding to some tens of turns will be available for beam manipulation prior to the onset of extraction. Excluding the beam dump itself, the total energy of the beam is not a limitation. Rather, the finite time (of much less than the period of revolution) during which the beam is swept across an extraction septum implies a possible limit on linear energy density rather than on total stored energy.

The third category is - hopefully - the normal mode of beam extraction, accomplished frequently during studies of machine behavior or at larger time intervals to terminate physics runs of a number of hours duration. There is no need for urgency in this circumstance. In principle, a slow resonant mode of extraction could be employed were it to prove advantageous. For the present, we will assume that a single turn fast extraction system will be used for both of the "controlled" cases.

The dispersion transition sections described in Section C provide space for the extraction equipment, as sketched below. The beam is bumped downward

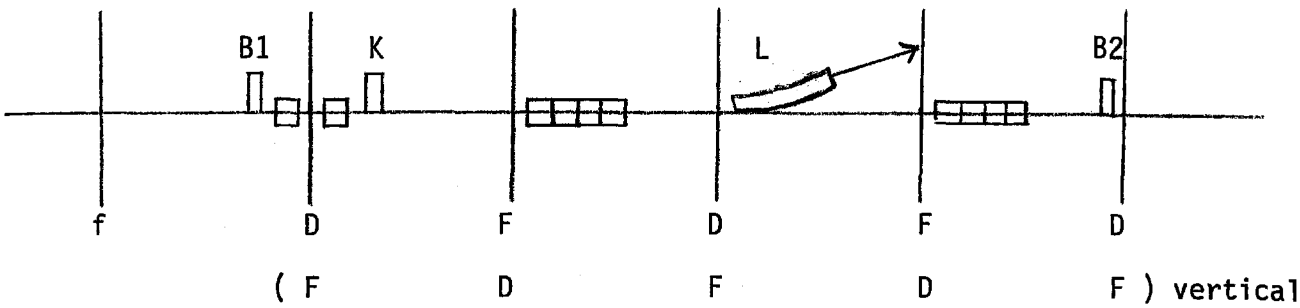

into the groove of a Lambertson septum L by bump magnets B1 and B2, then kicked across the septum by a full aperture kicker K. The Lambertson then deflects the beam in the horizontal plane. If the Lambertson magnet is 14 m in length at a field of 10 kG and is followed by a 14 m drift space, the horizontal deflection of the beam at the position of the next normal cell quadrupole will be 22 cm, which should be ample clearance.

In order to bump the beam 30 mm from the aperture center line, B1 and B2 must yield angular deflections of 0.36 mrad and 0.30 mrad respectively. These are relatively small magnets: at 4 kG, B1 is 1.2 m in length and B2 1.0 m.

At the upstream end of the Lambertson, the beam is almost round, for β is a maximum in the vertical plane, ~100 m, and the momentum dispersion function is only 0.8 m. For a stack of width 0.3% in momentum, and using the emittance of $\pi/40$ mm mrad at 400 GeV, the beam is 3.2 mm high and 3.7 mm wide. If we take the thickness of the septum to be 1 mm, then the kicker must yield an 8 mm deflection at the Lambertson. Since the kicker is located nearly $\pi/2$ in phase upstream at a point of maximum β, it must produce an angular deflection of 0.08 mrad.

That the kicker have a fast rise time is of prime importance in reducing extraction losses on the septum. The present fast extraction kicker in the main ring, which is 6 m in length and produces an angular deflection slightly larger than required here, has a rise time of 1/3 μsec. Shorter rise times would have been possible at greater expense, but were unnecessary in that application. We will take 100 nsec as the rise time; even shorter rise times may be contemplated[17] though associated with rapidly increasing costs and, in all likelihood, operational problems. With 100 nsec within which the beam is deflected 8 mm, the septum will in effect intercept the entire 10 ampere current for 12 nsec, corresponding to an incident energy of 5×10^4 joules. This amount of energy deposition is, we feel, near a tolerable level, though further study is clearly needed. It should be noted that, in addition to further reduction in rise time, it is also possible to install two such extraction systems in each storage ring - a step that may be advisable for reasons of reliability in any case.

The design of the beam dump is apt to be a non-trivial problem - we have not as yet devoted any time to it.

REFERENCES

1. Design Report - National Accelerator Laboratory, edited by F. T. Cole, January 1968.

   "The NAL Accelerator and Future Plans" presented by P. J. Reardon, Proceedings of the IXth International Conference on High Energy Accelerators, SLAC 1974, p. 7.

2. T. L. Collins, "An Electron Target for NAL," 1973 Summer Study, Vol. 2, page 97.

3. L. C. Teng, "Parameters for 1 TeV^2 P-P Storage Rings," Fermilab Technical Memorandum 475, 13 February 1974.

4. "Proton-Proton Colliding-Beam Storage Rings for the National Accelerator Laboratory," 1968 Design Study, edited by L. C. Teng.

5. W. W. Lee and L. C. Teng, "Insertions for Colliding-Beam Storage Rings," Proceedings of the IXth International Conference on High Energy Particle Accelerators, SLAC 1974, page 599.

6. M. J. Lee, W. W. Lee and L. C. Teng, "Magnet Insertion Code (MAGIC)," 1973 PEP Summer Study.

7. K. L. Brown, F. R. Rothacker, D. C. Carey, and Ch. Iselin, "TRANSPORT - A Computer Program for Designing Charged Particle Beam Transport Systems," NAL-91, or SLAC 91, or CERN 73-16, March 1974.

8. M. Sands in "Physics with Intersecting Storage Rings," editor B. Touschek, Academic Press (1971).

9. E. Keil, C. Pellegrini and A. M. Sessler, "Tune Shifts for Particle Beams Crossing at Small Angles in the Low-β Section of a Storage Ring," CERN Report CERN/ISR-TH/73-44, September 1973.

10. See, for example, J. Allinger, G. Danby, B. DeVito, S. Hsieh, J. Jackson, A. Prodell, "Studies of Performance and Field Reproducibility of a Precision 40 kG Superconducting Dipole Magnet," IEEE Transactions on Nuclear Science, Volume NS-20, 678 (1973).

11. R. Avery et al, "Experimental Superconducting Accelerator Ring (ESCAR)," Proceedings of the IXth International Conference on High Energy Particle Accelerators," SLAC 1974, page 179.

12. C. Benvenuti, "Vacuum System for Proton Storage Rings Equipped with Superconducting Magnets," FERMILAB-74/109, December 1974.

13. "A Proposal for Construction of a Proton-Proton Storage Accelerator Facility ISABELLE," edited by H. Hahn and M. Plotkin, BNL 18891, May 1974.

14. E. Keil, "Perspectives on Colliding Beams," Proceedings of the IXth International Conference on High Energy Particle Accelerators, SLAC 1974, page 660.

15. M. Month, "Effects of Matched Insertions in Low Periodicity Lattices," Particle Accelerators 3, 183 (1972).

16. M. J. de Jonge and E. W. Messerschmid, "Measurements of Stacking Efficiency in the CERN Intersecting Storage Rings (ISR)," IEEE Transactions on Nuclear Science, Vol. NS-20, 796 (1973).

17. Private Communications from J. C. Schnuriger, CERN/ISR, and J. D. McCarthy, Fermilab.

Figures and Tables

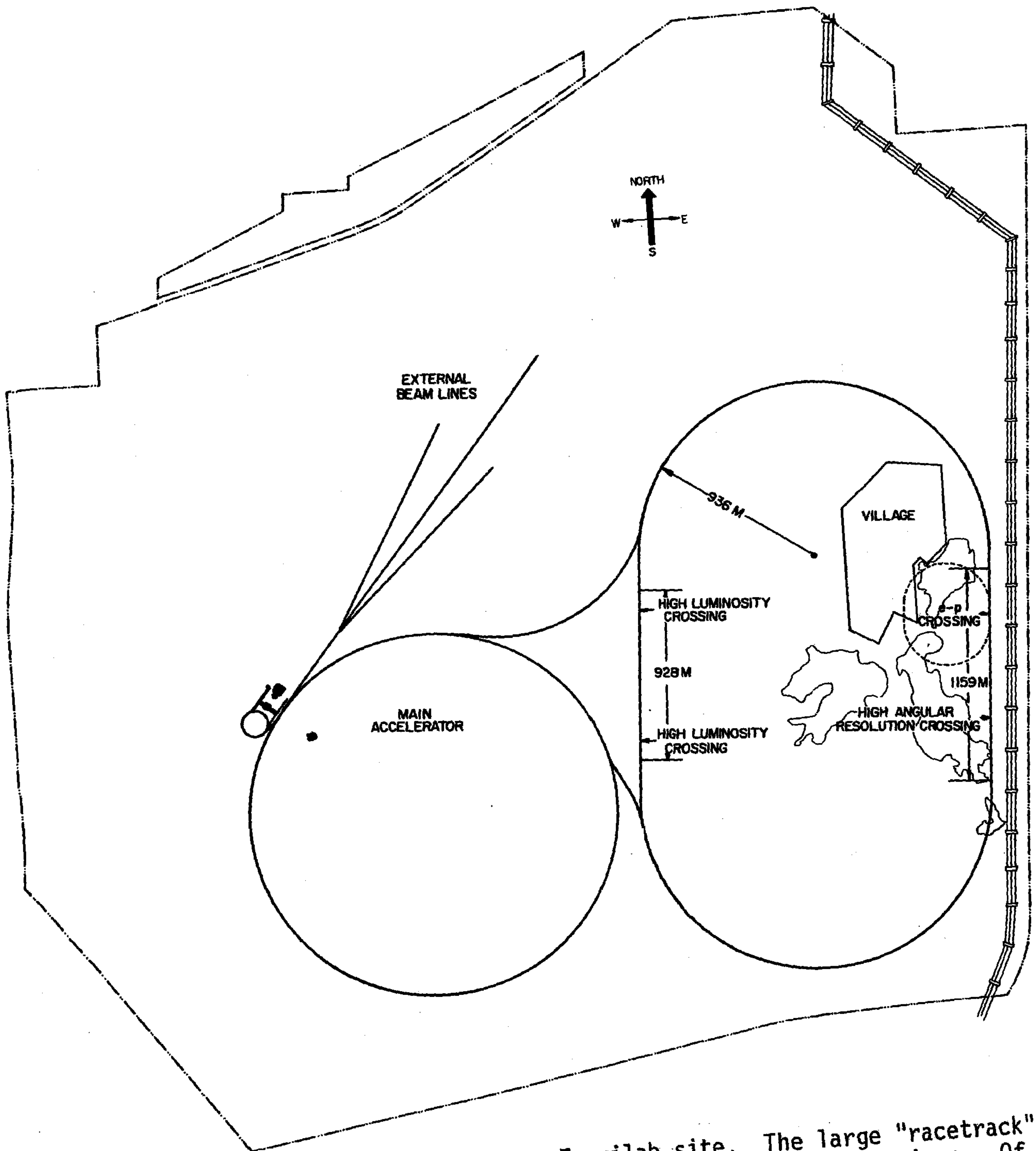

Fig. 1. Layout of POPAE on the Fermilab site. The large "racetrack" represents an enclosure containing the two proton storage rings. Of the two alternatives considered for the electron ring, one - the 20 GeV case - would share the same enclosure as the proton rings. The second possibility - a 10 GeV electron ring - is shown as the small dashed oval.

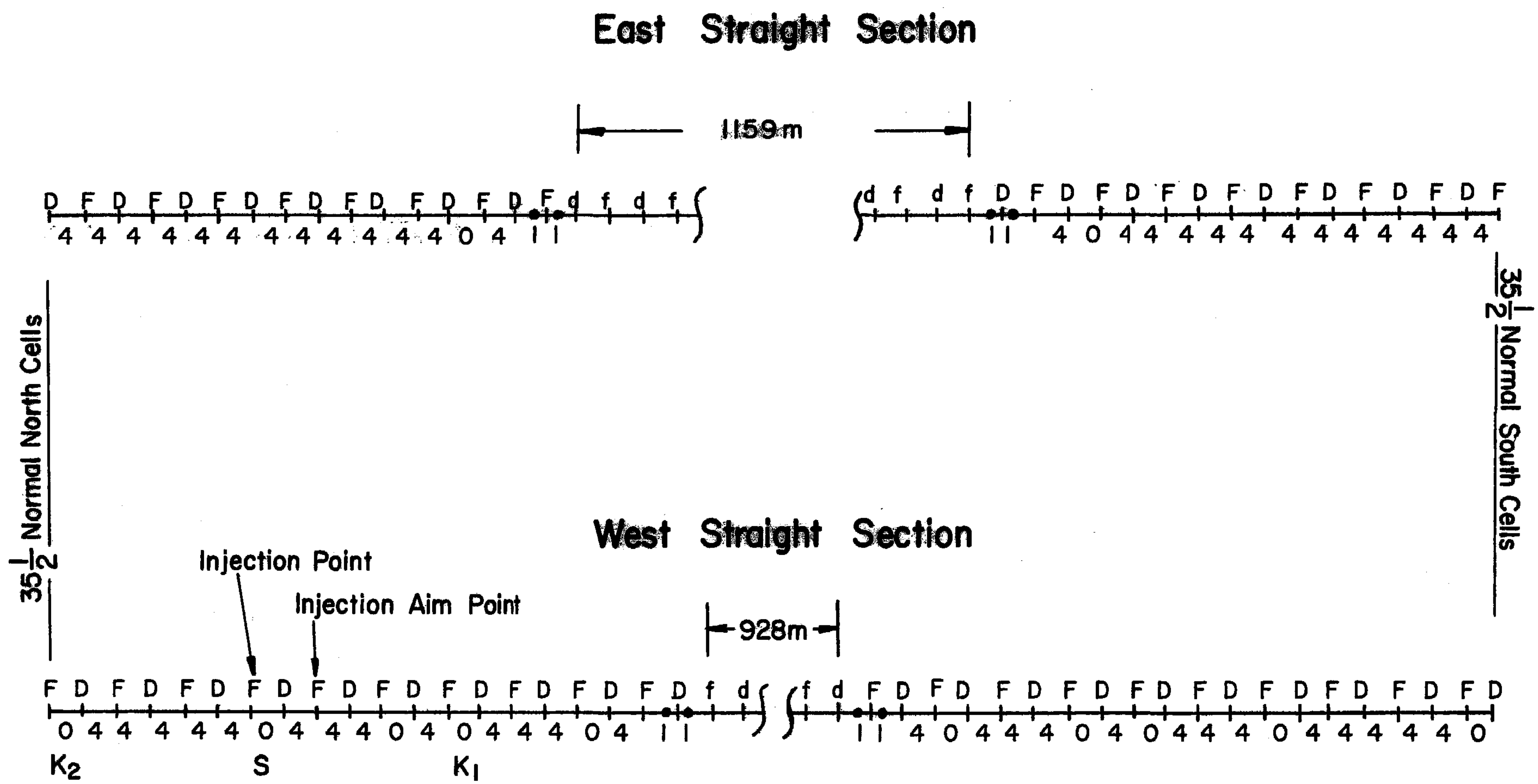

Fig. 2. Schematic of lattice for Beam 1 (clockwise). Lattice for Beam 2 is obtained by interchange of F, D designations, and by north-south reflection of the injection sequence. Quadrupole focusing character is referred to horizontal plane. Numerals below half-cell intervals indicate number of dipoles in half-cell.

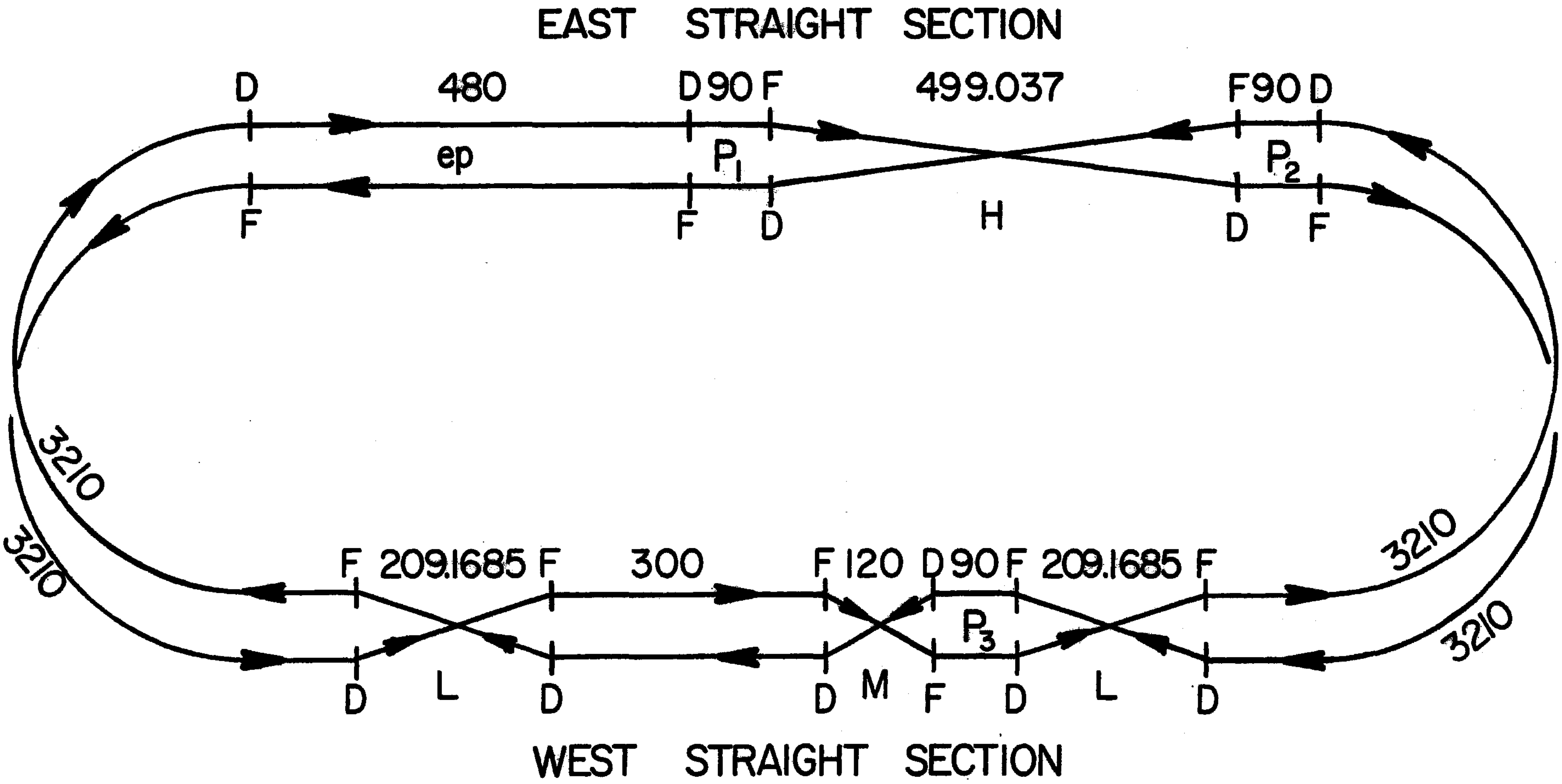

Total curved	-	6420
East S	-	1159.037
West S	-	928.337
		8507.374 = central orbit

Injection orbit = 8507.422 = $\frac{1507}{1113}$ x 6283.185307

Fig. 3. Composition of long straight sections. Insertions are: L - high luminosity, H - high angular resolution, P - phase adjusting, M - non-colliding crossing. All distances are in meters.

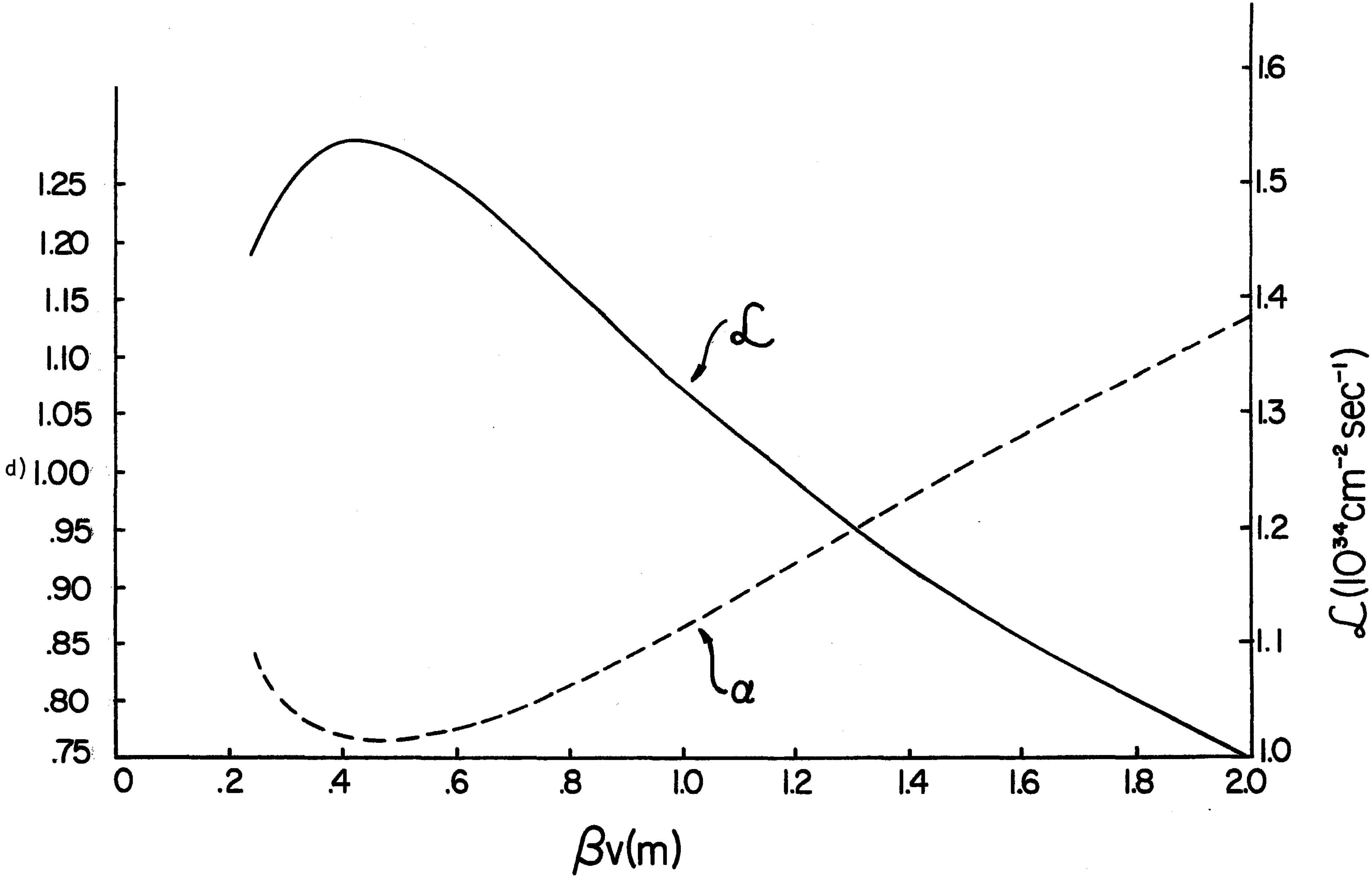

Fig. 4. Luminosity, $\mathcal{L}$, and crossing angle in vertical plane, α, versus β_v^* with the condition imposed that the luminosity per unit length diminish by a factor of 10^4 at a distance of 0.5 m from the center of the crossing.

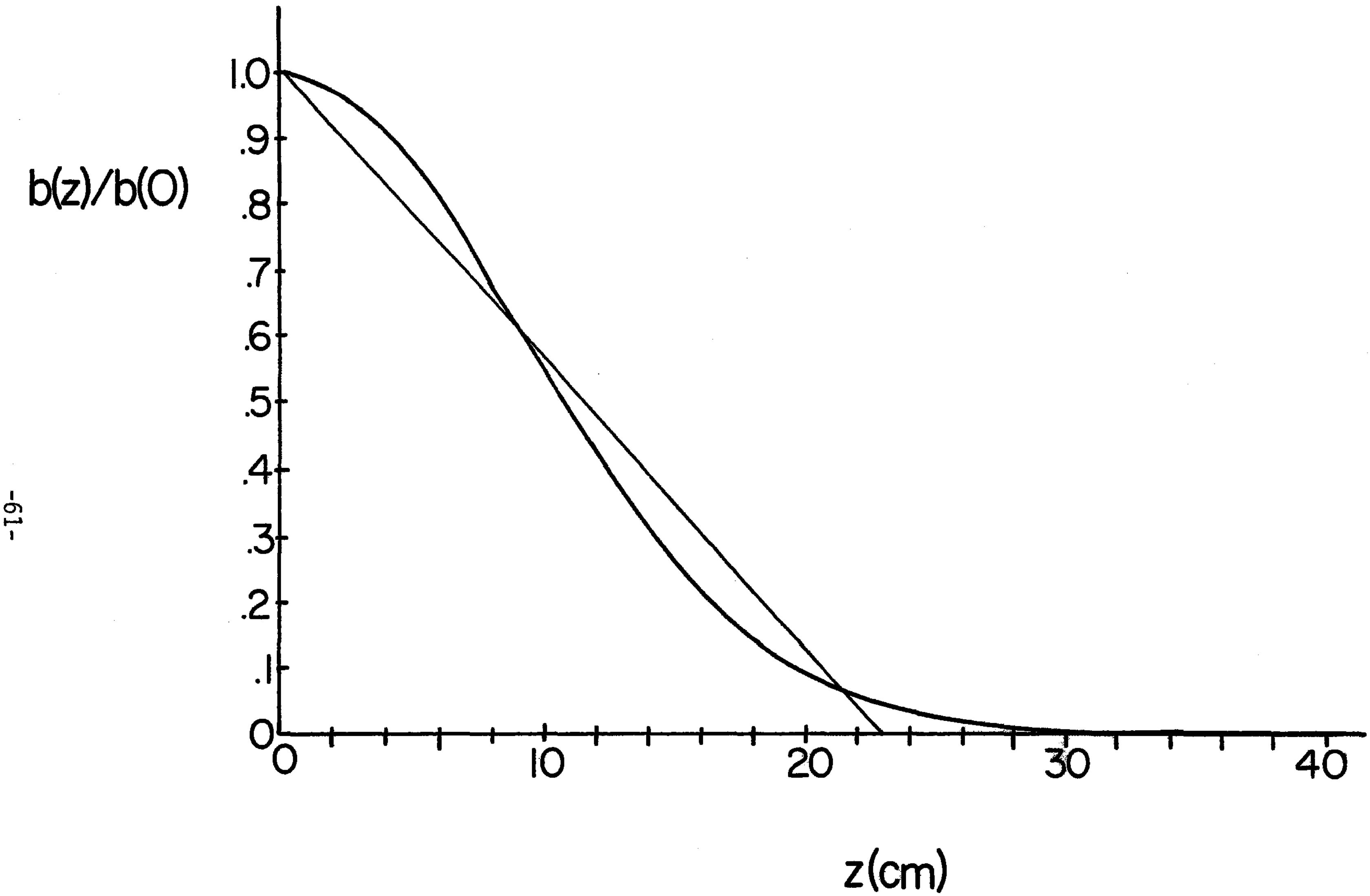

Fig. 5. Relative luminosity per unit length versus distance z from center of crossing for $\beta_H^* = \beta_V^* = 1$ m and $\alpha = 1$ mrad. The straight line shows as a comparison the luminosity distribution corresponding to a uniformly populated beam of square cross section.

High Luminosity Insertion

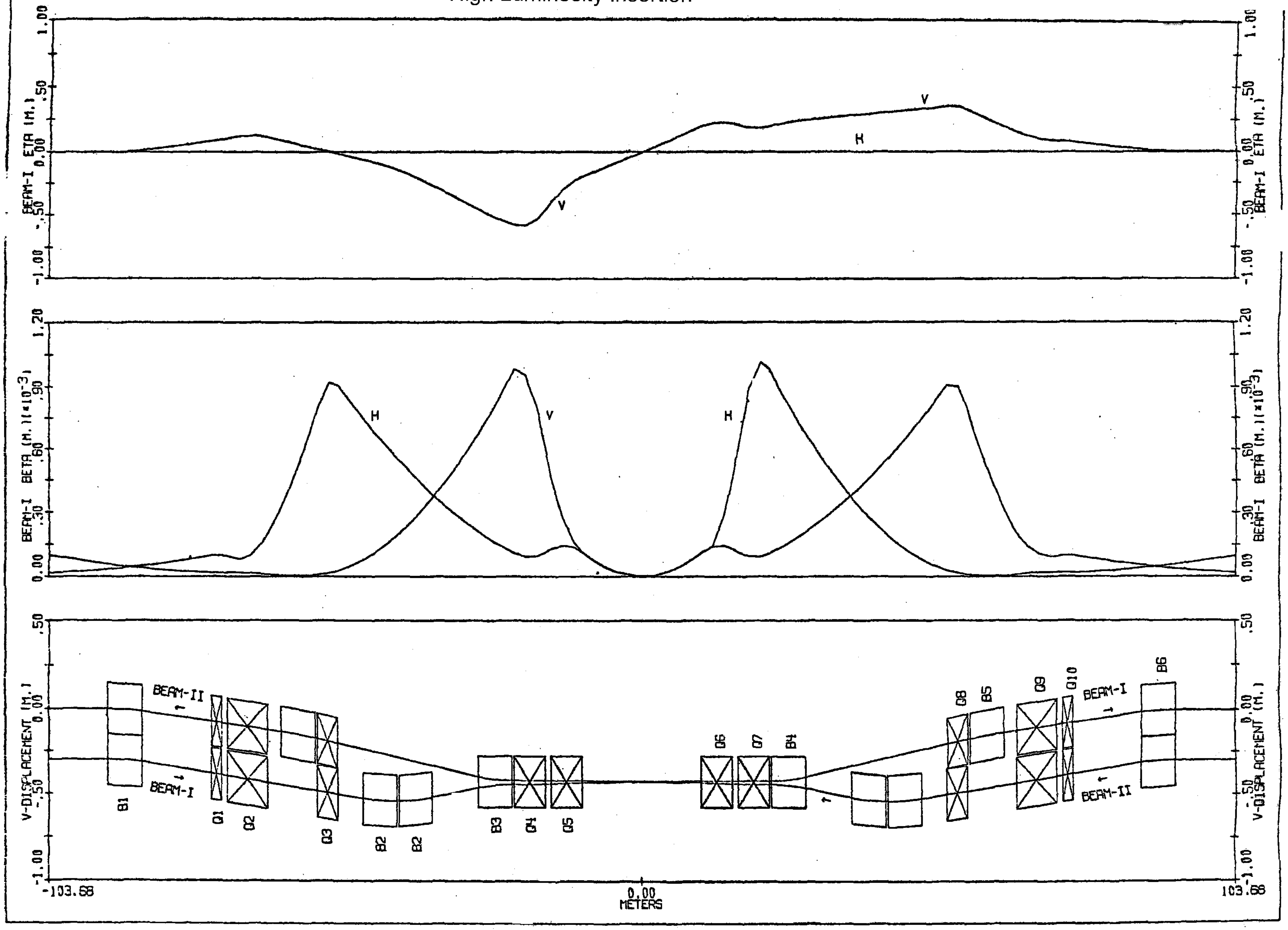

Fig. 6. Lattice elements and orbit parameters for high luminosity insertion. $\beta_H^* = \beta_V^* = 1$ meter and $\alpha = 1$ mrad.

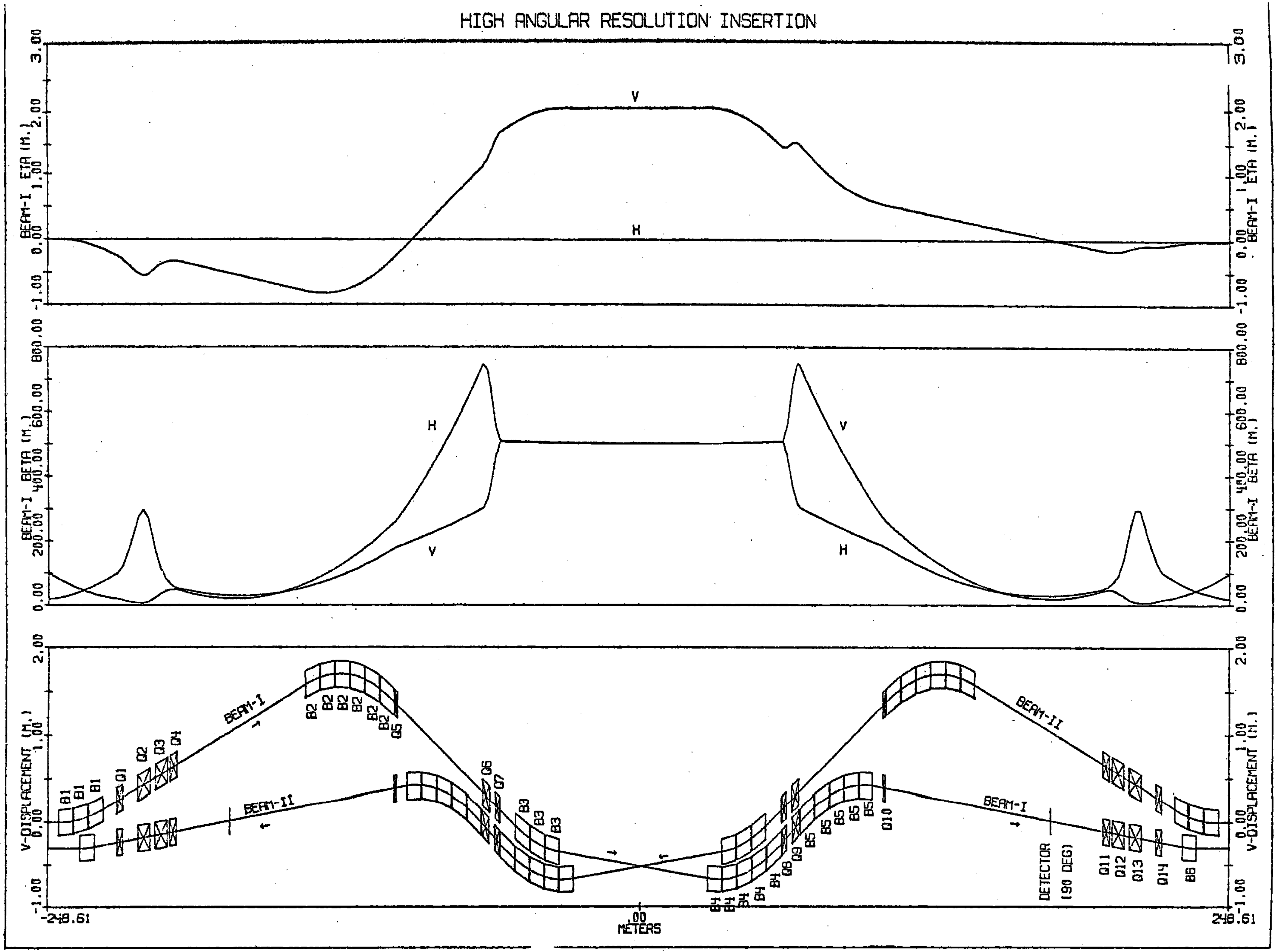

Fig. 7. Lattice elements and orbit parameters for high angular resolution insertion. $\beta_H^* = \beta_V^* = 500$ m and $\alpha = 10$ mrad.

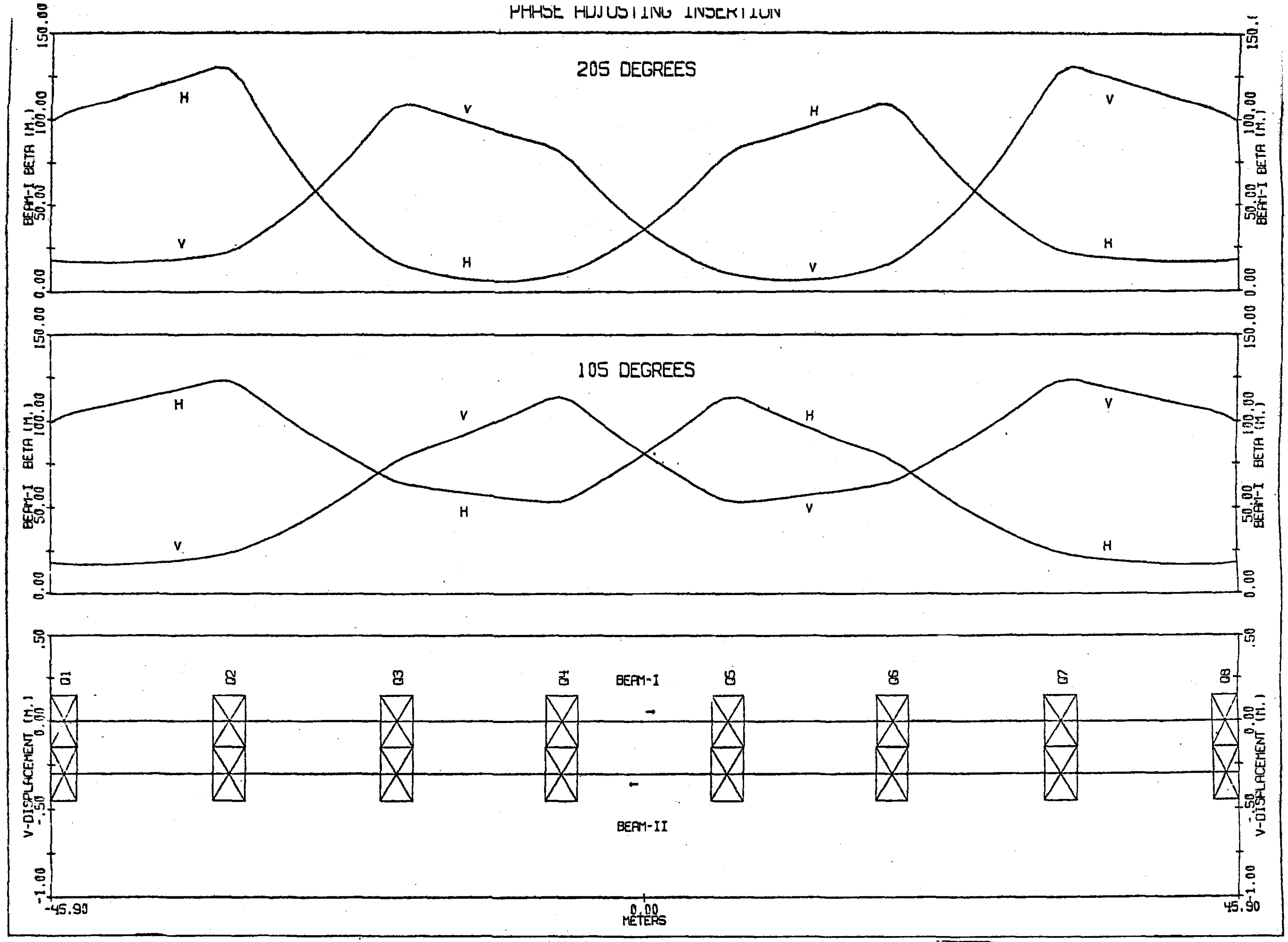

Fig. 8. Lattice elements and orbit parameters for phase adjusting insertion. Momentum dispersion is zero throughout. Amplitude functions are shown for phase advances through the insertion of 105° and 205°

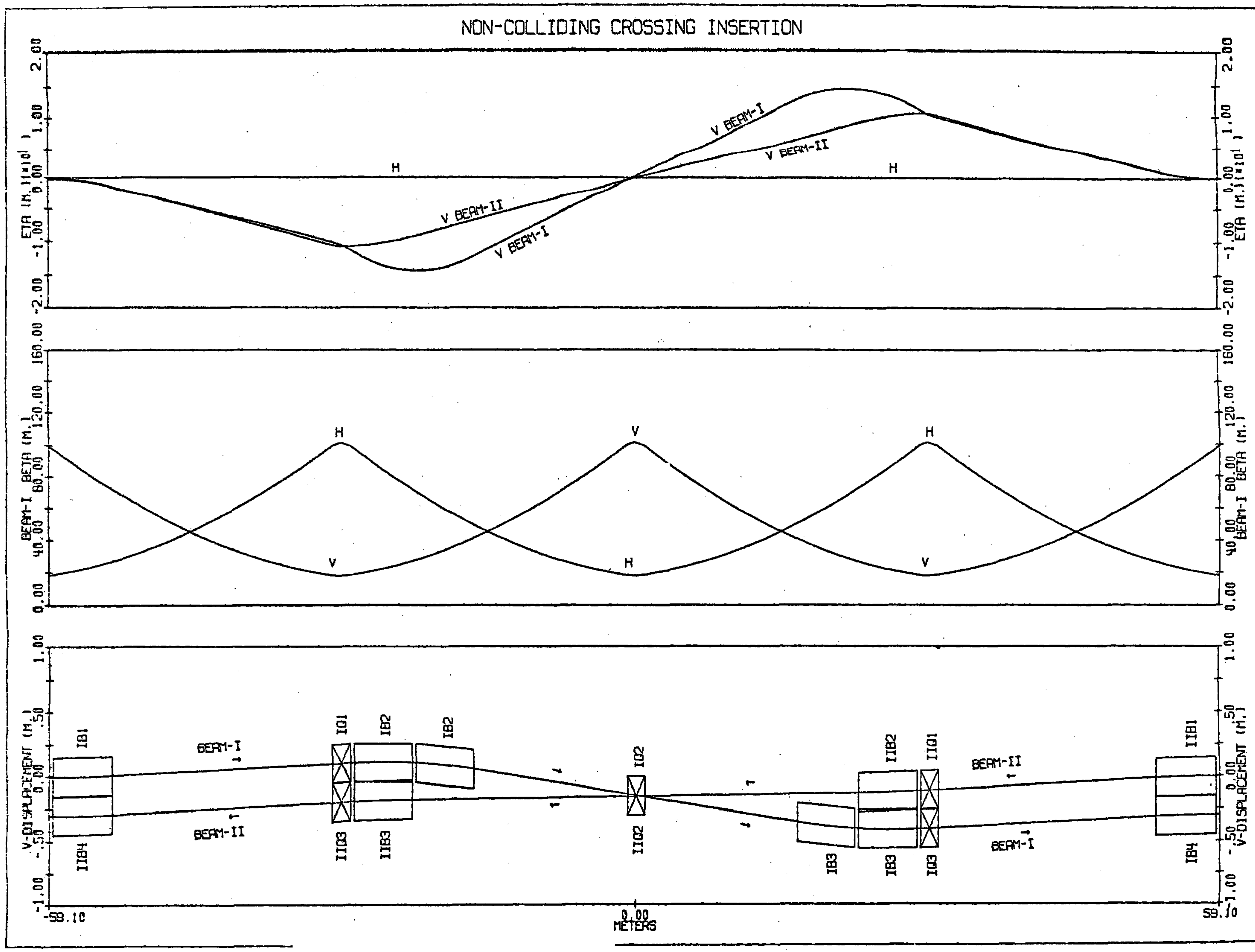

Fig. 9. Lattice elements and orbit parameters for the non-colliding crossing. Trimming elements to maintain separation of beams in horizontal plane are not shown.

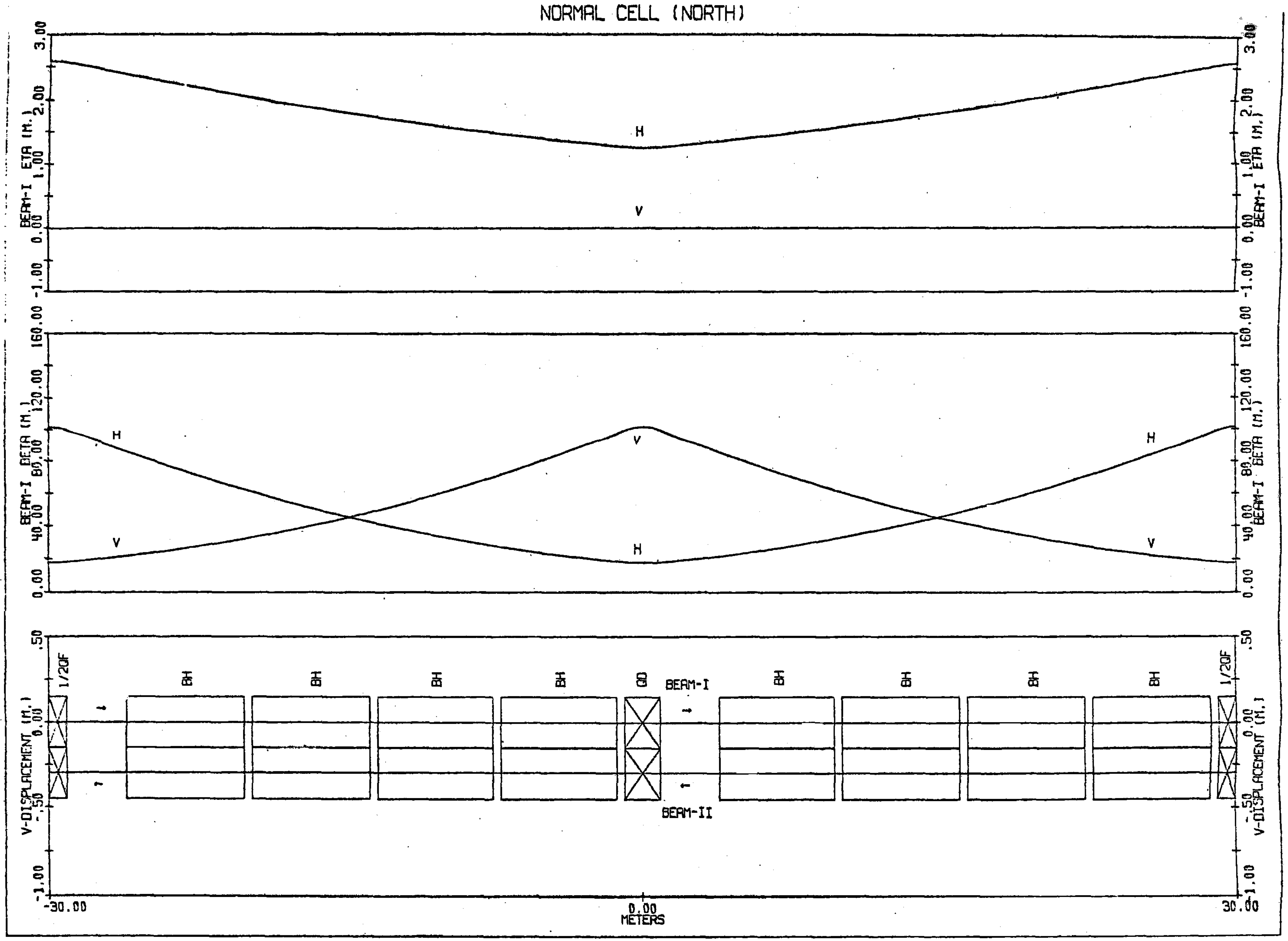

Fig. 10. Lattice elements and orbit parameters for a normal cell in north arc. A normal cell of the south arc differs only in that the 3 m drift appears at the other end of each half-cell

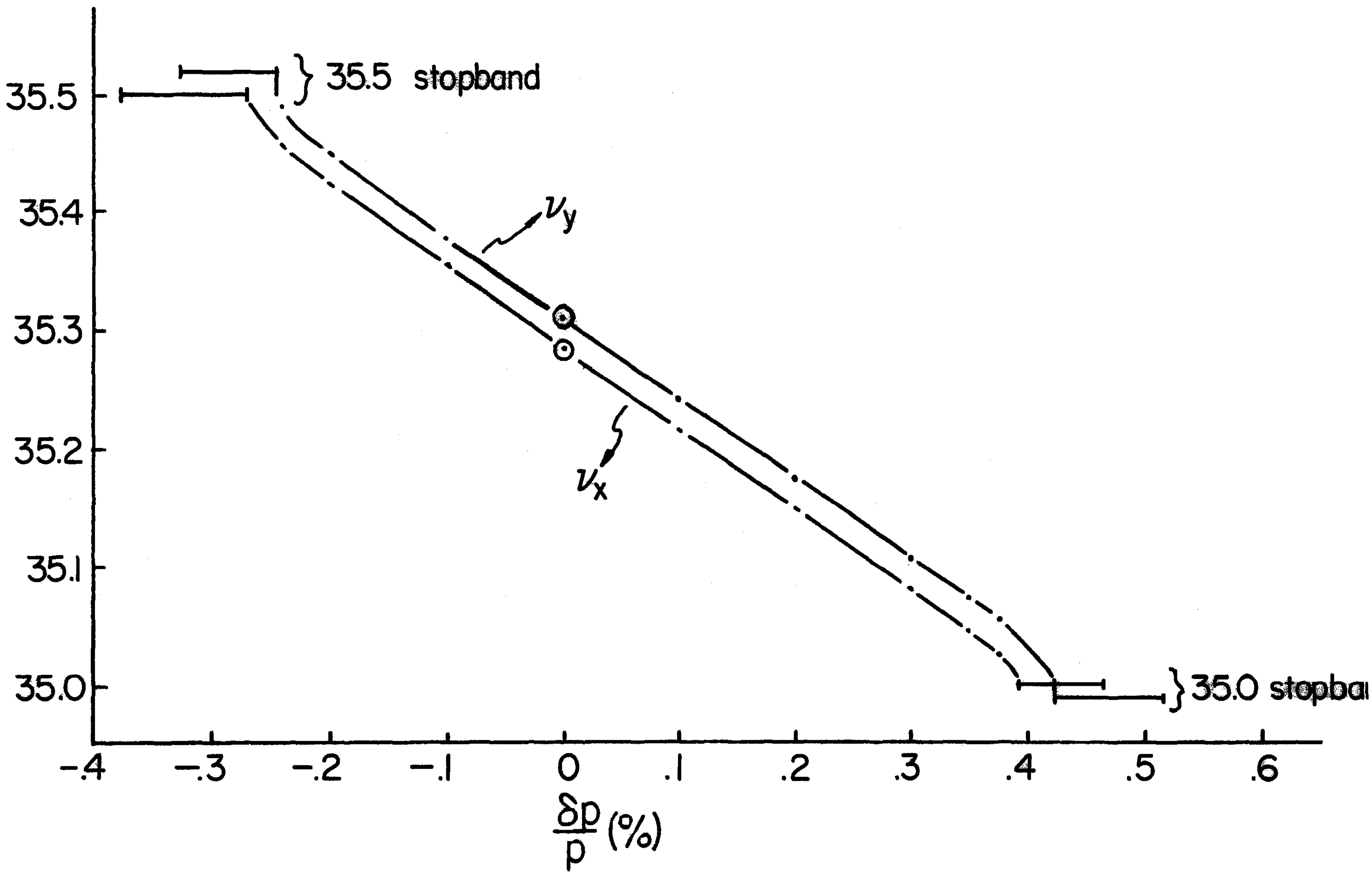

Fig. 11. Vertical (ν_y) and horizontal (ν_x) tunes versus momentum for storage ring lattice before introduction of sextupoles. Stopbands are displaced vertically from one another for clarity.

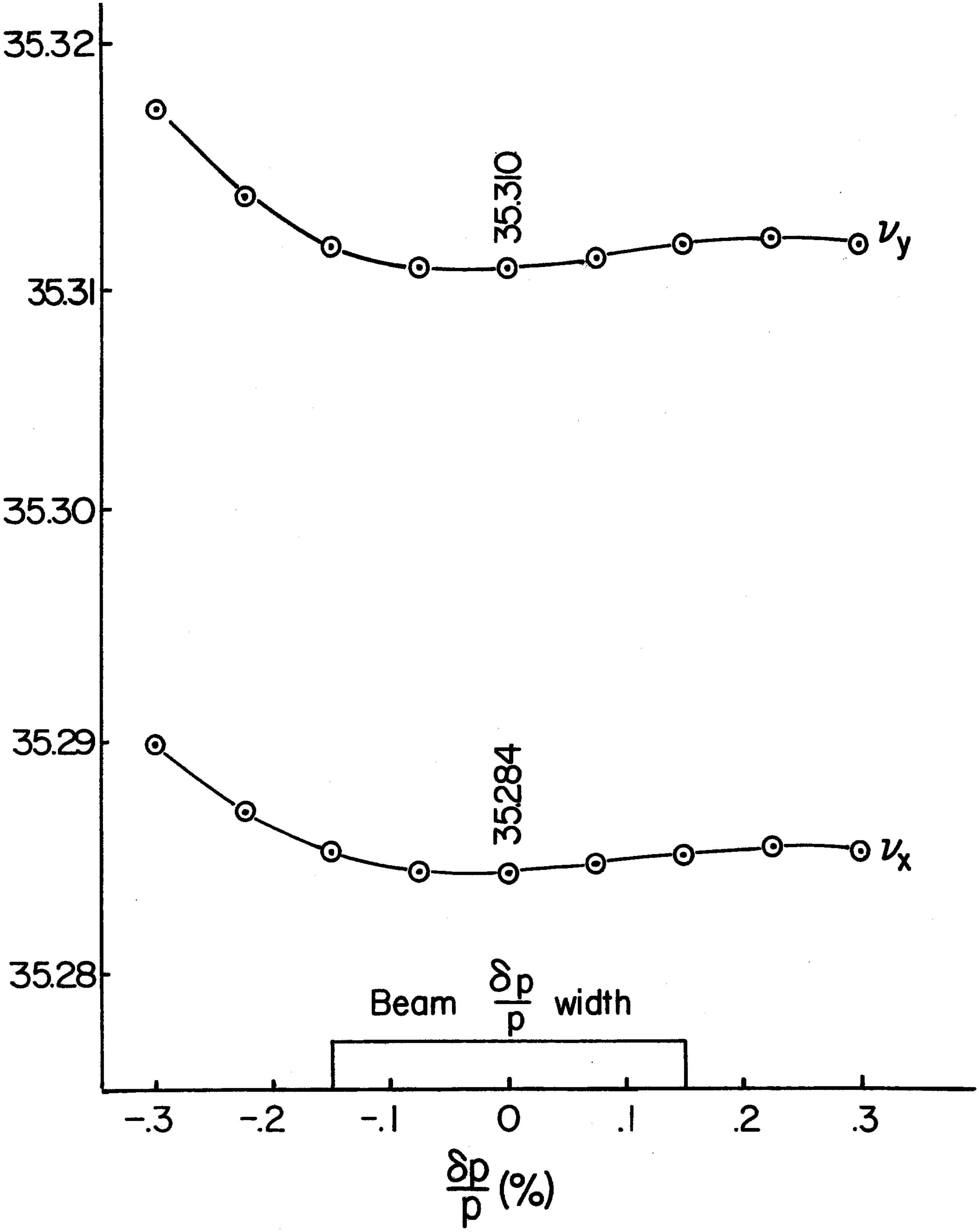

Fig. 12. Vertical and horizontal tunes versus momentum for storage ring lattice after introduction of 160 chromaticity compensating sextupoles in 40 normal cells in each of the north and south arcs.

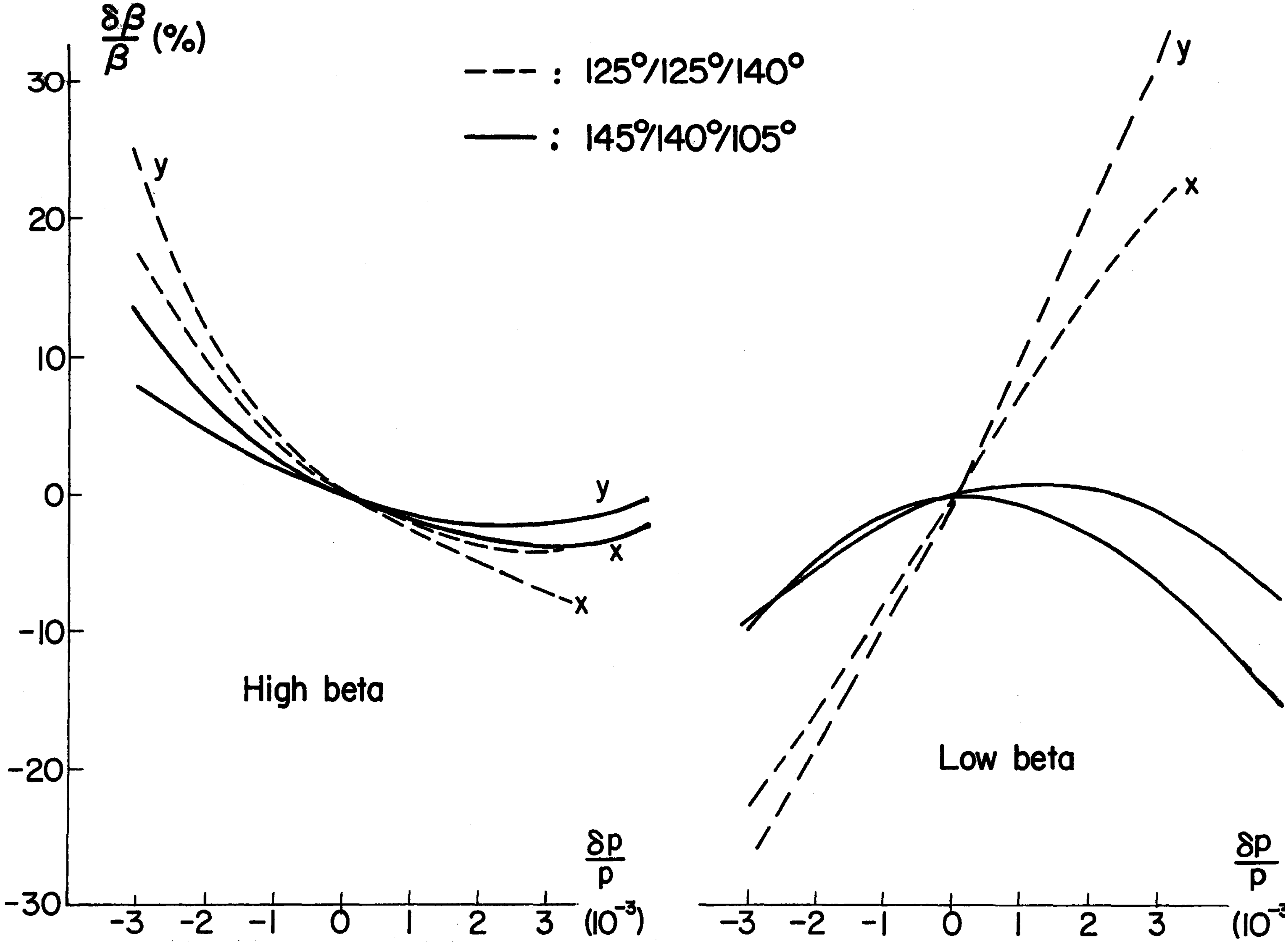

Fig. 13. Fractional change in the amplitude function as a function of momentum at the crossing point in the high angular resolution insertion and in one of the high luminosity insertions, for two settings of the phase adjusting insertions. The numbers separated by slashes at the top of the Figure are the settings of the three phase

APPENDIX I

TABLE 1

HIGH LUMINOSITY INSERTION

Element	Polarity	Length (m) (Drift)	Field (kG) or Field Gradient (kG/m)
		(10.32)	
B1	Down	5.9	12.561
		(11.98)	
Q1	F	1.8	357.17
		(1.0)	
Q2	D	7.0	-328.68
		(8.6)	
Q3	F	3.5	291.14
		(4.4)	
B2	Up	5.9	-14.318
		(0.4)	
B2	Up	5.9	-14.318
		(8.18425)	
B3 (Common)	Down	5.9	17.024
		(0.4)	
Q4 (Common)	D	5.5	-328.48
		(1.0)	
Q5 (Common)	F	5.5	355.27
		(10.5)	
Crossing Point	(β_H=β_V = 1.0 m, η_H= η_V = 0)		
		(10.5)	
Q6 (Common)	D	5.5	-355.27
		(1.0)	
Q7 (Common)	F	5.5	328.48
		(0.4)	
B4 (Common)	Up	5.9	-17.024
		(24.78425)	
Q8	D	3.5	-291.14
		(0.4)	
B5	Down	5.9	6.479
		(2.3)	

Table 1 (cont'd)
High Luminosity Insertion

Element	Polarity	Length (m) (Drift)	Field (kG) or Field Gradient (kG/m)
Q9	F	7.0	328.68
		(1.0)	
Q10	D	1.8	-357.17
		(11.98)	
B6	Down	5.9	11.256
		(10.32)	

TABLE 2

HIGH ANGULAR RESOLUTION INSERTION

Element	Polarity	Length (m) (Drift)	Field (kG) or Field Gradient (kG/m)
		(4.2)	
B1	Up	5.9	-12.836
		(0.4)	
B1	Up	5.9	-12.836
		(0.4)	
B1	Up	5.9	-12.836
		(5.5)	
Q1	F	2.5	305.92
		(6.2)	
Q2	D	5.0	-335.65
		(2.1)	
Q3	F	5.0	204.48
		(1.0)	
Q4	F	3.0	205.07
		(53.4364)	
B2	Down	5.9	16.909
		(0.4)	
B2	Down	5.9	16.909
		(0.4)	
B2	Down	5.9	16.909
		(0.4)	
B2	Down	5.9	16.909
		(0.4)	
B2	Down	5.9	16.909
		(0.4)	
B2	Down	5.9	16.909
		(0.4)	

Table 2 (cont'd)
High Angular Resolution Insertion

Element	Polarity	Length (m) (Drift)	Field (kG) or Field Gradient (kG/m)
Q5	D	1.0	-67.63
		(36.0102)	
Q6	F	3.0	226.92
		(2.3719)	
Q7	D	2.0	-311.71
		(6.7)	
B3	Up	5.9	-17.203
		(0.4)	
B3	Up	5.9	-17.203
		(0.4)	
B3	Up	5.9	-17.203
		(34.8)	
Crossing Point ($\beta_H = \beta_V = 500$ m, $\eta'_H = \eta'_V = 0$)			
		(28.5)	
B4	Up	5.9	-16.685
		(0.4)	
B4	Up	5.9	-16.685
		(0.4)	
B4	Up	5.9	-16.685
		(0.4)	
B4	Up	5.9	-16.685
		(0.4)	
B4	Up	5.9	-16.685
		(0.4)	
Q8	F	2.0	311.71
		(2.3719)	
Q9	D	3.0	-226.92
		(0.4)	

Table 2 (cont'd)
High Angular Resolution Insertion

Element	Polarity	Length (m) (Drift)	Field (kG) or Field Gradient (kG/m)
B5	Down	5.9	16.861
		(0.4)	
B5	Down	5.9	16.861
		(0.4)	
B5	Down	5.9	16.861
		(0.4)	
B5	Down	5.9	16.861
		(0.4)	
B5	Down	5.9	16.861
		(4.5102)	
Q10	F	1.0	67.63
		(69.2364)	
Detector	(β_H = 29.5 m, β_V = 19.4 m, $\eta_H = \eta_V$ = 0)		
		(22.0)	
Q11	D	3.0	-205.07
		(1.0)	
Q12	D	5.0	-204.48
		(2.1)	
Q13	F	5.0	335.65
		(6.2)	
Q14	D	2.5	-305.92
		(9.026)	
B6	Up	5.9	-12.197
		(13.274)	

TABLE 3

PHASE ADJUSTING INSERTION

Element	Polarity	Length (m) (Drift)	Field Gradient
Q1	F	2.0	G1
		(10.4)	
Q2	F&D	2.5	G2
		(10.4)	
Q3	D	2.5	G3
		(10.4)	
Q4	D	2.5	G4
		(10.4)	
Q5	F	2.5	-G4
		(10.4)	
Q6	F	2.5	-G3
		(10.4)	
Q7	D&F	2.5	-G2
		(10.4)	
Q8	D	2.0	-G1

TABLE 4

PHASE ADJUSTING INSERTION

$\psi_H=\psi_V$ (degree)	G1 (kG/m)	G2 (kG/m)	G3 (kG/m)	G4 (kG/m)
105	111.20	163.15	-110.00	-223.91
110	239.71	52.67	-103.01	
115	274.45	17.92	-100.26	
120	297.12	- 3.84	-100.24	
125	313.29	-17.14	-102.81	
130	325.11	-23.78	-107.78	
135	333.59	-24.77	-114.93	
140	339.28	-20.70	-123.96	
145	342.45	-11.97	-134.59	
150	343.15	1.16	-146.52	
155	341.29	18.52	-159.49	
160	336.63	40.01	-173.27	FIXED VALUE
165	328.77	65.52	-187.63	
170	317.14	94.88	-202.40	
175	300.99	127.76	-217.41	
180	279.49	163.51	-232.51	
185	251.94	201.01	-247.56	
190	218.17	238.64	-262.44	
195	179.01	274.52	-277.03	
200	136.40	307.06	-291.25	
205	92.69	335.47	-305.02	-223.91

TABLE 5

NON-COLLIDING CROSSING INSERTION

BEAM I

Element	Polarity	Length (m) (Drift)	Field (kG) or Field Gradient (kG/m)
		(0.4)	
IB1	Up	5.9	-9.033
		(21.9)	
IQ1	F	1.8	357.17
		(0.4)	
IB2	Down	5.9	18.663
		(0.4)	
IB2	Down	5.9	18.663
		(15.6)	
IQ2 (Common)	D	1.8	-357.17
		(15.6)	
IB3	Up	5.9	-18.663
		(0.4)	
IB3	Up	5.9	-18.663
		(0.4)	
IQ3	F	1.8	357.17
		(21.9)	
IB4	Down	5.9	9.033
		(0.4)	

Table 5 (cont'd)
Non-Colliding Crossing Insertion

BEAM II

Element	Polarity	Length (m) (Drift)	Field (kG) or Field Gradient (kG/m)
		(0.4)	
IIB1	Down	5.9	9.282
		(21.9)	
IIQ1	D	1.8	-357.17
		(0.4)	
IIB2	Up	5.9	-6.892
		(21.9)	
IIQ2 (Common)	F	1.8	357.17
		(21.9)	
IIB3	Down	5.9	6.892
		(0.4)	
IIQ3	D	1.8	-357.17
		(21.9)	
IIB4	Up	5.9	-9.282
		(0.4)	

TABLE 6

NORMAL CELL

Element	Length (m) (Drift)	Field (kG) or Field Gradient (kG/m)
	(3.0)	
B	5.9	18.166
	(0.4)	
B	5.9	18.166
	(0.4)	
B	5.9	18.166
	(0.4)	
B	5.9	18.166
	(0.4)	
D	1.8	-357.535
	(3.0)	
B	5.9	18.166
	(0.4)	
B	5.9	18.166
	(0.4)	
B	5.9	18.166
	(0.4)	
B	5.9	18.166
	(0.4)	
F	1.8	357.535

APPENDIX II

PROGRAM LISTING OF PROTON STORAGE RING PARAMETERS

The following pages constitute the output from the program SYNCH[1] for one of the proton storage rings. In particular, it follows "Beam 1," starting from the north end of the west long straight section, heading north in the upper ring. Lattice elements are designated in accord with the nomenclature below.

Regular Elements

F	1.8 m	357.535 kG/m	Quads
D	1.8 m	-357.535 kG/m	Quads
B	5.9 m	18.16634 kG	Dipole
G	0.4 m		Drift
O	2.6 m		Drift
R	21.9 m		Drift
S	25.6 m		Drift
C	GBGBGBGBG		

[1] "SYNCH, A Computer Program for Synchrotron Design and Orbit Analysis," A. A. Garren and A. S. Kenney, notes dated February, 1974. An earlier version of this code is described in UCID 10153 by A. A. Garren and J. W. Eusebio.

Appendix II

Insertion Elements

Three letter identifier, made up of element type, name of insertion, and sequence number of that element type in the insertion.

Types:	F,D	Quads
	U,V	Dipoles, U = up, V = down
	T	Drifts
Names:	H	High Luminosity
	L	High Angular Resolution
	P	Phase Adjusting
	M	Non-Colliding Crossing

Example: FH5 is the fifth horizontally focusing quadrupole in the high luminosity insertion.

SS, SE Flags indicating start and end of straight section respectively.

```
================================================================================================
***  GF               =              //  357.535
***  GD               =              //  -357.535
***  BRHO             =              //  13373.823
***  BO               =              //  18.1663369
***  B      MAG                      //  5.9        0.        BRHO      BO
***  F      MAG                      //  1.8        GF        BRHO
***  D      MAG                      //  1.8        GD        BRHO
***  G      DRF                      //  0.4
***  O      DRF                      //  2.6
***  R      DRF                      //  21.9
***  S      DRF                      //  25.6
***  C      MMM        9             //  G    B    G    B    G    B    G
***         REM                      //  HIGH BETA INSERTION COMPONENTS

     HIGH BETA INSERTION COMPONENTS
***  TH1    DRF                      //  4.2
***  TH2    DRF                      //  5.1
***  TH3    DRF                      //  6.2
***  TH4    DRF                      //  2.1
***  TH5    DRF                      //  1.0
***  TH6    DRF                      //  53.4364
***  TH7    DRF                      //  36.0102
***  TH8    DRF                      //  2.3719
***  TH9    DRF                      //  6.7
***  TH10   DRF                      //  34.4
***  TH11   DRF                      //  28.5
***  TH12   DRF                      //  4.5102
***  TH13   DRF                      //  69.2364
***  TH14   DRF                      //  22.0
***  TH15   DRF                      //  9.026
***  TH16   DRF                      //  13.274
***  FH1    MAG                      //  2.5          305.924   BRHO      0.
***  FH2    MAG                      //  5.0          335.649   BRHO      0.
***  FH3    MAG                      //  5.0          204.481   BRHO      0.
***  FH4    MAG                      //  3.0          205.072   BRHO      0.
***  FH5    MAG                      //  1.0          67.634    BRHO      0.
***  FH6    MAG                      //  3.0          226.918   BRHO      0.
***  FH7    MAG                      //  2.0          311.709   BRHO      0.
***  DH1    MAG                      //  2.5         -305.924   BRHO      0.
***  DH2    MAG                      //  5.0         -335.649   BRHO      0.
***  DH3    MAG                      //  5.0         -204.481   BRHO      0.
***  DH4    MAG                      //  3.0         -205.072   BRHO      0.
***  DH5    MAG                      //  1.0         -67.634    BRHO      0.
***  DH6    MAG                      //  3.0         -226.918   BRHO      0.
***  DH7    MAG                      //  2.0         -311.709   BRHO      0.
***  UH1    MAGV                     //  5.9        0.          BRHO     -12.83626 .162229    .162229
***  UH3    MAGV                     //  5.9        0.          BRHO     -17.20326 .217420    .217420
***  UH4    MAGV                     //  5.9        0.          BRHO     -16.68493 .210869    .210869
***  UH6    MAGV                     //  5.9        0.          BRHO     -12.19662 .154145    .154145
***  VH2    MAGV                     //  5.9        0.          BRHO      16.90855 S
***  VH5    MAGV                     //  5.9        0.          BRHO      16.86117 S
***         REM                      //  LOW BETA INSERTION ELEMENTS

     LOW BETA INSERTION ELEMENTS
***  TL1    DRF                      //  10.32
***  TL2    DRF                      //  11.98
***  TL3    DRF                      //  1.0
***  TL4    DRF                      //  8.6
***  TL5    DRF                      //  4.4
***  TL6    DRF                      //  7.78425
***  TL7    DRF                      //  10.5
```

```
***  TL8     DRF          //  24.78425
***  TL9     DRF          //  2.5
***  FL1     MAG          //  7.0        328.678  BRHO      0.
***  FL2     MAG          //  3.5        291.140  BRHO      0.
***  FL3     MAG          //  5.5        328.480  BRHO      0.
***  FL4     MAG          //  5.5        355.270  BRHO      0.
***  DL1     MAG          //  7.0       -328.678  BRHO      0.
***  DL2     MAG          //  3.5       -291.140  BRHO      0.
***  DL3     MAG          //  5.5       -328.480  BRHO      0.
***  DL4     MAG          //  5.5       -355.270  BRHO      0.
***  VL1     MAGV         //  5.9       0.        BRHO      12.561     $
***  VL3     MAGV         //  5.9       0.        BRHO      17.024     $
***  VL4     MAGV         //  5.9       0.        BRHO      6.479      $
***  VL5     MAGV         //  5.9       0.        BRHO      11.256     $
***  UL2     MAGV         //  5.9       0.        BRHO      -14.318    .180955    .180955
***  UL3     MAGV         //  5.9       0.        BRHO      -17.024    .215155    .215155
***          REM          //  MU-CROSSING INSERTION COMPONENTS

     MU-CROSSING INSERTION COMPONENTS
***  TM1     DRF          //  15.6
***  VM1     MAGV         //  5.9       0.        BRHO      9.0325     $
***  VM2     MAGV         //  5.9       0.        BRHO      18.6631    $
***  UM1     MAGV         //  5.9       0.        BRHO      -9.0325    .114156    .114156
***  UM2     MAGV         //  5.9       0.        BRHO      -18.6631   .235870    .235870
***          REM          //  PHASE-ADJUSTING INSERTION COMPONENTS

     PHASE-ADJUSTING INSERTION COMPONENTS
***  TP      DRF          //  10.4
***          REM          //  DPF1     125 DEG. PHASE ADVANCE

     DPF1    125 DEG. PHASE ADVANCE
***  DP11    MAG          //  2.0       -313.294  BRHO      0.
***  DP12    MAG          //  2.5        17.135   BRHO      0.
***  FP13    MAG          //  2.5       102.807   BRHO      0.
***  FP14    MAG          //  2.5       223.906   BRHO      0.
***  DP14    MAG          //  2.5       -223.906  BRHO      0.
***  DP13    MAG          //  2.5       -102.807  BRHO      0.
***  FP12    MAG          //  2.5       -17.135   BRHO      0.
***  FP11    MAG          //  2.0       313.294   BRHO      0.
***          REM          //  DPF2    125. DEG. PHASE ADVANCE

     DPF2   125. DEG. PHASE ADVANCE
***  DP21    MAG          //  2.0       -313.294  BRHO      0.
***  DP22    MAG          //  2.5        17.135   BRHO      0.
***  FP23    MAG          //  2.5       102.807   BRHO      0.
***  FP24    MAG          //  2.5       223.906   BRHO      0.
***  DP24    MAG          //  2.5       -223.906  BRHO      0.
***  DP23    MAG          //  2.5       -102.807  BRHO      0.
***  FP22    MAG          //  2.5       -17.135   BRHO      0.
***  FP21    MAG          //  2.0       313.294   BRHO      0.
***          REM          //  DPF3    125.  DEG.PHASE ADVANCE

     DPF3    125.  DEG.PHASE ADVANCE
***  DP31    MAG          //  2.0       -313.294  BRHO      0.
***  DP32    MAG          //  2.5        17.135   BRHO      0.
***  FP33    MAG          //  2.5       102.807   BRHO      0.
***  FP34    MAG          //  2.5       223.906   BRHO      0.
***  DP34    MAG          //  2.5       -223.906  BRHO      0.
***  DP33    MAG          //  2.5       -102.807  BRHO      0.
***  FP32    MAG          //  2.5       -17.135   BRHO      0.
***  FP31    MAG          //  2.0       313.294   BRHO      0.
***          REM          //  OCD 1ST HALF NORMAL CELL,NORTH

     OCD 1ST HALF NORMAL CELL,NORTH
***  OCD     NMM     3    //  0     C     D
***          REM          //  OCF 2ND HALF NORMAL CELL,NORTH
```

```
     OCF 2ND HALF NORMAL CELL,NORTH
***  OCF      MMM      3       //  O    C    F
***           REM              //  FCO 1ST HALF NORMAL CELL,SOUTH

     FCO 1ST HALF NORMAL CELL,SOUTH
***  FCO      MMM      3       //  F    C    O
***           REM              //  DCO 2ND HALF NORMAL CELL,SOUTH

     DCO 2ND HALF NORMAL CELL,SOUTH
***  DCO      MMM      3       //  D    C    O
***           REM              //  SS + ES  ARE START AND END OF LONG STRAIGHTS

     SS + ES  ARE START AND END OF LONG STRAIGHTS
***  SS       DRF              //  0,0
***  ES       DRF              //  0,0
***           REM              //  RT = ENTIRE RACETRACK

     RT = ENTIRE RACETRACK
***  RT       CYC    626       //  F    R    B    G    D    G    B    R    F    O    C    D
  *                            //  O    S    F    O    C    D    O    C    F    O    C    D
  *                            //  U    S    F    O    C    D    O    C    F    O    C    D
  *                            //  U    C    F    O    C    D    O    S    F    O    C    D
  *                            //  U    C    F    O    C    D    O    S    F    O    C    D
  *                            //  O    S    F    OCD  UCF  OCD  UCF  OCD  OCF  OCD  OCF  OCD
  *                            //  OCF  OCD  OCF  OCD  OCF  OCD  UCF  OCD  OCF  OCD  OCF  OCD
  *                            //  UCF  OCD  OCF  OCD  OCF  UCD  UCF  OCD  OCF  OCD  OCF  OCD
  *                            //  UCF  OCD  OCF  OCD  UCF  UCD  OCF  OCD  OCF  OCD  UCF  OCD
  *                            //  OCF  OCD  OCF  OCD  UCF  UCD  OCF  UCD  OCF  OCD  OCF  OCD
  *                            //  OCF  OCD  OCF  OCD  UCF  UCD  UCF  UCD  OCF  OCD  OCF  OCD
  *                            //  OCF  OCD  OCF  OCD  UCF  UCD  UCF  OCD  OCF  OCD  OCF  OCD
  *                            //  U    C    F    O    C    D    U    S    F    O    C    D
  *                            //  R    B    G    F    G    B    R    SS   D    O    S    F
  *                            //  U    S    D    O    S    F    U    S    O    O    S    F
  *                            //  O    S    D    O    S    F    O    S    D    O    S    F
  *                            //  O    S    D    O    S    F    U    S    D    O    S    F
  *                            //  U    S    D    O    S    F    U    S    DP11 TP   DP12 TP
  *                            //  FP13 TP   FP14 TP   DP14 TP   DP13 TP   FP12 TP   FP11 TH1
  *                            //  UH1  G    UH1  G    UH1  G    TH2  FH1  TH3  DH2  TH4  FH3
  *                            //  TH5  FH4  TH6  VH2  G    VH2  G    VH2  G    VH2  G    VH2
  *                            //  G    VH2  G    DH5  TH7  FH6  TH8  DH7  TH9  UH3  G    UH3
  *                            //  G    UH3  G    TH10 TH11 UH4  G    UH4  G    UH4  G    UH4
  *                            //  G    UH4  G    FH7  TH8  DH6  G    VH5  G    VH5  G    VH5
  *                            //  G    VH5  G    VH5  TH12 FH5  TH13 TH14 DH4  TH5  DH3  TH4
  *                            //  FH2  TH3  DH1  TH15 UH6  TH16 DP21 TP   DP22 TP   FP23 TP
  *                            //  FP24 TP   DP24 TP   DP23 TP   FP22 TP   FP21 ES   R    B
  *                            //  G    D    G    B    R    F    C    O    D    S    D    F
  *                            //  C    O    D    C    U    FCO  DCO  FCO  DCO  FCO  DCO  FCO
  *                            //  DCU  FCU  DCU  FCO  DCO  FCO  DCU  FCO  DCO  FCO  DCO  FCO
  *                            //  DCU  FCO  DCO  FCO  DCO  FCO  DCO  FCO  DCO  FCO  DCO  FCO
  *                            //  DCU  FCO  DCO  FCO  DCO  FCO  OCU  FCO  DCO  FCO  DCO  FCO
  *                            //  DCU  FCO  DCO  FCO  DCO  FCO  DCU  FCO  DCO  FCO  DCO  FCO
  *                            //  DCU  FCU  DCU  FCO  DCO  FCO  DCU  FCO  DCO  FCO  DCO  FCO
  *                            //  DCU  FCU  DCU  FCO  DCO  FCO  DCU  FCO  DCO  FCO  DCO  FCO
  *                            //  DCU  FCU  D    S    O    F    C    O    D    S    O    F
  *                            //  C    O    D    C    U    F    C    O    D    S    U    F
  *                            //  C    O    D    C    O    F    C    O    D    C    O    F
  *                            //  C    O    D    S    U    F    C    O    D    C    O    F
  *                            //  C    O    D    S    U    F    C    O    D    R    B    G
  *                            //  F    G    B    R    D    SS   TL1  VL1  TL2  F    TL3  DL1
  *                            //  TL4  FL2  TL5  UL2  G    UL2  G    TL6  VL3  G    DL3  TL3
  *                            //  FL4  TL7  TL7  DL4  TL3  FL3  G    UL3  TL8  DL2  G    VL4
  *                            //  TL9  FL1  TL3  D    TL2  VL5  TL1  FP31 TP   FP32 TP   DP33
  *                            //  TP   DP34 TP   FP34 TP   FP33 TP   DP32 TP   DP31 G    UM1
  *                            //  R    F    G    VM2  G    VM2  TM1  D    TM1  UM2  G    UM2
  *                            //  G    F    R    VM1  G    D    S    O    F    S    O    D
```

```
// S   O   F   S   O   D   S   D   F   S   O   D
// S   O   F   S   O   D   S   O   F   S   O   D
// TL1 VL1 TL2 F   TL3 DL1 TL4 FL2 TL5 UL2 G   UL2
// G   TL6 VL3 G   DL3 TL3 FL4 TL7 TL7 DL4 TL3 FL3
// G   UL3 TL8 DL2 G   VL4 TL9 FL1 TL3 D   TL2 VL3
// TL1 ES
```

POS	RT	S	PSIX	BETAX	ALPHAX	XEQ	DXEQ	PSIY	BETAY	ALPHAY	YEQ	DYEQ
0	'	0,00000	0,00000	99,666996	=2,42454	=,059914	=,00276	0,00000	18,040772	,47824	,00231	,00007
1	F	1,80000	,00283	99,730633	2,39021	=,062225	,00021	,01613	18,053365	=,48544	,00255	,00019
2	R	23,70000	,07174	27,323117	,91607	=,057733	,00021	,11991	72,142041	=1,98437	,00670	,00019
3	B	29,60000	,11358	18,856706	,51893	=,032881	,00822	,13109	97,934715	=2,38713	,00782	,00019
4	G	30,00000	,11700	18,452331	,49201	=,029593	,00822	,13174	99,855366	=2,41449	,00790	,00019
5	D	31,80000	,13278	18,446493	=,48867	=,015875	,00713	,13456	99,867102	2,40816	,00790	=,00019
6	G	32,20000	,13619	18,848173	=,51553	=,013022	,00713	,13521	97,951466	2,38093	,00782	=,00019
7	B	38,10000	,17809	27,269043	=,91175	,052706	,01515	,14638	72,221087	1,98001	,00668	=,00019
8	R	60,00000	,24719	99,412490	=2,38247	,384438	,01515	,24970	18,172545	,48796	,00245	=,00019
9	F	61,80000	,25003	99,348857	2,41680	,394782	=,00374	,26572	18,159923	=,48074	,00220	=,00008
10	O	64,40000	,25447	87,246988	2,23777	,385064	=,00374	,28692	21,118072	=,65701	,00199	=,00008
11	C	90,00000	,36701	17,799933	,47503	,699717	,02832	,38141	99,121282	=2,38884	=,00011	=,00008
12	D	91,80000	,38336	17,805774	=,47837	,781955	,06371	,38426	99,105375	2,39742	=,00025	=,00007
13	O	94,40000	,40495	20,759842	=,65781	,947613	,06371	,38871	87,099027	2,22040	=,00044	=,00007
14	S	120,00000	,50008	99,668331	=2,42456	2,578706	,06371	,50047	18,034994	,47741	=,00232	=,00007
15	F	121,80000	,50292	99,731918	2,39026	2,580866	=,06133	,51661	18,050154	=,48608	=,00255	=,00019
16	O	124,40000	,50734	87,757631	2,21524	2,421404	=,06133	,53791	21,040747	=,66415	=,00305	=,00019
17	C	150,00000	,61708	18,452284	,49203	1,261663	=,02927	,63219	99,866868	=2,41383	=,00790	=,00019
18	D	151,80000	,63286	18,446365	=,48864	1,263242	,03104	,63502	99,875261	2,40930	=,00789	,00019
19	O	154,40000	,65373	21,441286	=,66325	1,343950	,03104	,63944	87,807462	2,23216	=,00739	,00019
20	C	180,00000	,74727	99,409370	=2,38241	2,548937	,06310	,75024	18,142509	,48810	=,00244	,00019
21	F	181,80000	,75011	99,345786	2,41671	2,551285	=,06051	,76629	18,127066	=,47927	=,00219	,00008
22	O	184,40000	,75456	87,244364	2,23768	2,393962	=,06051	,78752	21,077879	=,65565	=,00198	,00008
23	C	210,00000	,86709	17,800127	,47501	1,255282	=,02845	,88216	99,041480	=2,38865	,00015	,00008
24	D	211,80000	,88345	17,806080	=,47841	1,258085	,03159	,88501	99,031770	2,39389	,00029	,00007
25	O	214,40000	,90503	20,760348	=,65785	1,340215	,03159	,88947	87,043000	2,21718	,00048	,00007
26	S	240,00000	1,00017	99,671411	=2,42462	2,148886	,03159	1,00116	18,065034	,47727	,00233	,00007
27	F	241,80000	1,00300	99,734948	2,39034	2,112532	=,07169	1,01727	18,082997	=,48754	,00256	,00019
28	O	244,40000	1,00742	87,760219	2,21532	1,926138	=,07169	1,03853	21,080893	=,66550	,00306	,00019
29	C	270,00000	1,11716	18,452083	,49205	,501223	=,03963	1,13267	99,945928	=2,41400	,00790	,00019
30	D	271,80000	1,13294	18,446051	=,48861	,450714	=,01689	1,13549	99,948116	2,41282	,00790	=,00019
31	O	274,40000	1,15381	21,440771	=,66321	,406794	=,01689	1,13991	87,862821	2,23537	,00739	=,00019
32	C	300,00000	1,24736	99,406251	=2,38235	,384680	,01516	1,25078	18,112407	,48823	,00243	=,00019
33	F	301,80000	1,25020	99,342717	2,41662	,395044	=,00373	1,26686	18,094191	=,47782	,00218	=,00008
34	O	304,40000	1,25464	87,241742	2,23760	,385340	=,00373	1,28813	21,037747	=,65432	,00196	=,00008
35	C	330,00000	1,36718	17,800320	,47498	,700120	,02832	1,38291	98,963366	=2,38850	=,00019	=,00008
36	D	331,80000	1,38353	17,806386	=,47845	,782385	,06374	1,38577	98,959872	2,39039	=,00033	=,00007
37	O	334,40000	1,40512	20,760856	=,65789	,948108	,06374	1,39023	86,988500	2,21399	=,00051	=,00007
38	C	360,00000	1,50025	99,673264	=2,42466	2,990150	,09580	1,50194	18,065885	,47728	=,00234	=,00007
39	F	361,80000	1,50308	99,736795	2,39039	3,031537	=,05014	1,51804	18,083876	=,48757	=,00257	=,00019

40	O	364.40000	1.50751	87.761830	2.21537	2.901164	-.05014	1.53930	21.081896	-.66552	-.00307	-.00019
41	C	390.00000	1.61724	18.452086	.49207	2.027836	-.01809	1.63344	99.946775	-2.41398	-.00790	-.00019
42	D	391.80000	1.63302	18.445986	-.48859	2.083269	.08012	1.63626	99.948792	2.41289	-.00790	.00019
43	O	394.40000	1.65389	21.440596	-.66319	2.291584	.08012	1.64068	87.863179	2.23542	-.00739	.00019
44	S	420.00000	1.74744	99.405602	-2.38232	4.342694	.08012	1.75146	18.141201	.48809	-.00242	.00019
45	F	421.80000	1.75028	99.342030	2.41661	4.298116	-.12929	1.76752	18.125694	-.47923	-.00217	.00008
46	O	424.40000	1.75473	87.241088	2.23760	3.961949	-.12929	1.78875	21.076285	-.65561	-.00195	.00008
47	C	450.00000	1.86726	17.800121	.47497	1.062360	-.09724	1.88339	99.039636	-2.38868	.00021	.00008
48	D	451.80000	1.88362	17.806212	-.47845	.931137	-.04962	1.88625	99.030189	2.39377	.00035	.00007
49	O	454.40000	1.90520	20.760704	-.65789	.802135	-.04962	1.89070	87.041977	2.21708	.00053	.00007
50	C	480.00000	2.00034	99.673954	-2.42469	-.057701	-.01756	2.00248	18.036988	.47741	.00235	.00007
51	F	481.80000	2.00317	99.737522	2.39040	-.086372	-.01407	2.01861	18.052300	-.48616	.00258	.00019
52	O	484.40000	2.00759	87.762520	2.21537	-.122947	-.01407	2.03991	21.043322	-.66423	.00307	.00019
53	C	510.00000	2.11733	18.452293	.49208	-.072739	.01799	2.13418	99.871178	-2.41382	.00790	.00019
54	D	511.80000	2.13511	18.446168	-.48858	-.043061	.01522	2.13701	99.879162	2.40951	.00789	-.00019
55	O	514.40000	2.15397	21.440756	-.66318	-.003479	.01522	2.14143	87.810321	2.23235	.00739	-.00019
56	S	540.00000	2.24752	99.404951	-2.38230	.386246	.01522	2.25215	18.170182	.48797	.00241	-.00019
57	F	541.80000	2.25036	99.341342	2.41661	.396648	-.00375	2.26818	18.157338	-.48063	.00216	-.00008
58	O	544.40000	2.25481	87.240433	2.23759	.386897	-.00375	2.28937	21.114908	-.65690	.00194	-.00008
59	C	570.00000	2.36735	17.799921	.47496	.701217	.02831	2.38388	99.114968	-2.38883	-.00023	-.00008
60	D	571.80000	2.38370	17.806038	-.47845	.783497	.06377	2.38672	99.099548	2.39715	-.00037	-.00007
61	O	574.40000	2.40529	20.760553	-.65790	.949310	.06377	2.39118	87.094587	2.22015	-.00056	-.00007
62	S	600.00000	2.50042	99.675870	-2.42473	2.581931	.06377	2.50294	18.037352	.47740	-.00236	-.00007
63	F	601.80000	2.50325	99.739432	2.39044	2.584059	-.06143	2.51907	18.052733	-.48619	-.00259	-.00019
64	OCD	631.80000	2.63319	18.446100	-.48856	1.263578	.03097	2.63747	99.881003	2.40958	-.00789	.00019
65	OCF	661.80000	2.75045	99.338273	2.41652	2.549417	-.06050	2.76874	18.124479	-.47916	-.00215	.00009
66	OCD	691.80000	2.88379	17.806345	-.47849	1.256543	.03153	2.88748	99.026077	2.39361	.00041	.00007
67	OCF	721.80000	3.00333	99.741280	2.39049	2.558892	-.06038	3.01984	18.053519	-.48623	.00260	.00019
68	OCD	751.80000	3.13327	18.446035	-.48854	1.270158	.03228	3.13823	99.883249	2.40968	.00789	-.00019
69	OCF	781.80000	3.25053	99.336425	2.41647	2.593528	-.06131	3.26951	18.123692	-.47912	.00214	-.00009
70	OCD	811.80000	3.38387	17.806411	-.47851	1.277187	.03172	3.38825	99.023851	2.39352	-.00045	-.00007
71	OCF	841.80000	3.50342	99.743127	2.39054	2.584036	-.06143	3.52062	18.054308	-.48627	-.00261	-.00019
72	OCD	871.80000	3.63335	18.445968	-.48852	1.263568	.03097	3.63900	99.885454	2.40977	-.00789	.00020
73	OCF	901.80000	3.75061	99.334578	2.41643	2.549404	-.06050	3.77028	18.122901	-.47908	-.00213	.00009
74	OCD	931.80000	3.88396	17.806478	-.47853	1.256546	.03153	3.88903	99.021666	2.39342	.00049	.00007
75	OCF	961.80000	4.00350	99.744974	2.39059	2.558915	-.06038	4.02139	18.055101	-.48631	.00262	.00019
76	OCD	991.80000	4.13343	18.445902	-.48850	1.270169	.03228	4.13977	99.887619	2.40987	.00788	-.00020
77	OCF	1021.80000	4.25070	99.332731	2.41638	2.593541	-.06131	4.27106	18.122107	-.47904	.00211	-.00009
78	OCD	1051.80000	4.38404	17.806544	-.47855	1.277184	.03172	4.38981	99.019521	2.39333	-.00053	-.00007
79	OCF	1081.80000	4.50358	99.746821	2.39063	2.584013	-.06143	4.52216	18.055896	-.48635	-.00263	-.00019
80	OCD	1111.80000	4.63351	18.445835	-.48848	1.263557	.03097	4.64054	99.889744	2.40996	-.00788	.00020
81	OCF	1141.80000	4.75078	99.330884	2.41633	2.549391	-.06049	4.77183	18.121309	-.47900	-.00210	.00009
82	OCD	1171.80000	4.88412	17.806611	-.47857	1.256550	.03153	4.89058	99.017417	2.39323	.00056	.00007
83	OCF	1201.80000	5.00366	99.748668	2.39068	2.558938	-.06038	5.02294	18.056695	-.48639	.00264	.00019
84	OCD	1231.80000	5.13360	18.445768	-.48846	1.270180	.03228	5.14131	99.891827	2.41005	.00788	-.00020
85	OCF	1261.80000	5.25086	99.329037	2.41628	2.593554	-.06131	5.27260	18.120509	-.47896	.00209	-.00009
86	OCD	1291.80000	5.38421	17.806679	-.47859	1.277180	.03171	5.39136	99.015354	2.39318	-.00060	-.00006

87	OCF	1321.80000	5.50375	99.750515	2.39073	2.583990	-.06143	5.52371	18.057497	-.48643	-.00265	-.00019
88	OCD	1351.80000	5.63368	18.445700	-.48844	1.263546	.03097	5.64208	99.893869	2.41014	-.00787	.00020
89	OCF	1381.80000	5.75095	99.327191	2.41624	2.549378	-.06049	5.77337	18.119706	-.47893	-.00208	.00009
90	OCD	1411.80000	5.88429	17.806747	-.47861	1.256553	.03153	5.89213	99.013333	2.39305	.00064	.00006
91	OCF	1441.80000	6.00383	99.752361	2.39077	2.558960	-.06038	6.02448	18.058302	-.48646	.00266	.00019
92	OCD	1471.80000	6.13376	18.445632	-.48842	1.270191	.03228	6.14285	99.895870	2.41024	.00787	-.00020
93	OCF	1501.80000	6.25103	99.325344	2.41619	2.593567	-.06131	6.27414	18.118900	-.47889	.00206	-.00009
94	OCD	1531.80000	6.38438	17.806815	-.47863	1.277177	.03171	6.39291	99.011353	2.39296	-.00068	-.00006
95	OCF	1561.80000	6.50391	99.754207	2.39082	2.583967	-.06143	6.52526	18.059109	-.48650	-.00267	-.00018
96	OCD	1591.80000	6.63384	18.445564	-.48840	1.263535	.03097	6.64362	99.897829	2.41033	-.00787	.00020
97	OCF	1621.80000	6.75111	99.323498	2.41614	2.549365	-.06049	6.77491	18.118091	-.47885	-.00205	.00009
98	OCD	1651.80000	6.88446	17.806883	-.47865	1.256556	.03153	6.89368	99.009415	2.39287	.00072	.00006
99	OCF	1681.80000	7.00399	99.756053	2.39087	2.558983	-.06038	7.02603	18.059920	-.48654	.00268	.00018
100	OCD	1711.80000	7.13392	18.445495	-.48838	1.270201	.03228	7.14438	99.899746	2.41042	.00786	-.00020
101	OCF	1741.80000	7.25119	99.321653	2.41610	2.593580	-.06131	7.27568	18.117279	-.47881	.00204	-.00009
102	OCD	1771.80000	7.38454	17.806952	-.47867	1.277173	.03171	7.39446	99.007519	2.39278	-.00075	-.00006
103	OCF	1801.80000	7.50408	99.757899	2.39091	2.583944	-.06143	7.52680	18.060733	-.48658	-.00269	-.00018
104	OCD	1831.80000	7.63400	18.445426	-.48836	1.263525	.03097	7.64515	99.901621	2.41050	-.00786	.00020
105	OCF	1861.80000	7.75128	99.319807	2.41605	2.549352	-.06049	7.77645	18.116465	-.47878	-.00202	.00009
106	OCD	1891.80000	7.88463	17.807021	-.47869	1.256560	.03153	7.89523	99.005664	2.39269	.00079	.00006
107	OCF	1921.80000	8.00416	99.759744	2.39096	2.559006	-.06038	8.02758	18.061548	-.48661	.00270	.00018
108	OCD	1951.80000	8.13408	18.445357	-.48834	1.270212	.03228	8.14592	99.903454	2.41059	.00786	-.00020
109	OCF	1981.80000	8.25136	99.317962	2.41600	2.593593	-.06131	8.27722	18.115647	-.47874	.00201	-.00010
110	OCD	2011.80000	8.38471	17.807091	-.47871	1.277170	.03171	8.39601	99.003852	2.39260	-.00083	-.00006
111	OCF	2041.80000	8.50424	99.761589	2.39101	2.583921	-.06142	8.52835	18.062367	-.48665	-.00271	-.00018
112	OCD	2071.80000	8.63416	18.445287	-.48832	1.263514	.03096	8.64669	99.905245	2.41068	-.00785	.00020
113	OCF	2101.80000	8.75144	99.316117	2.41596	2.549339	-.06049	8.77799	18.114828	-.47870	-.00200	.00010
114	OCD	2131.80000	8.88480	17.807161	-.47873	1.256563	.03153	8.89679	99.002083	2.39252	.00087	.00006
115	OCF	2161.80000	9.00432	99.763434	2.39105	2.559029	-.06038	9.02912	18.063188	-.48669	.00272	.00018
116	OCD	2191.80000	9.13424	18.445217	-.48830	1.270223	.03228	9.14746	99.906994	2.41077	.00785	-.00020
117	OCF	2221.80000	9.25152	99.314272	2.41591	2.593606	-.06131	9.27876	18.114006	-.47867	.00198	-.00010
118	OCD	2251.80000	9.38488	17.807231	-.47875	1.277166	.03171	9.39756	99.000356	2.39243	-.00091	-.00006
119	OCF	2281.80000	9.50441	99.765279	2.39110	2.583898	-.06142	9.52990	18.064011	-.48672	-.00273	-.00018
120	OCD	2311.80000	9.63433	18.445147	-.48828	1.263503	.03096	9.64823	99.908699	2.41085	-.00784	.00020
121	OCF	2341.80000	9.75161	99.312427	2.41586	2.549327	-.06049	9.77954	18.113182	-.47863	-.00197	.00010
122	OCD	2371.80000	9.88496	17.807301	-.47877	1.256567	.03153	9.89834	98.998671	2.39234	.00095	.00006
123	OCF	2401.80000	10.00449	99.767123	2.39115	2.559052	-.06038	10.03067	18.064836	-.48676	.00274	.00018
124	OCD	2431.80000	10.13441	18.445076	-.48826	1.270233	.03228	10.14900	99.910362	2.41094	.00784	-.00020
125	OCF	2461.80000	10.25169	99.310583	2.41582	2.593619	-.06131	10.28031	18.112355	-.47860	.00196	-.00010
126	OCD	2491.80000	10.38505	17.807372	-.47879	1.277163	.03171	10.39911	98.997030	2.39226	-.00098	-.00006
127	OCF	2521.80000	10.50457	99.768968	2.39119	2.583875	-.06142	10.53144	18.065664	-.48679	-.00275	-.00018
128	OCD	2551.80000	10.63449	18.445005	-.48824	1.263493	.03096	10.64976	99.911982	2.41102	-.00784	.00020
129	OCF	2581.80000	10.75177	99.308739	2.41577	2.549314	-.06049	10.78108	18.111526	-.47856	-.00194	.00010
130	OCD	2611.80000	10.88513	17.807444	-.47881	1.256570	.03153	10.89989	98.995431	2.39218	.00102	.00005
131	OCF	2641.80000	11.00465	99.770811	2.39124	2.559075	-.06038	11.03222	18.066494	-.48683	.00276	.00018
132	OCD	2671.80000	11.13457	18.444933	-.48822	1.270244	.03228	11.15053	99.913559	2.41110	.00783	-.00020
133	OCF	2701.80000	11.25186	99.306895	2.41572	2.593632	-.06131	11.28185	18.110695	-.47853	.00193	-.00010
134	OCD	2731.80000	11.38522	17.807515	-.47883	1.277159	.03171	11.40066	98.993876	2.39210	-.00106	-.00005

135	OCF	2761,8000011,50474	99,772655	2,39129	2,583852	-,06142	11,53299	18,067326	-,48686	-,00277	-,00018
136	OCD	2791,8000011,63465	18,444862	-,48820	1,263482	,03096	11,65130	99,915093	2,41118	-,00783	,00020
137	OCF	2821,8000011,75194	99,305052	2,41568	2,549301	-,06049	11,78262	18,109862	-,47850	-,00192	,00010
138	OCD	2851,8000011,88530	17,807587	-,47885	1,256574	,03154	11,90144	98,992364	2,39201	,00110	,00005
139	OCF	2881,8000012,00482	99,774499	2,39133	2,559098	-,06038	12,03376	18,068160	-,48689	,00277	,00018
140	OCD	2911,8000012,13473	18,444789	-,48818	1,270255	,03228	12,15207	99,916583	2,41127	,00782	-,00020
141	OCF	2941,8000012,25202	99,303208	2,41563	2,593644	-,06131	12,28339	18,109027	-,47846	,00190	-,00010
142	OCD	2971,8000012,38539	17,807659	-,47887	1,277156	,03171	12,40222	98,990896	2,39193	-,00114	-,00005
143	OCF	3001,8000012,50490	99,776342	2,39138	2,583829	-,06142	12,53454	18,068996	-,48693	-,00278	-,00018
144	OCD	3031,8000012,63481	18,444717	-,48816	1,263471	,03096	12,65284	99,918030	2,41135	-,00781	,00020
145	O	3034,4000012,65568	21,436987	-,66271	1,343979	,03096	12,65726	87,840076	2,23402	-,00729	,00020
146	C	3060,0000012,74926	99,364785	-2,38137	2,546993	,06302	12,76809	18,125260	,48818	-,00216	,00020
147	F	3061,8000012,75210	99,301365	2,41558	2,549288	-,06049	12,78416	18,108190	-,47843	-,00189	,00010
148	O	3064,4000012,75655	87,205640-	2,23662	2,392013	-,06049	12,80542	21,054780	-,65488	-,00162	,00010
149	C	3090,0000012,86912	17,800145	,47456	1,253805	-,02843	12,90014	98,995617	-2,38854	,00103	,00010
150	D	3091,8000012,88547	17,807732	-,47889	1,256577	,03154	12,90299	98,989471	2,39185	,00117	,00005
151	O	3094,4000012,90705	20,764652	-,65838	1,338571	,03154	12,90745	87,010809	2,21532	,00130	,00005
152	S	3120,0000013,00215	99,715995	-2,42565	2,145889	,03154	13,01910	18,082344	,47719	,00259	,00005
153	F	3121,8000013,00498	99,779366	2,39147	2,109570	-,07160	13,03520	18,101924	-,48838	,00279	,00018
154	O	3124,4000013,00941	87,798940	2,21639	1,923414	-,07160	13,05643	21,104034	-,66627	,00326	,00018
155	C	3150,0000013,11912	18,452060	,49250	,500844	-,03954	13,15049	99,991694	-2,41411	,00783	,00018
156	D	3151,8000013,13489	18,444395	-,48812	,450486	-,01682	13,15331	99,990313	2,41486	,00781	-,00020
157	R	3173,7000013,23748	72,022734	-1,95838	,082230	-,01682	13,22258	26,987489	,91861	,00342	-,00020
158	B	3179,6000013,24870	97,468256	-2,35447	,006662	-,00880	13,26508	18,524838	,51570	,00224	-,00020
159	G	3180,0000013,24935	99,362573	-2,38132	,003142	-,00880	13,26855	18,123215	,48836	,00216	-,00020
160	F	3181,8000013,25219	99,299172	2,41552	-,012608	-,00857	13,28462	18,105350	-,47815	,00188	-,00010
161	G	3182,2000013,25284	97,377766	2,38799	-,016036	-,00857	13,28810	18,498728	-,50529	,00184	-,00010
162	B	3188,1000013,26409	71,595692	1,98190	-,042966	-,00056	13,33077	26,822028	-,90539	,00123	-,00010
163	R	3210,0000013,36921	17,800020	,47452	-,055172	-,00056	13,40062	99,017001	-2,39119	-,00106	-,00010
164	SS	3210,0000013,36921	17,800020	,47452	-,055172	-,00056	13,40062	99,017001	-2,39119	-,00106	-,00010
165	D	3211,8000013,38556	17,807721	-,47893	-,058596	-,00328	13,40347	99,018400	2,39043	-,00120	-,00005
166	O	3214,4000013,40714	20,764815	-,65842	-,067111	-,00328	13,40793	87,046540	2,21413	-,00133	-,00005
167	S	3240,0000013,50224	99,719116	-2,42573	-,150953	-,00328	13,51941	18,121104	,47827	-,00260	-,00005
168	F	3241,8000013,50507	99,782502	2,39154	-,150273	,00403	13,53547	18,139748	-,48892	-,00280	-,00018
169	O	3244,4000013,50949	87,801709	2,21646	-,139807	,00403	13,55666	21,143897	-,66652	-,00326	-,00018
170	S	3270,0000013,61920	18,451941	,49252	-,036757	,00403	13,65062	100,034387	-2,41514	-,00783	-,00018
171	D	3271,8000013,63498	18,444204	-,48810	-,031010	,00241	13,65344	100,032977	2,41590	-,00781	,00020
172	O	3274,4000013,65585	21,436144	-,66265	-,024753	,00241	13,65785	87,932288	2,23821	-,00729	,00020
173	S	3300,0000013,74944	99,360895	-2,38129	,036853	,00241	13,76864	18,125421	,48862	-,00215	,00020
174	F	3301,8000013,75228	99,297513	2,41548	,039538	,00056	13,78471	18,106777	-,47797	-,00188	,00010
175	O	3304,4000013,75673	87,202315	2,23652	,040982	,00056	13,80597	21,050834	-,65436	-,00161	,00010
176	S	3330,0000013,86929	17,800027	,47450	,055192	,00056	13,90071	99,017035	-2,39119	,00106	,00010
177	D	3331,8000013,88565	17,807800	-,47895	,058613	,00327	13,90356	99,018454	2,39043	,00120	,00005
178	O	3334,4000013,90723	20,765011	-,65844	,067125	,00327	13,90802	87,046615	2,21413	,00133	,00005
179	S	3360,0000014,00233	99,721088	-2,42578	,150933	,00327	14,01950	18,121206	,47827	,00260	,00005
180	F	3361,8000014,00516	99,784466	2,39159	,150251	-,00403	14,03556	18,139849	-,48893	,00280	,00018

181	O	3364.4000014.00958	87.803419	2.21650	.139784	-.00403	14.05675	21.144005	-.66652	.00327	.00018
182	S	3390.0000014.11929	18.451935	.49254	.036727	-.00403	14.15070	100.034353	-2.41514	.00783	.00018
183	D	3391.8000014.13507	18.444126	-.48808	.030978	-.00241	14.15353	100.032923	2.41591	.00781	-.00020
184	O	3394.4000014.15594	21.435948	-.66262	.024716	-.00241	14.15794	87.932213	2.23821	.00729	-.00020
185	S	3420.0000014.24952	99.358923	-2.38124	-.036937	-.00241	14.26873	18.125318	.48862	.00215	-.00020
186	F	3421.8000014.25237	99.295550	2.41543	-.039622	-.00055	14.28480	18.106676	-.47796	.00188	-.00010
187	O	3424.4000014.25681	87.200605	2.23647	-.041059	-.00055	14.30606	21.050726	-.65436	.00161	-.00010
188	S	3450.0000014.36938	17.800033	.47448	-.055213	-.00055	14.40080	99.017069	-2.39120	-.00107	-.00010
189	D	3451.8000014.38574	17.807878	-.47897	-.058631	-.00327	14.40365	99.018509	2.39042	-.00121	-.00005
190	O	3454.4000014.40732	20.765208	-.65847	-.067139	-.00327	14.40811	87.046690	2.21412	-.00133	-.00005
191	S	3480.0000014.50242	99.723060	-2.42583	-.150912	-.00327	14.51959	18.121309	.47827	-.00260	-.00005
192	F	3481.8000014.50525	99.786429	2.39164	-.150229	.00403	14.53565	18.139950	-.48893	-.00280	-.00018
193	O	3484.4000014.50967	87.805129	2.21655	-.139762	.00403	14.55684	21.144113	-.66652	-.00327	-.00018
194	S	3510.0000014.61937	18.451928	.49256	-.036696	.00403	14.65079	100.034318	-2.41513	-.00783	-.00018
195	D	3511.8000014.63515	18.444047	-.48806	-.030945	.00241	14.65361	100.032868	2.41591	-.00781	.00020
196	O	3514.4000014.65602	21.435751	-.66260	-.024679	.00241	14.65803	87.932137	2.23822	-.00729	.00020
197	S	3540.0000014.74961	99.356951	-2.38120	.037021	.00241	14.76882	18.125216	.48862	-.00215	.00020
198	F	3541.8000014.75245	99.293586	2.41538	.039705	.00055	14.78489	18.106575	-.47796	-.00188	.00010
199	O	3544.4000014.75690	87.198895	2.23643	.041136	.00055	14.80615	21.050618	-.65436	-.00161	.00010
200	S	3570.0000014.86947	17.800040	.47447	.055233	.00055	14.90089	99.017104	-2.39120	.00107	.00010
201	D	3571.8000014.88583	17.807958	-.47899	.058648	.00327	14.90374	99.018564	2.39042	.00121	.00005
202	O	3574.4000014.90741	20.765405	-.65849	.067153	.00327	14.90820	87.046766	2.21412	.00134	.00005
203	S	3600.0000015.00250	99.725032	-2.42587	.150892	.00327	15.01968	18.121412	.47828	.00260	.00005
204	F	3601.8000015.00533	99.788392	2.39169	.150207	-.00403	15.03573	18.140051	-.48893	.00280	.00018
205	O	3604.4000015.00976	87.806839	2.21660	.139739	-.00403	15.05693	21.144220	-.66652	.00327	.00018
206	S	3630.0000015.11946	18.451921	.49258	.036666	-.00403	15.15088	100.034283	-2.41512	.00783	.00018
207	D	3631.8000015.13524	18.443967	-.48803	.030913	-.00241	15.15370	100.032813	2.41591	.00781	-.00020
208	O	3634.4000015.15611	21.435554	-.66258	.024642	-.00241	15.15812	87.932061	2.23822	.00729	-.00020
209	S	3660.0000015.24970	99.354979	-2.38115	-.037104	-.00241	15.26891	18.125113	.48861	.00215	-.00020
210	F	3661.8000015.25254	99.291623	2.41533	-.039788	-.00055	15.28498	18.106474	-.47796	.00188	-.00010
211	O	3664.4000015.25699	87.197185	2.23638	-.041214	-.00055	15.30624	21.050510	-.65436	.00160	-.00010
212	S	3690.0000015.36956	17.800047	.47445	-.055253	-.00055	15.40098	99.017140	-2.39121	-.00107	-.00010
213	DP11	3692.0000015.38777	17.786162	-.46729	-.058976	-.00320	15.40414	99.266526	2.27044	-.00123	-.00005
214	TP	3702.4000015.45629	34.914731	-1.17969	-.092294	-.00320	15.42588	58.747741	1.62560	-.00175	-.00005
215	DP12	3704.9000015.46681	40.929889	-1.21995	-.099923	-.00290	15.43313	51.436533	1.30669	-.00189	-.00006
216	TP	3715.3000015.49730	72.880204	-1.85220	-.130037	-.00290	15.47581	29.950611	.75927	-.00247	-.00006
217	FP13	3717.8000015.50251	78.775518	-.46804	-.134107	-.00035	15.48972	27.827945	.10335	-.00267	-.00011
218	TP	3728.2000015.52220	90.184537	-.62898	-.137718	-.00035	15.54873	29.606469	-.27436	-.00376	-.00011
219	FP14	3730.7000015.52669	84.095840	2.97891	-.131429	.00534	15.56141	34.518575	-1.75854	-.00423	-.00027
220	TP	3741.1000015.55747	34.833810	1.75782	-.075944	.00534	15.59236	83.919368	-2.99154	-.00705	-.00027
221	DP14	3743.6000015.57001	29.952282	.26243	-.066381	.00238	15.59685	90.091625	.60936	-.00735	.00003
222	TP	3754.0000015.62809	28.353583	-.10871	-.041606	.00238	15.61651	79.063337	.45106	-.00701	.00003
223	DP13	3756.5000015.64174	30.525517	-.77394	-.036607	.00163	15.62170	73.235083	1.84279	-.00676	.00017
224	TP	3766.9000015.68365	52.289023	-1.31871	-.019617	.00163	15.65195	41.397259	1.21854	-.00503	.00017
225	FP12	3769.4000015.69079	59.665911	-1.63992	-.015606	.00158	15.66234	35.380575	1.18171	-.00460	.00018
226	TP	3779.6000015.71223	100.464125	-2.28299	.000798	.00158	15.72969	18.127067	.47728	-.00272	.00018
227	FP11	3781.8000015.71536	100.152436	2.43393	.003866	.00147	15.74756	18.128208	-.47787	-.00248	.00006
228	TM1	3786.0000015.72276	80.926948	2.14357	.010028	.00147	15.78029	23.337616	-.76246	-.00222	.00006

230	G	3792,3000015,73761	56,659553	1,70832	,019271	,00147	15,81534	35,633958	-1,18935	-,02081	-,00560
231	UH1	3798,2000015,75767	38,907246	1,30050	,027926	,00147	15,83722	52,026867	-1,58913	-,07057	-,01127
232	G	3798,6000015,75932	37,877912	1,27283	,028513	,00147	15,83843	53,309010	-1,61623	-,07508	-,01127
233	UH1	3804,5000015,78987	25,265405	,86485	,037168	,00147	15,85332	74,739123	-2,01601	-,15825	-,01693
234	G	3804,9000015,79242	24,584597	,83717	,037754	,00147	15,85417	76,362773	-2,04311	-,16502	-,01693
235	TH2	3810,0000015,83157	17,844907	,48434	,045235	,00147	15,86351	98,964975	-2,38869	-,25135	-,01693
236	FH1	3812,5000015,85658	13,627759	1,12136	,045620	-,00116	15,86714	127,359895	-9,50546	-,31287	-,03287
237	TH3	3818,7000015,97571	6,090519	,09433	,038412	-,00116	15,87243	272,800219	-13,95265	-,51668	-,03287
238	DH2	3823,7000016,07614	14,473909	-2,10783	,044667	,00379	15,87525	237,116219	19,53041	-,51059	,03518
239	TH4	3825,8000016,09375	24,985184	-2,89754	,052633	,00379	15,87695	162,201247	16,14339	-,43671	,03518
240	FH3	3830,8000016,11560	46,990200	-,92789	,060674	-,00068	15,88477	72,409458	4,04685	-,33556	,00656
241	TH5	3831,8000016,11892	48,885574	-,96749	,059993	-,00068	15,88710	64,555746	3,80687	-,32899	,00656
242	FH4	3834,8000016,12655	48,069578	1,22686	,053905	-,00333	15,89561	51,141795	,86827	-,33181	-,00846
243	TH6	3888,2364016,42889	65,765612	-1,55802	-,124096	-,00333	16,13151	56,274112	-,96432	-,78397	-,00846
244	VH2	3894,1364016,44139	85,960216	-1,86470	-,143746	-,00333	16,14662	68,846722	-1,16665	-,81189	-,00100
245	G	3894,5364016,44212	87,460309	-1,88553	-,145077	-,00333	16,14754	69,785532	-1,18037	-,81229	-,00100
246	VH2	3900,4364016,45164	111,517141	-2,19178	-,164719	-,00333	16,15975	84,907569	-1,38271	-,79620	,00646
247	G	3900,8364016,45220	113,278894	-2,21260	-,166051	-,00333	16,16050	86,019223	-1,39643	-,79362	,00646
248	VH2	3906,7364016,45963	141,192237	-2,51834	-,185683	-,00333	16,17044	103,690686	-1,59876	-,73351	,01392
249	G	3907,1364016,46008	143,215231	-2,53914	-,187014	-,00333	16,17106	104,975184	-1,61248	-,72795	,01392
250	VH2	3913,0364016,46601	174,978452	-2,84430	-,206636	-,00332	16,17925	125,196073	-1,81482	-,62384	,02138
251	G	3913,4364016,46637	177,262207	-2,86508	-,207966	-,00332	16,17976	126,653415	-1,82854	-,61529	,02138
252	VH2	3919,3364016,47121	212,867755	-3,16959	-,227577	-,00332	16,18658	149,423730	-2,03087	-,46716	,02884
253	G	3919,7364016,47151	215,411728	-3,19034	-,228906	-,00332	16,18701	151,053917	-2,04459	-,45563	,02884
254	VH2	3925,6364016,47551	254,851143	-3,49412	-,248504	-,00332	16,19276	176,373658	-2,24693	-,26350	,03629
255	G	3926,0364016,47576	257,654729	-3,51485	-,249832	-,00332	16,19312	178,176688	-2,26065	-,24898	,03629
256	DH5	3927,0364016,47637	266,065274	-4,90987	-,253788	-,00459	16,19400	181,817436	-1,37396	-,21209	,03746
257	TH7	3963,0466016,48928	742,040393	-8,30792	-,419198	-,00459	16,21858	301,366413	-1,94590	1,13690	,03746
258	FH6	3966,0466016,48994	680,110652	27,88953	-,401029	,01655	16,22007	362,828829	-19,57396	1,34008	,09971
259	TH8	3968,4185016,49055	554,250808	25,17335	-,361769	,01655	16,22099	461,640117	-22,08517	1,57659	,09971
260	DH7	3970,4185016,49116	505,204434	,10723	-,345144	,00020	16,22164	506,979049	,12461	1,70000	,02274
261	TH9	3977,1185016,49328	503,857396	,09382	-,343788	,00020	16,22374	505,399167	,11119	1,85239	,02274
262	UH3	3983,0185016,49514	502,791050	,08691	-,342583	,00021	16,22560	504,156850	,09937	1,96420	,01516
263	G	3983,4185016,49527	502,721639	,08611	-,342501	,00021	16,22573	504,077672	,09857	1,97026	,01516
264	UH3	3989,3185016,49714	501,746548	,07919	-,341277	,00021	16,22759	502,984261	,08675	2,03729	,00757
265	G	3989,7185016,49727	501,683519	,07838	-,341193	,00021	16,22772	502,915179	,08595	2,04031	,00757
266	UH3	3995,6185016,49914	500,799523	,07144	-,339950	,00021	16,22959	501,970676	,07413	2,06256	-,00002
267	G	3996,0185016,49927	500,742692	,07064	-,339865	,00021	16,22972	501,911689	,07333	2,06255	-,00002
268	TH10	4030,4185016,51024	498,257797	,00160	-,332556	,00021	16,24066	499,236759	,00443	2,06174	-,00002
269	TH11	4058,9185016,51933	499,796935	-,05560	-,326501	,00021	16,24974	500,611462	-,05266	2,06107	-,00002
270	UH4	4064,8185016,52121	500,495808	-,06285	-,325239	,00022	16,25162	501,302592	-,06448	2,03922	-,00738
271	G	4065,2185016,52134	500,546407	-,06365	-,325153	,00022	16,25174	501,354496	-,06528	2,03626	-,00738
272	UH4	4071,1185016,52321	501,340162	-,07088	-,323873	,00022	16,25361	502,194533	-,07710	1,97098	-,01475
273	G	4071,5185016,52334	501,397188	-,07168	-,323786	,00022	16,25374	502,256533	-,07790	1,96508	-,01475
274	UH4	4077,4185016,52521	502,285642	-,07890	-,322488	,00022	16,25561	503,245477	-,08972	1,85637	-,02211

275	G	4077,8185016,52534	502,349081	-,07970	-,322400	,00022	16,25573	503,317573	-,09052	1,84753	-,02211
276	UH4	4083,7185016,52720	503,332030	-,08690	-,321085	,00022	16,25760	504,455424	-,10234	1,69539	-,02947
277	G	4084,1185016,52733	503,401868	-,08770	-,320995	,00022	16,25772	504,537615	-,10314	1,68361	-,02947
278	UH4	4090,0185016,52919	504,479082	-,09488	-,319663	,00023	16,25958	505,824375	-,11496	1,48804	-,03683
279	G	4090,4185016,52932	504,555303	-,09568	-,319572	,00023	16,25971	505,916661	-,11576	1,47331	-,03683
280	FH7	4092,4185016,52997	459,326705	22,00279	-,304343	,01488	16,26032	555,067793	-25,21883	1,46772	,03119
281	TH8	4094,7904016,53090	360,891718	19,49769	-,269041	,01488	16,26093	681,157083	-27,94079	1,54171	,03119
282	DH6	4097,7904016,53239	299,599410	1,96261	-,244052	,00199	16,26159	743,233099	8,31293	1,51670	-,04765
283	G	4098,1904016,53260	298,031910	1,95614	-,243257	,00199	16,26167	736,597848	8,27520	1,49764	-,04765
284	VH5	4104,0904016,53588	275,497377	1,86317	-,231520	,00199	16,26304	642,234757	7,71869	1,23843	-,04021
285	G	4104,4904016,53611	274,009437	1,85668	-,230724	,00199	16,26314	636,074895	7,68096	1,22235	-,04021
286	VH5	4110,3904016,53968	252,651057	1,76329	-,218975	,00199	16,26473	548,723732	7,12446	1,00703	-,03278
287	G	4110,7904016,53993	251,243031	1,75678	-,218178	,00199	16,26484	543,039260	7,08673	,99392	-,03278
288	VH5	4116,6904016,54383	231,065852	1,66299	-,206416	,00199	16,26672	462,700025	6,53022	,82249	-,02534
289	G	4117,0904016,54410	229,738071	1,65647	-,205618	,00199	16,26686	457,490941	6,49249	,81235	-,02534
290	VH5	4122,9904016,54837	210,746861	1,56229	-,193846	,00200	16,26910	384,163634	5,93598	,68481	-,01790
291	G	4123,3904016,54868	209,499639	1,55576	-,193047	,00200	16,26926	379,429940	5,89825	,67765	-,01790
292	VH5	4129,2904016,55336	191,698887	1,46123	-,181264	,00200	16,27199	313,114561	5,34175	,59400	-,01046
293	TH12	4133,8006016,55724	178,850687	1,38747	-,172252	,00200	16,27447	266,848610	4,91633	,54682	-,01046
294	FH5	4134,8006016,55814	175,198466	2,25859	-,169820	,00286	16,27508	258,429040	3,51743	,53773	-,00772
295	TH13	4204,0370016,76589	29,383416	-,15255	,028430	,00286	16,49135	19,407763	-,06518	,00332	-,00772
296	TH14	4226,0370016,86006	52,950723	-,91869	,091425	,00286	16,62065	47,320306	-1,20357	-,16650	-,00772
297	DH4	4229,0370016,86627	66,962147	-3,96468	,106595	,00737	16,63044	48,104609	,95427	-,17777	,00029
298	TH5	4230,0370016,87051	75,141180	-4,21435	,113961	,00737	16,63381	46,235784	,91455	-,17747	,00029
299	DH3	4235,0370016,87804	168,527693	-16,78418	,175668	,01810	16,65601	24,588592	2,84867	-,14325	,01296
300	TH4	4237,1370016,87969	246,419103	-20,30697	,213672	,01810	16,67390	14,258965	2,07020	-,11604	,01296
301	FH2	4242,1370016,88239	283,595996	14,49586	,231389	-,01139	16,77512	6,100296	-,11067	-,08261	,00111
302	TH3	4248,3370016,88748	132,464907	9,88012	,160801	-,01139	16,89293	13,851151	-1,13947	-,07575	,00111
303	DH1	4250,8370016,89097	102,956452	2,48047	,143287	-,00279	16,91755	18,121694	-,48656	-,06770	,00526
304	TH15	4259,8630016,90873	63,838851	1,85341	,118082	-,00279	16,97824	32,464991	-1,10255	-,02025	,00526
305	UH6	4265,7630016,92640	44,385506	1,44372	,101606	-,00279	17,00215	47,850653	-1,50520	-,00510	-,00012
306	TH16	4279,0370017,00351	18,301563	,52132	,064532	-,00279	17,03291	99,835690	-2,41110	-,00673	-,00012
307	DP21	4281,0370017,02129	18,139480	-,43776	,061905	,00015	17,03604	100,086986	2,28941	-,00666	,00019
308	TP	4291,4370017,08969	34,350219	-1,12097	,063424	,00015	17,05761	59,212164	1,64087	-,00465	,00019
309	DP22	4293,9370017,10041	40,060323	-1,15698	,063535	-,00006	17,06480	51,830173	1,31981	-,00418	,00018
310	TP	4304,3370017,13177	70,439477	-1,76410	,062938	-,00006	17,10721	30,100000	,76963	-,00232	,00018
311	FP23	4306,8370017,13716	76,008785	-,42784	,061289	-,00126	17,12106	27,932815	,11108	-,00193	,00014
312	TP	4317,2370017,15762	86,591229	-,58971	,048228	-,00126	17,18002	29,542274	-,26584	-,00049	,00014
313	FP24	4319,7370017,16230	80,683181	2,86992	,042641	-,00317	17,19273	34,401244	-1,74508	-,00016	,00013
314	TP	4330,1370017,19442	33,370802	1,67935	,009628	-,00317	17,22383	83,417491	-2,96803	,00114	,00013
315	DP24	4332,6370017,20751	28,732086	,24041	,002061	-,00293	17,22835	89,525084	,61080	,00139	,00007
316	TP	4343,0370017,26758	27,713593	-,14248	-,028430	-,00293	17,24815	78,479331	,45129	,00213	,00007
317	DP23	4345,5370017,28150	30,035778	-,80123	-,036505	-,00355	17,25338	72,678258	1,83186	,00226	,00003
318	TP	4355,9370017,32363	52,614051	-1,36976	-,073459	-,00355	17,28387	41,057806	1,20857	,00256	,00003
319	FP22	4358,4370017,33070	60,264507	-1,69858	-,082649	-,00380	17,29434	35,092825	1,17105	,00263	,00002
320	TP	4368,8370017,35182	102,568019	-2,36906	-,122201	-,00380	17,36215	18,043795	,46828	,00284	,00002
321	FP21	4370,8370017,35488	102,398680	2,45107	-,124009	,00201	17,38009	18,074532	-,48413	,00302	,00016
322	ES	4370,8370017,35488	102,398680	2,45107	-,12[illegible]	[illegible]	17,38009	18,074532	-,48413	,00302	,00016

323	R	4392.7370017.42211	27.864359	.95232	-.079990	[illegible]	17.48389	72.033711	-1.97976	[illegible]	[illegible]
324	B	4398.6370017.46337	19.009256	.54856	-.044489	.01002	17.48509	97.766037	-2.38164	.00739	.00016
325	G	4399.0370017.46676	18.581360	.52118	-.040479	.01002	17.49574	99.683072	-2.40694	.00740	.00016
326	D	4400.8370017.48247	18.479563	-.46301	-.023940	.00849	17.49857	99.689989	2.40521	.00741	-.00020
327	G	4401.2370017.48588	18.860482	-.48929	-.020546	.00849	17.49921	97.776710	2.37799	.00733	-.00020
328	B	4407.1370017.52804	26.921526	-.87700	.053160	.01650	17.51041	72.080301	1.97720	.00613	-.00020
329	R	4429.0370017.59859	96.851518	-2.31615	.414504	.01650	17.61394	18.144778	.48561	.00168	-.00020
330	F	4430.8370017.60151	96.773627	2.35816	.425955	-.00387	17.62998	18.138545	-.48205	.00138	-.00013
331	C	4456.4370017.69905	20.467217	.62258	.737228	.02819	17.74119	87.291774	-2.21823	-.00195	-.00013
332	O	4459.0370017.72086	17.688085	.44631	.810516	.02819	17.74563	99.285045	-2.39457	-.00228	-.00013
333	D	4460.8370017.73728	17.789892	-.50450	.897347	.06899	17.74848	99.275322	2.39982	-.00242	-.00002
334	S	4486.4370017.84789	89.835034	-2.30977	2.663385	.06899	17.84314	21.024658	.65685	-.00283	-.00002
335	O	4489.0370017.85220	102.322532	-2.49312	2.842749	.06899	17.86444	18.069282	.47983	-.00287	-.00002
336	F	4490.8370017.85496	102.400326	2.45115	2.842908	-.06881	17.88055	18.078272	-.48497	-.00303	-.00016
337	C	4516.4370017.94620	21.753689	.69914	1.491713	-.03675	17.99171	87.631614	-2.23093	-.00704	-.00016
338	O	4519.0370017.96684	18.580816	.52120	1.396155	-.03675	17.99614	99.693531	-2.40827	-.00745	-.00016
339	D	4520.8370017.98255	18.478922	-.46297	1.389945	.02980	17.99897	99.697150	2.40632	-.00741	.00020
340	C	4546.4370018.09412	85.248448	-2.14525	2.563208	.06186	18.09322	21.093891	.66296	-.00220	.00020
341	O	4549.0370018.09868	96.847954	-2.31610	2.724043	.06186	18.11445	18.107804	.48553	-.00167	.00020
342	FCO	4579.0370018.22095	17.688776	.44629	1.236362	-.03794	18.24639	99.212536	-2.39493	.00232	.00013
343	DCO	4609.0370018.35228	102.324847	-2.49314	2.300111	.05282	18.36521	18.069692	.47983	.00288	.00002
344	FCO	4639.0370018.46692	18.580334	.52121	1.137592	-.02640	18.49691	99.694356	-2.40826	.00744	.00016
345	DCO	4669.0370018.59876	96.845640	-2.31608	2.419037	.05995	18.61522	18.107393	.48553	.00166	-.00020
346	FCO	4699.0370018.72103	17.689257	.44628	1.297436	-.02531	18.74716	99.211722	-2.39493	-.00235	-.00013
347	DCO	4729.0370018.85236	102.327160	-2.49317	2.842907	.06899	18.86598	18.070104	.47983	-.00289	-.00001
348	FCO	4759.0370018.96700	18.579853	.52122	1.396124	-.03676	18.99768	99.695158	-2.40826	-.00743	-.00016
349	DCO	4789.0370019.09885	96.843329	-2.31605	2.723761	.06185	19.11599	18.106980	.48553	-.00164	.00020
350	FCO	4819.0370019.22112	17.689739	.44627	1.236228	-.03794	19.24794	99.210931	-2.39494	.00239	.00013
351	DCO	4849.0370019.35244	102.329469	-2.49320	2.299953	.05282	19.36676	18.070518	.47983	.00290	.00001
352	FCO	4879.0370019.46708	18.579371	.52124	1.137624	-.02648	19.49845	99.695938	-2.40826	.00742	.00015
353	DCO	4909.0370019.59893	96.841021	-2.31602	2.419319	.05996	19.61677	18.106565	.48553	.00163	-.00020
354	FCO	4939.0370019.72120	17.690221	.44625	1.297571	-.02531	19.74871	99.210162	-2.39494	-.00243	-.00013
355	DCO	4969.0370019.85252	102.331775	-2.49322	2.843065	.06899	19.86753	18.070934	.47984	-.00290	-.00001
356	FCO	4999.0370019.96716	18.578889	.52125	1.396092	-.03677	19.99922	99.696695	-2.40825	-.00740	-.00015
357	DCO	5029.0370020.09902	96.838716	-2.31599	2.723479	.06184	20.11754	18.106149	.48553	-.00161	.00020
358	FCO	5059.0370020.22129	17.690704	.44624	1.236094	-.03793	20.24949	99.209417	-2.39495	.00246	.00013
359	DCO	5089.0370020.35260	102.334079	-2.49325	2.299795	.05282	20.36830	18.071351	.47984	.00291	.00001
360	FCO	5119.0370020.46725	18.578406	.52126	1.137656	-.02648	20.49999	99.697429	-2.40824	.00739	.00015
361	DCO	5149.0370020.59910	96.836414	-2.31597	2.419601	.05996	20.61831	18.105731	.48552	.00160	-.00020
362	FCO	5179.0370020.72137	17.691187	.44623	1.297705	-.02532	20.75026	99.208695	-2.39496	-.00250	-.00013
363	DCO	5209.0370020.85268	102.336379	-2.49328	2.843223	.06899	20.86908	18.071770	.47984	-.00292	-.00001
364	FCO	5239.0370020.96733	18.577922	.52127	1.396060	-.03677	21.00076	99.698140	-2.40824	-.00738	-.00015
365	DCO	5269.0370021.09919	96.834115	-2.31594	2.723197	.06183	21.11908	18.105311	.48552	-.00159	.00020
366	FCO	5299.0370021.22146	17.691671	.44622	1.235960	-.03793	21.25103	99.207995	-2.39496	.00253	.00018
367	DCO	5329.0370021.35276	102.338677	-2.49331	2.299637	.05281	21.36985	18.072190	.47984	.00293	.00001
368	FCO	5359.0370021.46741	18.577438	.52129	1.137688	-.02647	21.50153	99.698828	-2.40823	.00737	.00015
369	DCO	5389.0370021.59927	96.831819	-2.31591	2.419883	.05997	21.61985	18.104890	.48552	.00157	-.00020

370	FCO	5419.0370021.72154	17.692155	.44620	1.297839	-.02532	21.75181	99.207319	-2.39497	-.00257	-.00014
371	DCO	5449.0370021.85284	102.340971	-2.49333	2.843380	.06899	21.87062	18.072612	.47984	-.00293	-.00001
372	FCO	5479.0370021.96749	18.576954	.52130	1.396028	-.03678	22.00230	99.699493	-2.40822	-.00736	-.00015
373	DCO	5509.0370022.09936	96.829526	-2.31589	2.722915	.06183	22.12062	18.104467	.48552	-.00156	.00020
374	FCO	5539.0370022.22163	17.692639	.44619	1.235825	-.03792	22.25258	99.206666	-2.39498	.00260	.00014
375	DCO	5569.0370022.35293	102.343263	-2.49336	2.299480	.05281	22.37139	18.073036	.47985	.00294	.00001
376	FCO	5599.0370022.46757	18.576469	.52131	1.137720	-.02646	22.50307	99.700134	-2.40821	.00734	.00015
377	DCO	5629.0370022.59944	96.827236	-2.31586	2.420165	.05998	22.62139	18.104043	.48551	.00154	-.00020
378	FCO	5659.0370022.72171	17.693124	.44618	1.297973	-.02533	22.75336	99.206036	-2.39499	-.00264	-.00014
379	DCO	5689.0370022.85301	102.345551	-2.49338	2.843537	.06899	22.87217	18.073461	.47985	-.00295	-.00001
380	FCO	5719.0370022.96765	18.575984	.52132	1.395995	-.03679	23.00384	99.700753	-2.40820	-.00733	-.00015
381	DCO	5749.0370023.09953	96.824949	-2.31583	2.722632	.06182	23.12217	18.103617	.48551	-.00153	.00020
382	FCO	5779.0370023.22180	17.693610	.44617	1.235691	-.03792	23.25413	99.205429	-2.39500	.00268	.00014
383	DCO	5809.0370023.35309	102.347837	-2.49341	2.299323	.05281	23.37294	18.073888	.47985	.00296	.00001
384	FCO	5839.0370023.46773	18.575498	.52134	1.137752	-.02646	23.50461	99.701348	-2.40819	.00732	.00015
385	DCO	5869.0370023.59961	96.822665	-2.31581	2.420448	.05999	23.62294	18.103190	.48551	.00152	-.00020
386	FCO	5899.0370023.72188	17.694096	.44615	1.298107	-.02533	23.75491	99.204846	-2.39501	-.00271	-.00014
387	DCO	5929.0370023.85317	102.350120	-2.49344	2.843694	.06899	23.87371	18.074315	.47986	-.00296	-.00000
388	FCO	5959.0370023.96781	18.575012	.52135	1.395963	-.03679	24.00538	99.701919	-2.40818	-.00730	-.00015
389	DCO	5989.0370024.09970	96.820384	-2.31578	2.722350	.06181	24.12371	18.102761	.48550	-.00150	.00020
390	FCO	6019.0370024.22197	17.694583	.44614	1.235557	-.03791	24.25568	99.204286	-2.39502	.00275	.00014
391	DCO	6049.0370024.35325	102.352399	-2.49346	2.299166	.05281	24.37448	18.074745	.47986	.00297	.00000
392	FCO	6079.0370024.46789	18.574525	.52136	1.137785	-.02645	24.50615	99.702467	-2.40817	.00729	.00015
393	DCO	6109.0370024.59978	96.818106	-2.31576	2.420731	.06000	24.62448	18.102331	.48550	.00149	-.00020
394	FCO	6139.0370024.72205	17.695070	.44613	1.298241	-.02534	24.75645	99.203749	-2.39503	-.00278	-.00014
395	DCO	6169.0370024.85333	102.354676	-2.49349	2.843851	.06899	24.87526	18.075175	.47987	-.00298	-.00000
396	FCO	6199.0370024.96797	18.574038	.52137	1.395930	-.03680	25.00692	99.702992	-2.40816	-.00728	-.00015
397	DCO	6229.0370025.09987	96.815831	-2.31573	2.722067	.06180	25.12525	18.101900	.48550	-.00147	.00020
398	FCO	6259.0370025.22214	17.695557	.44612	1.235423	-.03791	25.25723	99.203236	-2.39504	.00282	.00014
399	DCO	6289.0370025.35341	102.356950	-2.49352	2.299010	.05281	25.37603	18.075607	.47987	.00299	.00000
400	FCO	6319.0370025.46805	18.573550	.52138	1.137817	-.02644	25.50770	99.703494	-2.40815	.00726	.00015
401	DCO	6349.0370025.59995	96.813558	-2.31570	2.421014	.06001	25.62602	18.101468	.48549	.00146	-.00020
402	FCO	6379.0370025.72222	17.696045	.44611	1.298375	-.02534	25.75800	99.202747	-2.39505	-.00285	-.00014
403	DCO	6409.0370025.85349	102.359220	-2.49354	2.844007	.06899	25.87680	18.076040	.47987	-.00299	-.00000
404	FCO	6439.0370025.96813	18.573062	.52140	1.395898	-.03681	26.00847	99.703971	-2.40814	-.00725	-.00015
405	DCO	6469.0370026.10004	96.811289	-2.31568	2.721784	.06179	26.12680	18.101034	.48549	-.00144	.00020
406	FCO	6499.0370026.22230	17.696533	.44609	1.235289	-.03790	26.25878	99.202281	-2.39507	.00289	.00014
407	DCO	6529.0370026.35357	102.361488	-2.49357	2.298854	.05281	26.37758	18.076474	.47988	.00300	-.00000
408	FCO	6559.0370026.46821	18.572573	.52141	1.137850	-.02644	26.50924	99.704425	-2.40812	.00724	.00015
409	DCO	6589.0370026.60012	96.809023	-2.31565	2.421297	.06002	26.62757	18.100599	.48548	.00143	-.00020
410	FCO	6619.0370026.72239	17.697022	.44608	1.298509	-.02535	26.75955	99.201838	-2.39508	-.00292	-.00014
411	DCO	6649.0370026.85365	102.363753	-2.49359	2.844163	.06899	26.87835	18.076909	.47988	-.00301	.00000
412	FCO	6679.0370026.96829	18.572084	.52142	1.395865	-.03681	27.01001	99.704856	-2.40811	-.00722	-.00014
413	DCO	6709.0370027.10021	96.806760	-2.31563	2.721501	.06178	27.12834	18.100163	.48548	-.00141	.00020
414	FCO	6739.0370027.22247	17.697512	.44607	1.235155	-.03789	27.26032	99.201420	-2.39510	.00296	.00014
415	DCO	6769.0370027.35373	102.366015	-2.49362	2.298698	.05281	27.37912	18.077346	.47989	.00301	-.00000
[illegible]	[illegible]	[illegible]	[illegible]	[illegible]	1.137883	-.02643	27.51078	99.705263	-2.40809	.00721	.00014

417	DCO	6829.0370027.60029	96.804500	-2.31560	2.421580	.06002	27.62911	18.099726	.48547	.00140	-.00020
418	FCO	6859.0370027.72256	17.698002	.44606	1.298643	-.02535	27.76110	99.201025	-2.39511	-.00299	-.00014
419	DCO	6889.0370027.85381	102.368273	-2.49364	2.844319	.06900	27.87989	18.077783	.47990	-.00302	.00000
420	FCO	6919.0370027.96845	18.571104	.52144	1.395832	-.03682	28.01155	99.705646	-2.40808	-.00719	-.00014
421	DCO	6949.0370028.10038	96.802242	-2.31558	2.721217	.06178	28.12988	18.099288	.48546	-.00138	.00020
422	FCO	6979.0370028.22264	17.698492	.44605	1.235021	-.03789	28.26187	99.200654	-2.39513	.00303	.00015
423	D	6980.8370028.23905	17.802066	-.50524	1.219707	.02075	28.26472	99.200187	2.39538	.00316	-.00000
424	S	7006.4370028.34958	89.881276	-2.31036	1.750919	.02075	28.35931	21.069928	.65658	.00304	-.00000
425	O	7009.0370028.35389	102.371789	-2.49369	1.804870	.02075	28.38055	18.114837	.47999	.00303	-.00000
426	F	7010.8370028.35665	102.447361	2.45292	1.764079	-.06575	28.39662	18.126747	-.48680	.00315	.00014
427	C	7036.4370028.44789	21.745027	.69954	.491336	-.03369	28.50754	87.717847	-2.23058	.00682	.00014
428	O	7039.0370028.46854	18.570406	.52146	.403746	-.03369	28.51197	99.777363	-2.40770	.00719	.00014
429	D	7040.8370028.48426	18.466747	-.46222	.359840	-.01545	28.51480	99.771718	2.41074	.00713	-.00020
430	S	7066.4370028.59591	85.203330	-2.14468	-.035620	-.01545	28.60904	21.084904	.66296	.00191	-.00020
431	O	7069.0370028.60046	96.799914	-2.31555	-.075783	-.01545	28.63029	18.099018	.48545	.00138	-.00020
432	F	7070.8370028.60338	96.724352	2.35631	-.099931	-.01119	28.64638	18.089854	-.48022	.00106	-.00015
433	C	7096.4370028.70093	20.476301	.62216	.023961	.02087	28.75783	87.205290	-2.21858	-.00267	-.00015
434	O	7099.0370028.72273	17.698999	.44603	.078218	.02087	28.76228	99.200997	-2.39515	-.00305	-.00015
435	D	7100.8370028.73913	17.802656	-.50527	.119737	.02560	28.76512	99.200582	2.39537	-.00317	.00001
436	C	7126.4370028.84966	89.882297	-2.31036	1.185343	.05765	28.85979	21.034076	.65685	-.00304	.00001
437	D	7129.0370028.85597	102.372856	-2.49370	1.335244	.05765	28.88107	18.078492	.47991	-.00303	.00001
438	F	7130.8370028.85673	102.448365	2.45296	1.380118	-.00815	28.89717	18.087899	-.48529	-.00315	-.00014
439	C	7156.4370028.94797	21.744758	.69955	1.581692	.02390	29.00829	87.644795	-2.23075	-.00680	-.00014
440	O	7159.0370028.96862	18.570106	.52147	1.643839	.02390	29.01272	99.705652	-2.40804	-.00717	-.00014
441	D	7160.8370028.98434	18.466409	-.46220	1.759196	.10520	29.01555	99.707413	2.40709	-.00711	.00020
442	S	7186.4370029.09599	85.202296	-2.14467	4.452204	.10520	29.10974	21.120784	.66270	-.00190	.00020
443	O	7189.0370029.10055	96.798833	-2.31554	4.725713	.10520	29.13095	18.135364	.48554	-.00137	.00020
444	F	7190.8370029.10347	96.723333	2.35627	4.709151	-.12347	29.14700	18.128685	-.48172	-.00105	.00015
445	C	7216.4370029.20101	20.476567	.62215	1.958800	-.09141	29.25825	87.277701	-2.21839	.00269	.00015
446	O	7219.0370029.22282	17.699296	.44603	1.721139	-.09141	29.26270	99.271968	-2.39479	.00307	.00015
447	D	7220.8370029.23922	17.802992	-.50529	1.629300	-.01137	29.26554	99.264141	2.39901	.00319	-.00001
448	C	7246.4370029.34974	89.883317	-2.31037	1.748521	.02069	29.36026	20.998112	.65710	.00305	-.00001
449	O	7249.0370029.35405	102.373920	-2.49370	1.802304	.02069	29.38159	18.042117	.47982	.00303	-.00001
450	F	7250.8370029.35681	102.449368	2.45301	1.761509	-.06569	29.39772	18.049076	-.48380	.00315	.00014
451	C	7276.4370029.44805	21.744488	.69956	.490295	-.03363	29.50904	87.573482	-2.23098	.00678	.00014
452	O	7279.0370029.46870	18.569806	.52147	.402861	-.03363	29.51347	99.635951	-2.40844	.00715	.00014
453	D	7280.8370029.48442	18.466070	-.46219	.359025	-.01543	29.51631	99.645136	2.40348	.00710	-.00020
454	C	7306.4370029.59608	85.200180	-2.14464	.374390	.01663	29.61051	21.120603	.66272	.00188	-.00020
455	O	7309.0370029.60063	96.796584	-2.31552	.417625	.01663	29.63172	18.135079	.48555	.00135	-.00020
456	F	7310.8370029.60355	96.721189	2.35619	.429170	-.00389	29.64777	18.128316	-.48169	.00104	-.00015
457	C	7336.4370029.70110	20.476980	.62213	.739816	.02816	29.75903	87.275560	-2.21835	-.00272	-.00015
458	O	7339.0370029.72290	17.699788	.44602	.813041	.02816	29.76347	99.269627	-2.39475	-.00310	-.00015
459	D	7340.8370029.73930	17.803564	-.50533	.899937	.06908	29.76632	99.261866	2.39894	-.00323	.00001
460	S	7366.4370029.84982	89.886599	-2.31042	2.668476	.06908	29.86097	21.034428	.65682	-.00306	.00001
461	O	7369.0370029.85414	102.377428	-2.49375	2.848093	.06908	29.88225	18.078968	.47989	-.00304	.00001
462	F	7370.8370029.85689	102.452725	2.45313	2.848196	-.06897	29.89835	18.088484	-.48533	-.00316	-.00014
463	C	7396.4370029.94813	21.743917	.69959	1.492905	-.03691	30.00947	87.647607	-2.23080	-.00678	-.00014
464	O	7399.0370029.96878	18.569107	.52149	1.396931	-.03691	30.01389	99.708695	-2.40808	-.00715	-.00014

465	D	7400.8370029.98450	18.465245	-.46214	1.390462	.02907	30.01073	99.710352	2.40717	-.00709	.00020
466	C	7426.4370030.09616	85.196913	-2.14460	2.560420	.06173	30.11099	21.084089	.66299	-.00187	.00020
467	O	7429.0370030.10072	96.793094	-2.31547	2.720919	.06173	30.13223	18.098103	.48547	-.00134	.00020
468	F	7430.8370030.10364	96.717849	2.35606	2.713445	-.06998	30.14832	18.088819	-.48016	-.00103	.00015
469	C	7456.4370030.20118	20.477555	.62210	1.332424	-.03792	30.25978	87.202089	-2.21855	.00275	.00015
470	O	7459.0370030.22299	17.700490	.44600	1.233837	-.03792	30.26423	99.197648	-2.39512	.00313	.00015
471	D	7460.8370030.23939	17.804392	-.50538	1.218418	.02066	30.26708	99.197426	2.39524	.00326	-.00001
472	S	7486.4370030.34990	89.889878	-2.31046	1.747374	.02066	30.36167	21.071068	.65657	.00307	-.00001
473	O	7489.0370030.35422	102.380932	-2.49379	1.801096	.02066	30.38291	18.116029	.47998	.00305	-.00001
474	F	7490.8370030.35697	102.456078	2.45325	1.760311	-.06565	30.39897	18.128046	-.48685	.00317	.00014
475	C	7516.4370030.44821	21.743345	.69962	.489991	-.03359	30.50989	87.720827	-2.23059	.00678	.00014
476	O	7519.0370030.46886	18.568407	.52151	.402647	-.03359	30.51431	99.780378	-2.40770	.00714	.00014
477	D	7520.8370030.48459	18.464420	-.46208	.358866	-.01540	30.51714	99.774489	2.41088	.00708	-.00020
478	R	7542.7370030.58864	70.224655	-1.90140	.021552	-.01540	30.58657	26.924530	.91561	.00262	-.00020
479	B	7548.6370030.60014	94.948647	-2.28915	-.045679	-.00739	30.62916	18.495737	.51296	.00141	-.00020
480	G	7549.0370030.60081	96.790486	-2.31544	-.048635	-.00739	30.63264	18.096298	.48564	.00133	-.00020
481	F	7550.8370030.60373	96.715360	2.35597	-.059651	-.00476	30.64873	18.086250	-.47990	.00102	-.00015
482	G	7551.2370030.60439	94.841423	2.32888	-.061557	-.00476	30.65221	18.481053	-.50711	.00096	-.00015
483	B	7557.1370030.61595	69.718638	1.92927	-.066020	.00325	30.69489	26.831472	-.90817	.00009	-.00015
484	R	7579.0370030.72308	17.700879	.44597	.005166	.00325	30.76465	99.227085	-2.39756	-.00315	-.00015
485	D	7580.8370030.73948	17.804908	-.50542	.011328	.00364	30.76750	99.232984	2.39438	-.00328	.00001
486	SS	7580.8370030.73948	17.804908	-.50542	.011328	.00364	30.76750	99.232984	2.39438	-.00328	.00001
487	TL1	7591.1570030.80655	35.746516	-1.23310	.048940	.00364	30.78940	57.039247	1.69416	-.00320	.00001
488	VL1	7597.0570030.82824	52.750333	-1.64885	.070442	.00364	30.80926	39.410147	1.29384	.01320	.00555
489	TL2	7609.0370030.85430	102.374595	-2.49340	.114100	.00364	30.88318	18.147766	.48098	.07968	.00555
490	F	7610.8370030.85706	102.448919	2.45331	.115659	-.00192	30.89922	18.158584	-.48717	.09329	.00968
491	TL3	7611.8370030.85865	97.610804	2.38480	.113735	-.00192	30.90775	19.201057	-.55531	.10297	.00968
492	DL1	7618.8370030.86814	208.106983	-24.04970	.173032	.02053	30.97856	9.062439	1.36952	.10191	-.00995
493	TL4	7627.4370030.87144	827.672990	-47.99286	.349615	.02053	31.27723	8.974819	-1.35934	.01632	-.00995
494	FL2	7630.9370030.87204	936.397555	19.74041	.372738	-.00761	31.31489	27.133293	-4.28199	-.01786	-.01001
495	TL5	7635.3370030.87287	770.759288	17.90465	.339235	-.00761	31.33007	78.610864	-7.41746	-.06191	-.01001
496	UL2	7641.2370030.87428	573.981365	15.44688	.294303	-.00762	31.33774	190.941891	-11.62182	-.13961	-.01633
497	G	7641.6370030.87439	561.690653	15.27990	.291256	-.00762	31.33807	200.353365	-11.90687	-.14614	-.01633
498	UL2	7647.5370030.87638	395.900295	12.81960	.246312	-.00762	31.34154	365.658998	-16.11122	-.26110	-.02264
499	G	7647.9370030.87655	385.711437	12.65254	.243265	-.00762	31.34171	378.661995	-16.39627	-.27016	-.02264
500	TL6	7655.7212530.88086	214.036743	9.40156	.183961	-.00762	31.34415	677.107464	-21.94339	-.44643	-.02264
501	VL3	7661.6212530.88678	117.627249	6.93857	.139008	-.00762	31.34532	960.842431	-26.14774	-.55787	-.01513
502	G	7662.0212530.88733	112.143242	6.77145	.135960	-.00762	31.34538	981.874637	-26.43278	-.56392	-.01513
503	DL3	7667.5212530.89596	117.083344	-7.88181	.142377	.01010	31.34639	599.459612	77.82478	-.44039	.05724
504	TL3	7668.5212530.89723	133.386087	-8.42094	.152474	.01010	31.34669	453.915315	67.71952	-.38315	.05724
505	FL4	7674.0212530.90340	114.785188	10.84445	.143592	-.01311	31.35114	111.076427	10.48056	-.18898	.01803
506	TL7	7684.5212531.13951	.967839	-.00470	.005969	-.01311	31.58557	1.002121	.00271	.00038	.01803
507	TL7	7695.0212531.37414	114.982765	-10.85386	-.131654	-.01311	31.82085	110.962670	-10.47514	.18974	.01803
508	DL4	7700.5212531.37843	469.973747	-70.11806	-.270329	-.04065	31.82723	128.873312	8.14156	.20490	-.01290
509	TL3	7701.5212531.37872	620.673300	-80.58150	-.310981	-.04065	31.82855	113.112295	7.61946	.19201	-.01290
510	FL3	7707.0212531.37969	1016.651393	27.36678	-.399345	.01053	31.83748	108.302141	-6.53831	.18783	.01128

511	G	7707,4212531,37976	994,875992	27,07172	-,395131	,01053	31,83805	113,597421	-6,69989	,19234	,01120
512	UL3	7713,3212531,38088	701,060463	22,72612	-,332964	,01054	31,84418	206,716897	-9,08322	,23675	-,00377
513	TL8	7738,1055031,40920	27,966259	4,43202	-,071778	,01054	31,85330	905,093064	-19,09501	,33022	,00377
514	DL2	7741,6055031,44593	9,144665	1,41531	-,043018	,00626	31,85393	800,095478	46,37898	,29978	-,02078
515	G	7742,0055031,45335	8,064961	1,28395	-,040514	,00626	31,85401	763,422644	45,30310	,29147	-,02078
516	VL4	7747,9055031,69017	4,345927	-,65561	-,003582	,00626	31,85590	322,474645	29,43395	,17732	-,01792
517	TL9	7750,2055031,74979	9,089758	-1,40893	,010815	,00626	31,85734	201,306956	23,24766	,13610	-,01792
518	FL1	7757,2055031,81940	19,768201	,55136	,040469	,00134	31,86714	94,632591	-2,33210	,07444	-,00143
519	TL3	7758,2055031,82767	18,731449	,48539	,041814	,00134	31,86878	99,364827	-2,40014	,07301	-,00143
520	D	7760,0055031,84520	18,771201	-,50811	,046094	,00344	31,87162	99,367968	2,39844	,06734	-,00483
521	TL2	7771,9855031,91467	40,565310	-1,31110	,087365	,00344	31,89836	51,654172	1,58434	,00944	-,00483
522	VL5	7777,8855031,93402	58,368260	-1,70632	,107689	,00344	31,92041	35,324469	1,18341	-,00442	,00013
523	TL1	7788,2055031,95550	100,723821	-2,39790	,143237	,00344	31,98725	18,136170	,48212	-,00304	,00013
524	FP31	7790,2055031,95861	100,840129	2,34158	,143361	-,00332	32,00513	18,118532	-,47303	-,00291	-,00001
525	TP	7800,6055031,98012	59,088872	1,67296	,108810	-,00332	32,07261	35,262799	-1,17546	-,00297	-,00001
526	FP32	7803,1055031,98734	51,556636	1,34797	,100930	-,00299	32,08304	41,248161	-1,21229	-,00297	,00000
527	TP	7813,5055032,03036	29,428699	,77972	,069870	-,00299	32,11340	72,939671	-1,83497	-,00292	,00000
528	DP33	7816,0055032,04456	27,187713	,13099	,064029	-,00170	32,11861	78,743098	-,44910	-,00284	,00006
529	TP	7826,4055032,10549	28,509746	-,25810	,046297	-,00170	32,13835	89,735105	-,60782	-,00222	,00006
530	DP34	7828,9055032,11866	33,223014	-1,69251	,044403	,00018	32,14287	83,591943	2,97877	-,00196	,00015
531	TP	7839,3055032,15078	81,008598	-2,90226	,046242	,00018	32,17393	34,408315	1,75042	-,00041	,00015
532	FP34	7841,8055032,15544	87,045564	,57229	,044278	-,00173	32,18664	29,524826	,27064	-,00006	,00014
533	TP	7852,2055032,17574	76,791391	,41368	,026242	-,00173	32,24574	27,827291	-,10741	,00138	,00014
534	FP33	7854,7055032,18107	71,251662	1,76661	,021313	-,00219	32,25964	29,971072	-,76379	,00176	,00017
535	TP	7865,1055032,21198	40,761789	1,16511	-,001495	-,00219	32,30225	51,572039	-1,31322	,00351	,00017
536	DP32	7867,6055032,22251	35,002243	1,13255	-,006965	-,00218	32,30948	58,918422	-1,63317	,00395	,00018
537	TP	7878,0055032,28952	18,498823	,45432	-,029631	-,00218	32,33115	99,620468	-2,28049	,00582	,00018
538	DP31	7880,0055032,30697	18,623233	-,51845	-,035458	-,00369	32,33430	99,377613	2,39810	,00590	-,00010
539	G	7880,4055032,31035	19,048895	-,54570	-,036955	-,00369	32,33495	97,470001	2,37093	,00587	-,00010
540	UM1	7886,3055032,35157	27,859431	-,94760	-,058720	,00369	32,34618	71,857807	1,97013	-,00646	-,00408
541	R	7908,2055032,41894	102,037801	-2,43954	-,139583	,00369	32,44989	18,146717	,48243	-,09584	-,00408
542	F	7910,0055032,42171	101,950110	2,48685	-,140132	,00309	32,46593	18,152203	-,48556	-,10747	-,00894
543	G	7910,4055032,42234	99,971907	2,45866	-,138897	,00309	32,46940	18,551547	-,51280	-,11105	-,00894
544	VM2	7916,3055032,43331	73,406994	2,04372	-,120681	,00309	32,51188	26,972217	-,91445	-,13950	-,00070
545	G	7916,7055032,43419	71,783305	2,01551	-,119446	,00309	32,51421	27,714672	-,94168	-,13978	-,00070
546	VM2	7922,6055032,44981	50,451111	1,60000	-,101221	,00309	32,54214	41,196179	-1,34334	-,11965	,00753
547	TM1	7938,2055032,53722	17,703475	,49921	-,053025	,00309	32,58128	99,676012	-2,40536	-,00220	,00753
548	D	7940,0055032,55371	17,614253	-,44822	-,049696	,00064	32,58411	99,670844	2,40815	,01125	,00731
549	TM1	7955,6055032,64363	48,190512	-1,51180	-,039780	,00064	32,62328	41,137661	1,34397	,12528	,00731
550	UM2	7961,5055032,66002	68,399100	-1,91327	-,036028	,00064	32,65126	27,653502	,94150	,14411	-,00092
551	G	7961,9055032,66094	69,940620	-1,94053	-,035773	,00064	32,65360	26,911216	,91422	,14374	-,00092
552	UM2	7967,8055032,67246	95,205255	-2,34146	-,032019	,00064	32,69619	18,498162	,51174	,11400	-,00916
553	G	7968,2055032,67312	97,089301	-2,36870	-,031765	,00064	32,69967	18,099682	,48446	,11034	-,00916
554	F	7970,0055032,67603	97,177329	2,32122	-,029270	,00212	32,71576	18,094199	-,48132	,09843	-,00417
555	R	7991,9055032,74629	27,055669	,88160	,017064	,00212	32,81967	71,823112	-1,97205	,00710	-,00417
556	VM1	7997,8055032,78829	18,920727	,49380	,029547	,00212	32,83090	97,462779	-2,37366	-,00575	-,00019
557	G	7998,2055032,79169	18,536202	,46751	,030393	,00212	32,83155	99,372602	-2,40089	-,00583	-,00019
558	D	8000,0055032,80736	18,625968	-,51881	,035582	,00369	32,83439	99,377752	2,39811	-,00590	,00010

559	S	8025,6055032,91497	89,844974	-2,26318	,130089	,00369	32,92877	21,114360	,65905	-,00338	,00010
560	O	8028,2055032,91929	102,074143	-2,44034	,139688	,00369	32,94997	18,146526	,48243	-,00312	,00010
561	F	8030,0055032,92206	101,986155	2,48781	,140231	-,00309	32,96601	18,152009	-,48556	-,00308	-,00005
562	S	8055,6055033,01584	20,807917	,68322	,061067	-,00309	33,07694	87,628775	-2,22838	-,00434	-,00005
563	O	8058,2055033,03745	17,731709	,49994	,053027	-,00309	33,08137	99,676549	-2,40538	-,00447	-,00005
564	D	8060,0055033,05391	17,641992	-,44867	,049693	-,00064	33,08420	99,671396	2,40816	-,00437	,00016
565	S	8085,6055033,16866	85,239297	-2,19185	,033346	-,00064	33,17851	21,079941	,66182	-,00015	,00016
566	O	8088,2055033,17321	97,097247	-2,36890	,031686	-,00064	33,19976	18,099637	,48445	,00028	,00016
567	F	8090,0055033,17612	97,185283	2,32141	,029190	-,00211	33,21584	18,094157	-,48132	,00059	,00019
568	S	8115,6055033,27095	21,412389	,63847	-,024926	-,00211	33,32719	87,348242	-2,22392	,00535	,00019
569	O	8118,2055033,29178	18,536742	,46755	-,030422	-,00211	33,33164	99,372759	-2,40090	,00583	,00019
570	D	8120,0055033,30744	18,626409	-,51879	-,035610	-,00369	33,33448	99,377915	2,39812	,00591	-,00010
571	S	8145,6055033,41505	89,842752	-2,26310	-,130108	-,00369	33,42886	21,114405	,65905	,00338	-,00010
572	O	8148,2055033,41938	102,071458	-2,44025	-,139705	-,00369	33,45006	18,146559	,48243	,00312	-,00010
573	F	8150,0055033,42214	101,983374	2,48777	-,140247	,00309	33,46610	18,152036	-,48556	,00308	,00005
574	S	8175,6055033,51593	20,807174	,68318	-,061053	,00309	33,57702	87,628645	-2,22837	,00434	,00005
575	O	8178,2055033,53754	17,731168	,49990	-,053010	,00309	33,58145	99,676392	-2,40538	,00447	,00005
576	D	8180,0055033,55400	17,641552	-,44868	-,049673	,00064	33,58429	99,671233	2,40816	,00436	-,00016
577	S	8205,6055033,66875	85,241520	-2,19194	-,033274	,00064	33,67860	21,079896	,66181	,00015	-,00016
578	O	8208,2055033,67330	97,099934	-2,36899	-,031608	,00064	33,69984	18,099604	,48445	-,00028	-,00016
579	F	8210,0055033,67621	97,188066	2,32145	-,029113	,00211	33,71593	18,094130	-,48132	-,00060	-,00019
580	S	8235,6055033,77103	21,413132	,63851	,024960	,00211	33,82728	87,348372	-2,22392	-,00535	-,00019
581	O	8238,2055033,79186	18,537282	,46759	,030452	,00211	33,83172	99,372916	-2,40090	-,00583	-,00019
582	D	8240,0055033,80753	18,626848	-,51877	,035637	,00369	33,83457	99,378078	2,39812	-,00591	,00010
583	S	8265,6055033,91514	89,840527	-2,26301	,130126	,00369	33,92895	21,114450	,65905	-,00338	,00010
584	O	8268,2055033,91946	102,068769	-2,44016	,139723	,00369	33,95015	18,146592	,48243	-,00312	,00010
585	F	8270,0055033,92223	101,980589	2,48773	,140263	-,00309	33,96619	18,152063	-,48556	-,00308	-,00005
586	S	8295,6055034,01602	20,806431	,68314	,061039	-,00309	34,07711	87,628516	-2,22837	-,00434	-,00005
587	O	8298,2055034,03763	17,730628	,49986	,052993	-,00309	34,08154	99,676235	-2,40537	-,00446	-,00005
588	D	8300,0055034,05409	17,641113	-,44870	,049653	-,00064	34,08437	99,671070	2,40816	-,00436	,00016
589	TL1	8310,3255034,12315	34,154993	-1,15148	,043021	-,00064	34,10619	57,231938	1,70416	-,00266	,00016
590	VL1	8316,2255034,14592	50,111704	-1,55301	,039229	-,00064	34,12599	39,497526	1,30169	,01466	,00571
591	TL2	8328,2055034,17339	97,093245	-2,36866	,031528	-,00064	34,19993	18,099601	,48445	,08302	,00571
592	F	8330,0055034,17630	97,180781	2,32144	,029032	-,00211	34,21602	18,094127	-,48132	,09706	,01001
593	TL3	8331,0055034,17798	92,603647	2,25570	,026921	-,00211	34,22458	19,124843	-,54939	,10707	,01001
594	DL1	8338,0055034,18797	197,677253	-22,85739	,026901	,00210	34,29575	9,013727	1,36140	,10563	-,01038
595	TL4	8346,6055034,19145	786,674677	-45,63068	,044998	,00210	34,59407	9,010636	-1,36104	,01640	-,01038
596	FL2	8350,1055034,19208	890,122647	18,74938	,046173	-,00145	34,63161	27,183752	-4,28483	-,01931	-,01048
597	TL5	8354,5055034,19295	732,795795	17,00673	,039800	-,00145	34,64678	78,678062	-7,41842	-,06544	-,01048
598	UL2	8360,4055034,19443	545,877926	14,67364	,031255	-,00145	34,65444	191,005576	-11,62026	-,14593	-,01680
599	G	8360,8055034,19455	534,202420	14,51513	,030675	-,00145	34,65476	200,415736	-11,90514	-,15265	-,01680
600	UL2	8366,7055034,19665	376,700208	12,17963	,022129	-,00145	34,65823	365,686101	-16,10698	-,27041	-,02312
601	G	8367,1055034,19682	367,019936	12,02105	,021549	-,00145	34,65840	378,685631	-16,39185	-,27966	-,02312
602	TL6	8374,8897534,20135	203,893036	8,93497	,010272	-,00145	34,66085	677,036409	-21,93564	-,45961	-,02312
603	VL3	8380,7897534,20755	112,252328	6,59691	,001725	-,00145	34,66201	960,665120	-26,13747	-,57384	-,01561
604	G	8381,1897534,20814	107,038252	6,43827	,001145	-,00145	34,66208	981,689046	-26,42234	-,58008	-,01561

605	DL3	8386,6897534,21716	112,101422	-7,57629	-,007595	-,00185	34,66409	599,305139	77,81016	-,45320	,05885
606	TL3	8387,6897534,21849	127,770965	-8,09725	-,009201	-,00185	34,66339	455,788886	67,70609	-,39435	,05885
607	FL4	8393,1897534,22492	110,243010	10,38149	-,014619	,00002	34,66783	111,011853	10,47988	-,19487	,01848
608	TL7	8403,6897534,45625	1,013951	,02127	-,014373	,00002	34,90313	1,001668	-,00272	-,00085	,01848
609	TL7	8414,1897534,69429	109,349529	-10,33895	-,014126	,00002	35,13756	111,125925	-10,48531	,19317	,01848
610	DL4	8419,6897534,69880	447,409771	-66,77114	-,020045	-,00232	35,14393	129,008181	8,15542	,20917	-,01305
611	TL3	8420,6897534,69911	590,919168	-76,73826	-,022363	-,00232	35,14525	113,220640	7,63212	,19612	-,01305
612	FL3	8426,1897534,70013	968,162835	26,04123	-,025786	,00115	35,15417	108,340219	-6,53517	,19257	,01169
613	G	8426,5897534,70019	947,442089	25,76063	-,025325	,00115	35,15475	113,632909	-6,69655	,19724	,01169
614	UL3	8432,4897534,70137	667,840203	21,62818	-,018530	,00115	35,16088	206,694840	-9,07681	,24403	,00418
615	TL8	8457,2740034,73095	26,931633	4,23133	,010017	,00115	35,17000	904,433692	-19,07570	,34752	,00418
616	DL2	8460,7740034,76671	8,992665	1,34180	,015596	,00211	35,17063	799,478684	46,34861	,31617	-,02169
617	G	8461,1740034,77624	7,969054	1,21723	,016439	,00211	35,17071	762,829913	45,27332	,30750	-,02169
618	VL4	8467,0740035,00512	4,445939	-,62010	,028867	,00211	35,17261	322,183044	29,41270	,18798	-,01883
619	TL9	8469,3740035,06454	8,945749	-1,53634	,033712	,00211	35,17404	201,105453	23,22973	,14468	-,01883
620	FL1	8476,3740035,13662	18,814953	,54376	,027329	-,00374	35,18386	94,476439	-2,32307	,08101	-,00115
621	TL3	8477,3740035,14533	17,796293	,47490	,023586	-,00374	35,18550	99,190281	-2,39077	,07985	-,00115
622	D	8479,1740035,16168	17,802352	-,47836	,017779	-,00276	35,18835	99,175268	2,39887	,07437	-,00489
623	TL2	8491,1540035,23662	39,170546	-1,30529	-,015227	-,00276	35,21516	51,473116	1,58294	,01576	-,00489
624	VL5	8497,0540035,25655	56,974671	-1,71232	-,031482	-,00276	35,23730	35,165267	1,18111	,00155	,00007
625	TL1	8507,3740035,27842	99,666996	-2,42454	-,059914	-,00276	35,30449	18,040772	,47824	,00231	,00007
626	ES	8507,3740035,27842	99,666996	-2,42454	-,059914	-,00276	35,30449	18,040772	,47824	,00231	,00007

R=1353,99062 TGAM=(28,20497, 0,00000) QX= 35,27842 QY= 35,30449

MAXIMA	BETAX(510)=1016,65139	XEQ=(443)= 4,72571	BETAY(502)= 981,87464	YEQ(266)= 2,06256
MINIMA	BETAX(506)= ,96784	XEQ=(226)= ,00080	BETAY(608)= 1,00167	YEQ(532)= -,00006